

School of Science and the Environment

**The Manipulation of Inflammation, Immunity and
Infection by Novel Derivatives of Halichlorine**

**A thesis submitted in partial fulfilment of the requirements of the
Manchester Metropolitan University for the degree of Doctor of Philosophy**

Sasha Blackshaw

2017

Abstract

Halichlorine **1** is a marine spirocyclic alkaloid, which has shown to exhibit anti-inflammatory properties.¹ Due to the complexity of this structure, and the low abundance in nature, the development of total and partial syntheses of this compound have become of interest to the organic chemist.

This project aimed to evaluate the therapeutic potential of this class of compounds by producing a library of simplified halichlorine derivatives by addition of Grignard reagents onto a key spironitrone that maps onto the core structure of halichlorine and thence to monitor potential bioactivity by conducting a series of biological assays to determine what effects these compounds have on human U937 cells.

Addition of a wide range of Grignard reagents to spironitrone **128** was successful and generally proceed with high diastereoselectivity. In addition, reductive cleavage of the resulting *N*-hydroxyspirocycles with Zn/AcOH provided a host of *N*-acetyl-C7-substituted spirocyclic derivatives **167-172**. Reduction with indium provided free amines **173-181**.

As additions to spironitrone **128** proceeded with undesired stereoselectivity attempts were made to access O-protected spironitrone **204** by oxidation of spiroamines such as **199**. This strategy was unsuccessful. In order to explore alternative spirocyclic derivatives, synthetic studies were also directed in attempts to access un-substituted derivatives by ring closing metathesis (RCM) of diene precursors **222-224**. While RCM substrates were accessed cyclisation of these did not proceed.

It was discovered that heating 6,5-spiroisoxazolidine **102** under pressure in a microwave reactor provided access to the corresponding 6,6-isomer **164** which maps onto the core structure of the amphibian toxin histrionicotoxin (HTX). Oxidation to 6,6-spiro-nitrone **192**, as followed by conversion to cycloadducts **193-195**, which represent new analogues of the HTX family of alkaloids. Grignard additions to this nitrone, did not proceed in general.

Biological screenings using undifferentiated and LPS activated U937 cells helped to identify a number of biologically active derivatives, when tested in the NO and growth and viability assays. The NO assay using LPS activated cells, identified that the adducts containing larger alkyl or aryl chains, particularly the pentyl, hexyl and benzyl adducts, expressed significant differences in NO inhibition at both 10^{-4} M and 10^{-5} M concentrations tested, compared to the untreated cells.

Acknowledgements

I would like to thank my beloved son Koby Lin for being so well behaved during the busy evenings I spent working on this project. I am very thankful to my auntie Pat for always being there for me, as well as Devon July and Koby Lin for providing me with all the love and support in the world.

I would also like to thank Dr Jenny Gibson, Dr Nyevero Simbanegavi, Dr Jay Dixon, James Ryan, Michael Foley and Lee Harman and colleagues for all the laughs, support, guidance and friendship.

A big thank you to my supervisory team, in particular Dr Vittorio Caprio, for all his guidance, patience, support and endless knowledge during the length of this project.

Contents

Abstract	i
Acknowledgements	iii
Abbreviations	viii
List of Figures	xii
List of Tables	xv
Chapter 1. Halichlorine, a natural product	
1.1 Introduction.....	1
1.1.1 The history of natural products.....	1
1.1.2 Halichlorine and Pinnaic acid.....	3
1.2 Biological Processes.....	5
1.2.1 An introduction into Inflammation.....	5
1.2.2 NF- κ B and Inflammation.....	8
1.2.3 The role of NF- κ B in Inflammatory Diseases.....	10
Chapter 2. Previous syntheses of Halichlorine and Histrionicotoxin	
2.1 Literature studies.....	12
2.1.1 The Danishefsky Group.....	13
2.1.2 The Uemura Group.....	17
2.1.2.1 Synthesis of a tricyclic Halichlorine Core.....	17
2.1.2.2 Enantioselective Total Synthesis of Halichlorine.....	19
2.1.3 The Clive Group.....	23
2.1.3.1 Synthesis of Spirobicyclic core Structures.....	23

2.1.3.2 Clive's Total Synthesis of Halichlorine.....	26
2.2.1 The White Group.....	31
2.2.2 The Zhao Group.....	33
2.3 Synthetic Studies towards Histrionicotoxin.....	35
2.3.1 The Gossinger Group.....	37
2.3.2 The Holme's Group.....	39
2.3.3 The Brossi Group.....	42
2.4 Previous Syntheses by the Caprio Group.....	44

Chapter 3. Synthetic Studies

3.1 The History of Nitrones.....	47
3.2 Preparation of Nitrones.....	49
3.3 Reactions of Nitrones.....	52
3.3.1 Oxidation of Nitrones.....	54
3.3.2 Reduction of Nitrones.....	56
3.3.3 The 1,3-dipolar Cycloaddition.....	57
3.3.3.1 Stereochemistry of the Cycloaddition.....	60
3.3.4 Nucleophilic Addition to Nitrones.....	62
3.4 Project Aims.....	64

Chapter 4. Additions to [6,5,5]-spironitrone

4.1 Synthesis of the Spironitrone.....	65
4.2 Nucleophilic additions to the Spironitrone.....	71
4.2.1 Stereochemistry of the acetylated cycloadducts.....	75

4.3 Indium-Mediated Reductive Method.....	78
4.4 Further Studies into the Allyl-adduct.....	83
Chapter 5. Additions to the 6,6-Spirotrone	
5.1 Synthesis of the 6,6-Spirotrone.....	89
5.2 Cycloadditions to the 6,6-Spirotrone.....	92
5.3 Grignard additions to the 6,6-Spirotrone.....	97
Chapter 6. Alternative routes to access Spirocyclic structures	
6.1 Alternative Methods to Ring Open the Isoxazolidine.....	103
6.2 Di-alkenyl Additions to Access a Spirocyclic Core.....	111
Chapter 7. Biological Studies	
7.1 Cell Culture.....	117
7.2 Growth and Viability Assay.....	118
7.3 Nitric Oxide Assay.....	122
7.3.1 Results of the NO Assay.....	123
7.4 Discussion.....	127
Chapter 8. Summary and Future Work	
8.1 Summary.....	130
8.2 Future Work.....	131
Chapter 9. Experimental	133
Chapter 10. References	185
Chapter 11 Appendix	

10.1 Statistical Data.....	188
----------------------------	-----

Abbreviations

9-BBN	9-Borabicyclo[3.3.1]nonane
Ac	Acetyl
AIBN	Azobisisobutyronitrile
Aq.	Aqueous
Bn	Benzyl
BOC	<i>tert</i> -Butyloxycarbonyl
C	Carbon
cPLA2	Cytosolic phospholipase A2
CAN	Ceric ammonium nitrate
Cat.	Catalyst
CBz	Carboxybenzyl
COX	Cyclooxygenase
CSA	Camphorsulfonic acid
DABCO	1,4-Diazabicyclo[2.2.2]octane
DBU	1,8-Diazabicyclo[5.4.0]undec-7-ene
DCC	<i>N, N'</i> -Dicyclohexylcarbodiimide
DEPT	Distortionless enhancement by polarisation transfer
DIBAL	Diisobutylaluminium hydride
(DHQD)₂PHAL	Hydroquinidine 1,4-phthalazinediyl diether
DMAP	4-Dimethylaminopyridine
DMAP•HCl	4-(<i>N, N</i> -Dimethylamino)pyridine hydrochloride
DMF	Dimethylformamide
DMSO	Dimethyl sulfoxide
DNA	Deoxyribonucleic acid
ECAM	Endothelial cell adhesion molecule
EDCI	1-Ethyl-3-(3-dimethylaminopropyl)carbodiimide
EDTA	Ethylenediaminetetraacetic acid

eNOS	Endothelial nitric oxide synthase
EPR	Electron paramagnetic resonance
equiv.	Equivalence
Et	Ethyl
EtOAc	Ethyl acetate
EtOH	Ethanol
FBS	Fetal bovine serum
FMO	Frontier molecular orbital
FT-IR	Fourier transform infrared spectroscopy
h	Hour
H	Hydrogen
HMPA	Hexamethylphosphoramide
HOMO	Highest occupied molecular orbital
HTX	Histrionicotoxin
ICAM-1	Intracellular adhesion molecule-1
IκB	Inhibitory protein
iNOS	Inducible nitric oxide synthase
LDA	Lithium diisopropylamide
LiDBB	4,4'-Di- <i>tert</i> -butylbiphenylide
LiHMDS	Lithium bis(trimethylsilyl)amide
LTA	Lead tetraacetate
LUMO	Lowest unoccupied molecular orbital
mCPBA	<i>meta</i> -Chloroperoxybenzoic acid
Me	Methyl
MeOH	Methanol
MEM	Methoxyethoxymethyl
mg	Milligram
MHz	Megahertz

MNBA	2-Methyl-6-nitrobenzoic anhydride
MOMCl	Methoxymethyl acetal chloride
MSH	Mesitylenesulphonylhydroxylamine
MW	Microwave
Nf-$\kappa$$\beta$	Nuclear factor kappa beta
NMO	<i>N</i> -Methylmorpholine <i>N</i> -oxide
NMR	Nuclear magnetic resonance
nNOS	Neuronal nitric oxide synthase
NOESY	Nuclear overhauser effect spectroscopy
PBN	α -Phenyl <i>N</i> -tertiary-butyl nitron
PCC	Pyridinium chlorochromate
Ph	Phenyl
ppm	Parts per million
PPTS	Pyridinium <i>p</i> -toluenesulfonate
Pr	Propyl
Py	Pyridine
quant.	Quantitative
RCM	Ring closing metathesis
r.t.	Room temperature
sat.	Saturated
S_N2	Nucleophilic substitution
TBAF	Tetra- <i>n</i> -butylammonium fluoride
TBDMSCl	tert-Butyldimethylsilyl chloride
TBDPSCI	<i>tert</i> -Butyl(chloro)diphenylsilane
TBSOTf	<i>tert</i> -Butyldimethylsilyltrifluoromethanesulfonate
^tBu	Tertiary butyl
TEA	Triethylamine
TEA-HF	triethylamine trihydrofluoride

Temp.	Temperature
TMSCI	Trimethylsilyl chloride
TFA	Trifluoroacetic acid
TFAA	Trifluoroacetic anhydride
THF	Tetrahydrofuran
THP	Tetrahydropyran
TLC	Thin layer chromatography
TPAP	Tetrapropylammonium perruthenate
TREAT•HF	Triethylamine trihydrofluoride
Ts	Tosylate
UV	Ultraviolet
VCAM-1	Vascular cell adhesion molecule-1

List of Figures

Figure 1. Halichlorine 1 , Pinnaic acid 2 and Tauropinnaic acid 3 , with the 6-azaspiro[4.5]decane core.....	3
Figure 2. The inflammatory Process.....	6
Figure 3. The structures of the most studied and widely used nitron spin traps.....	47
Figure 4. The delocalisation of electrons in the 1,3 dipole of a nitron.....	52
Figure 5. The nitron 147 and oxime 148 studied.....	52
Figure 6. A frontier molecular orbital diagram showing the various types of HOMO-LUMO interaction in the 1,3-dipolar cycloaddition.....	58
Figure 7. Shows the FMO for the dipole and dipolarophile, leading to two possible transition states, depending on the electronegativity of the dipolarophile.....	59
Figure 8. Showing the differences in the endo and exo reaction, which illustrates why the exo product is favoured.....	60
Figure 9. A representation of an <i>endo</i> orbital interaction in a Diels Alder cycloaddition.....	61
Figure 10. The stereoselective bond formation in a 1,3 dipolar cycloaddition.....	61
Figure 11. Spironitron 130	70
Figure 12. ¹ H-NMR of the methyl adduct 168	73
Figure 13. Structures of <i>N</i> -acetylated reduced compounds 168-173	74
Figure 14. Possible conformers generated from a nucleophilic addition of a Grignard species to nitron 130	75
Figure 15. The different sides of attack leading to conformers a, a'; and b, b'.....	76
Figure 16. Spirocyclic amines synthesised via Grignard addition/ indium reduction one pot method.....	79

Figure 17a. ¹ H-NMR spectrum of the propyl adduct 176	80
Figure 17b. NOESY spectrum of the propyl adduct 176 , showing the cross peaks for overlapping peaks C1'/C7.....	80
Figure 18. ¹ H-NMR spectrum of the [6,6,5]-cycloadduct 165 product.....	90
Figure 19. ¹ H-NMR spectrum of the 6,6-spiro nitrone 194	91
Figure 20. The possible conformers of a cycloaddition if attack occurs from the top face.....	94
Figure 21. The possible conformers of a cycloaddition if attack occurs from the bottom face.....	95
Figure 22. Shows the expected stereochemistry for the series of cycloadditions, with the unassigned conformation of C2''	96
Figure 23. The pentyl adduct synthesised by the Brossi group.....	98
Figure 24. The possible conformers of spirocyclic nitrone 194	100
Figure 25. The bulky silyl protection groups of interest.....	101
Figure 26. The expected conformer of a silyl-protected 6,5-spiro nitrone....	102
Figure 27. Retroanalysis of the intended RCM route.....	111
Figure 28. Effect of the molecules at 10 ⁻⁴ M and 10 ⁻⁵ M on undifferentiated U937 cells.....	119
Figure 29. Average viable cell counts for LPS activated cells and treated cells at 10 ⁻⁴ M and 10 ⁻⁵ M.....	121
Figure 30. Average NO concentrations (μM) calculated for undifferentiated cells compared to the treated cells at 10 ⁻⁴ M and 10 ⁻⁵ M concentrations....	124
Figure 31. Average NO concentrations (μM) per million viable undifferentiated cells compared to the treated cells following treatment with molecules at 10 ⁻⁴ M and 10 ⁻⁵ M concentrations.....	125
Figure 32. Average NO concentrations (μM) LPS activated cells compared to the treated cells following treatments with molecules at 10 ⁻⁴ M and 10 ⁻⁵ M concentrations.....	126

Figure 33. Average NO concentrations (μM) per million viable LPS activated cells compared to the treated cells following treatment with molecules at 10^{-4} M and 10^{-5} M concentrations.....127

Figure 34. The molecules which shown a significant difference at both concentration in the NO assay with LPS activated cells, suggesting a higher potency.....129

Figure 35. Alternate methods to oxidise the free hydroxyl group.....131

List of Tables

Table 1. The histrionicotoxin family of alkaloids.....	35
Table 2. Reductions of the spirocyclic adducts with zinc powder, with the addition of an acetate group.....	77
Table 3. Grignard addition/ indium reduction onto nitron 130	81
Table 4. Cycloadditions onto spirocyclic nitron 194	92
Table 5. Shows the reaction conditions for the attempted nucleophilic additions onto the 6,6-spiro-nitron.....	99
Table 6. Protection of the C1-hydroxy group as a silyl ether.....	104
Table 7. Reagents screened for oxidation of spirocycles 207/ 209 to nitrones.....	106
Table 8. Reagents screened for deprotection of the silylethers on 207/208 to the free hydroxyl.....	110
Table 9. Series of mono-additions to nitron 100	113
Table 10. Series of Grignard additions onto mono-additions 101, 231	114

Chapter 1. Halichlorine, a natural product

1.1 Introduction

1.1.1 The history of natural products

Nature is an ancient pharmacy. For thousands of years, natural products have been the source of therapeutic medicines all over the world. Plants have formed the basis of sophisticated traditional medicines, but natural remedies have also been sourced from microorganisms, marine organisms and animals.²

In recent years, natural products have been the most successful source of potential drug leads.³ Bioactive natural products act as the inspiration for structural scaffolds to the medicinal chemist,⁴ because they are generally small molecules with drug-like properties.⁵ Thousands of extracts from plant sources have undergone extensive screenings, although it is estimated that thousands remain unexplored.⁵ As well as being the inspiration for drug development, plants have also been a rich source of directly isolated medicinal drugs, for instance, morphine; cocaine; codeine and quinine.⁶

Microorganisms have yielded some of the most important products of the pharmaceutical industry,⁷ which started with the development of penicillin in the late 1930's- early 1940's.⁸ This expanded drug discovery from microorganisms, which has led to important modern day drugs including antibiotics, immunosuppressants and lipid-lowering statins.⁵ Interestingly, these drugs have all been produced from a small range of the world's microbial

diversity, and it is thought that there are potentially millions of bacterial species yet to be discovered.⁵

Marine natural products do not have an extensive history unlike the other sources, resulting from a previous lack of technology (mainly scuba diving). This has rapidly improved in recent years, with more than 20,000 compounds having been discovered since the 1960's.⁹ The earliest published work on marine organisms dates back to 1951 by the group of Werner Bergmann,¹⁰ which documents the discovery of nucleosides obtained from marine sponges, leading to the development of a successful anticancer drug.¹¹ Systematic investigations into marine organisms only began properly during the mid 1970's, during which time thousands of compounds were isolated.⁷ Marine organisms produce a unique and wide array of biologically diverse, fascinating molecular structures.¹² As many of the marine life are soft bodied, they require the deadly yet intriguing ability to either synthesise toxic compounds or obtain them from microorganisms as a defensive mechanism, or a way to paralyse their prey.¹³

The discovery of bioactive compounds is on-going from all natural resources. Halichlorine is one example of such an isolated compound, which was involved in a mass biological screening and showed potential biological properties.¹

1.1.2 Halichlorine and Pinnaic acid

Halichlorine **1** is a marine alkaloid isolated from marine sponge *Halichondria Okadai*, which was discovered whilst on a search for biologically active compounds.¹⁴ Sponges exhibit a high frequency of bioactive compounds for their chemical defences, it is also therefore reasonable to see that the highest concentrations of toxic or antioxidant properties are found in areas such as coral reefs, where there is feeding pressure from fish, and a constant competition for space.¹⁵

The complex structure of halichlorine shares a 6-azaspiro[4.5]decane core with similar marine compounds, pinnaic acid **2** and tauropinnaic acid **3** (Fig. 1).¹

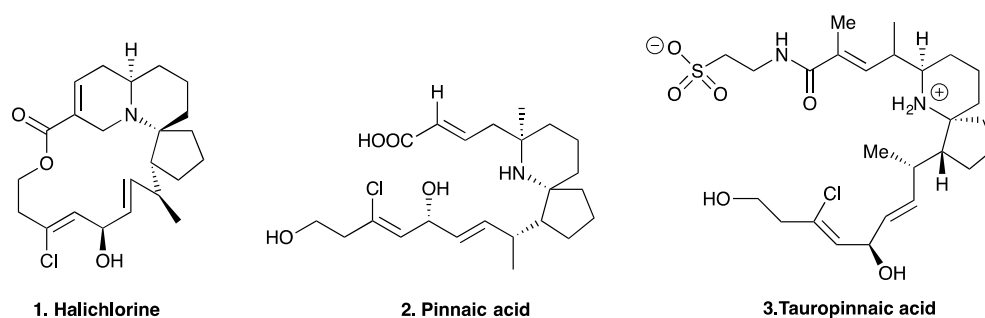


Figure 1. Halichlorine **1**, Pinnaic acid **2** and Tauropinnaic acid **3**, with the 6-azaspiro[4.5]decane core.

Pinnaic acid and tauropinnaic acid have activity against expressed cytosolic phospholipase A2 (cPLA₂) activity.¹⁴ The hydrolytic process catalysed by the cPLA₂ enzyme forms products which are precursors to a wide array of pro-inflammatory mediators, which act as either intracellular messengers within

the cell, or interact with specific receptors on the cell surface of the parent cell or neighbouring cells.¹⁶ The therapeutic potential in controlling this enzyme make cPLA₂ a drug target, thus, making pinnaic acid and taupinnaic acid biologically interesting molecules.

Halichlorine has been shown to inhibit lipopolysaccharide-induced nuclear factor-kappa beta (NF-κB). NF-κB results in the suppression of vascular cell adhesion molecule-1 (VCAM-1); intracellular adhesion molecule-1 (ICAM-1); E-selectin gene expression and endothelial cells adhesion molecules (ECAM).¹⁷ It has been reported, however, that although halichlorine has shown inhibitory properties towards VCAM-1, the same can not be said for ICAM-1. According to a review of bioactive alkaloids from the sea by the Uemura group,¹⁸ halichlorine does not affect ICAM-1, the reason for this remains unknown, but it may lead to ideas on how the biological mechanism may work. Drugs which block the expression of VCAM-1 may be useful in treating atherosclerosis, coronary heart disease, angina and non-cardiovascular inflammatory diseases.¹⁴

Beyond this knowledge, the specific biological capabilities and biological mechanisms of halichlorine remain to be investigated in detail.

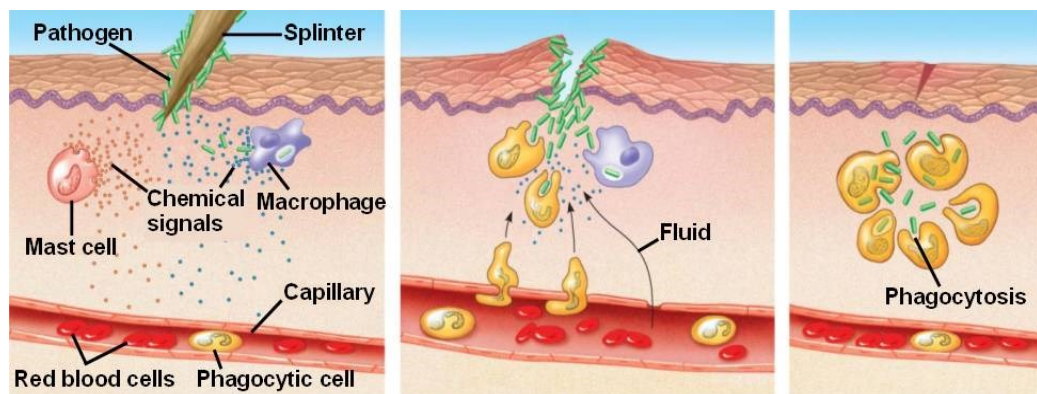
1.2 Biological Processes

1.2.1 An introduction into Inflammation

Inflammation is an essential response provided as a protective strategy against microbial infection, tissue injury and other noxious conditions. What was once seen as a fairly straight-forward immune response, has now emerged to operate in a sophisticated manner.¹⁹ The ultimate goal of inflammation is to remove the cause as well as any injured cells or tissue from the organism. The process simultaneously destroys, dilutes and defends against the unwanted agent, as well as healing the injured tissue with either native parenchymal cells (local cellular tissue) or with fibroblastic cells (scar tissue).²⁰ Inflammation is considered an 'adaptive response', as it is closely connected to homeostasis, the system responsible for maintaining the stability of the body.¹⁹

The inflammatory process is initiated by chemical mediators, or signals, expressed upon injury or injection. Figure 2 shows the release of chemical mediators from mass cells, causing the nearby blood vessels to dilate, becoming more permeable. The chemical signals released from the macrophages increases the blood flow to the local area, visible by a reddening of the injured area. The increased blood flow brings in phagocytes, which engulf the pathogens, dead cells and any cellular debris, which is recognised as pus from the wound, a fluid containing white blood cells with the engulfed debris and pathogens. Finally, the platelets will move out of the capillary to seal the wounded area.²¹

Figure 2. The inflammatory Process²¹ Shows the stages of acute inflammation, lasting between



a few hours to a few days.

Once the potential danger to the body has subsided, the reversion of the inflammatory response to the homeostatic state should proceed quickly, failure to do so turns acute inflammation into the chronic stage.

Acute inflammation is the initial response upon being injured (described above), and lasts for a relatively short period of time, usually between minutes to a few days. Chronic inflammation on the other hand is a prolonged inflammatory response and can have damaging consequences to the host. Chronic inflammation is believed to develop if the triggering stimuli isn't eliminated, such as chronic cellular injury or a persistent infection. Although it has been the subject of extensive studies, the underlying mechanism of the cause remains largely undetermined. It is extremely problematic as the major damages done to the host are mediated by the host's inflammatory response, not by the foreign pathogens.^{19, 20} Research into chronic inflammation has been unable to identify an inducer, which aids the continuation of the inflammatory response. Without this knowledge, an intervention is extremely difficult. Further research

is required into the mechanisms which induce and sustain chronic inflammation to ensure any therapeutic designed will have minimal risk of damaging side effects for the host.

It has recently been reported that inflammatory diseases can also play a role in promoting cancer, particularly tumorigenesis (tumour formation), as well as various inflammatory cells being present within tumours.²² It is also said that environmental factors, which promote inflammation are connected to an increased cancer risk, such as carcinogen exposure; inhalation of tobacco smoke or other pollutants and infectious microbes, particularly in lung tumorigenesis.¹⁹

With inflammation being a vital defensive mechanism for the body, research into novel, potentially anti-inflammatory bio-active species could prove extremely important in the quest to control chronic inflammation.

1.2.2 NF- κ B and Inflammation

Upon its discovery in 1986 by Sen and Baltimore,²³ NF- κ B was identified as a nuclear factor that bound to an enhancer element of the immunoglobulin light-chain gene and was believed to be specific to B cells. Since then, research has discovered that NF- κ B is actually a eukaryotic transcription factor²⁴ and serves as an important regulator of inducible inflammatory gene expression. This includes regulation of ECAMs and pro-inflammatory cytokines, activating NF- κ B dependent gene expression.²⁵

NF- κ B exists in virtually all cell types in its inactive form, and is bound to inhibitory proteins (I κ Bs) residing in the cytoplasm.²⁶ On activation, which is induced by agents including mitogens, chemical substances that encourage cell division, cytokines and inducible messengers that are generally produced and act for immune cells, NF- κ B is dissociated from I κ B, allowing the free NF- κ B to be transported into the nucleus, where it can regulate genes involved in immune and inflammatory responses.²⁴

As well as the usual activation pathways, researchers have suggested that reactive oxygen species, may also trigger the signalling process. Studies involving peroxynitrite, (formed *in vivo* from a reaction of free radicals superoxide and nitric oxide (NO)), suggested the peroxynitrite amplifies signalling mechanisms under inflammatory conditions. The amount of peroxynitrite synthesised increase in inflammation, with excessive amounts shown to have detrimental effects to the host, including DNA damage, cell

damage due to depletion of cellular energies, apoptosis leading to cell/ tissue damage.²⁷

NF- κ B exist as hetero- or homogeneous dimers, in a combination of NF- κ B and Rel proteins, which can bind to DNA through a terminal amino acid, this region is also responsible for the dimerisation. There are various dimer combinations possible, most of which have shown to be transcriptionally active, although there are some homodimer exceptions, which have shown to be transcriptionally repressive.²⁴

NF- κ B regulates pro-inflammatory cytokines, adhesion molecules and growth factors, but it also regulates genes encoding cyclooxygenase 2 (COX2) and inducible nitric oxide synthase (iNOS).²⁸ The onset of inflammation is associated with the expression of COX-2 and iNOS, with COX-2 being induced by inflammatory stimuli hormones, which is said to be the dominant source of prostaglandin formation in inflammation.²⁹ iNOS is responsible for the overproduction of NO, which is often observed during inflammation.

1.2.3 Nitric Oxide and Inflammation

Since the discovery that mammalian cells have the ability to synthesise free radical nitric oxide in 1987, it has been the focus for many research groups. NO is a gaseous molecule, produced, *in vivo*, in a reaction catalysed by NOS enzymes and has emerged to be a fundamental signalling device, responsible for regulating a variety of physiological and pathophysiological responses. The NOS family currently consists of three isoforms. All of the NOS family have the ability to produce NO, although eNOS and nNOS only produce relatively low amounts compared to iNOS.²⁵ Exposing the enzyme to microbial molecules such as lipopolysaccharide (LPS) induces the expression of the iNOS gene in various inflammatory cells.²⁷

The role of NO seems to be dependent on the quantity released at a particular site, for example, low concentrations of NO has shown to be protective and anti-inflammatory, whereas much larger quantities of NO released by cells have shown to destroy tissue and impair discrete cellular responses,³⁰ and may cause injury to the host during prolonged inflammation. The concentration of NO is also an important factor in respects of cytotoxicity. Low quantities of NO act as a defensive mechanism against invading microbial organisms for example, bacteria, viruses or parasites, an anti-inflammatory effect, whereas an inflated amount of NO can also start destroying cells and tissue, causing it to have a pro-inflammatory effect,³⁰ making it an important modulator in the inflammatory process.

Studies have reported a close link between NO and NF- κ B, with NO causing an inhibitory effects on NF- κ B activation and subsequent gene expression, as well as inhibiting NF- κ B's interaction with DNA. The inhibitory effect of NO is not restricted to NF- κ B though, as it is thought to inhibit the expression of many genes involved in inflammatory diseases. Studies also suggest that NO can effect both acute and chronic inflammation through influencing many pathophysiological processes, including leucocyte-endothelial interaction; ECAM expression and infiltration of activated leucocytes at inflammation sites.^{25, 27}

Research has shown that NO plays a vital role within the inflammatory process, therefore inhibition of an NO expression could provide a method to control inflammation.

Chapter 2. Previous Syntheses of Halichlorine

2.1 Literature Studies

Since the discovery of the bioactive alkaloids, halichlorine **1** and pinnaic acid **2** have interested many research groups with their unique structure and expressed bioactivity. Many groups have used similar strategies to access both core structures/natural products, due to the structural similarities.³¹⁻³⁷ Those up to 2005 have been comprehensively reviewed by the group of Clive.³⁸

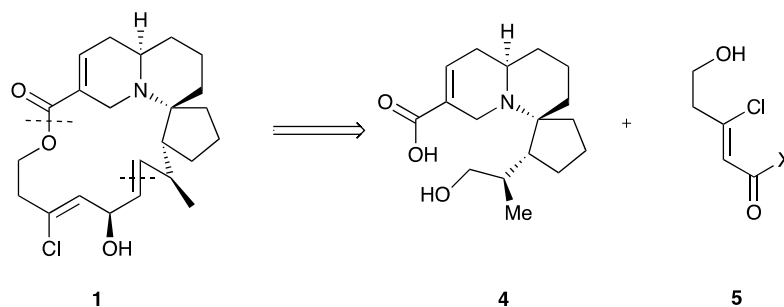
Owing to the volume of work in this area only a select number of routes to halichlorine will be reviewed here. There are a number of total syntheses, some of which are similar to the first total synthesis by the Danishefsky group, all of which will be covered here. Only those partial syntheses utilising nitrone chemistry, of particular relevance to this thesis, will be reviewed here.

This section will also cover some synthetic approaches to the terrestrial-sourced spiroalkaloid histrionicotoxin. While this compound is exclusively isolated from frogs of the *Dendrobates* species, surprisingly, it exhibits a similar structure to the marine alkaloids halichlorine and pinnaic acid and thus synthesis of the core structure of this potentially useful neuroactive compound has also been the subject of this thesis.

2.1.1 The Danishefsky's Lab

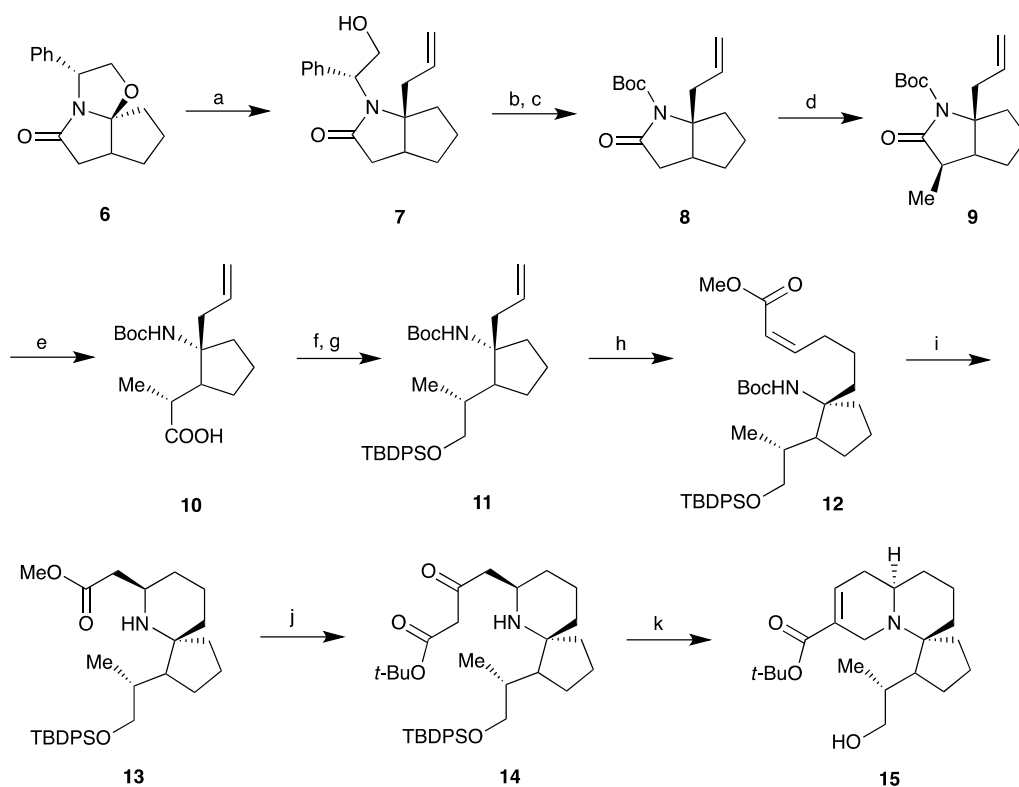
Danishefsky's lab were the first to achieve the total synthesis of halichlorine.³⁹

Retrosynthesis focuses on bisecting the target compound into a spiroquinolizidine core **4** and a highly functionalised fragment **5** (Scheme 1).⁴⁰



Scheme 1. Shows the disconnection of Halichlorine to the spiroquinolizidine core.⁴⁰

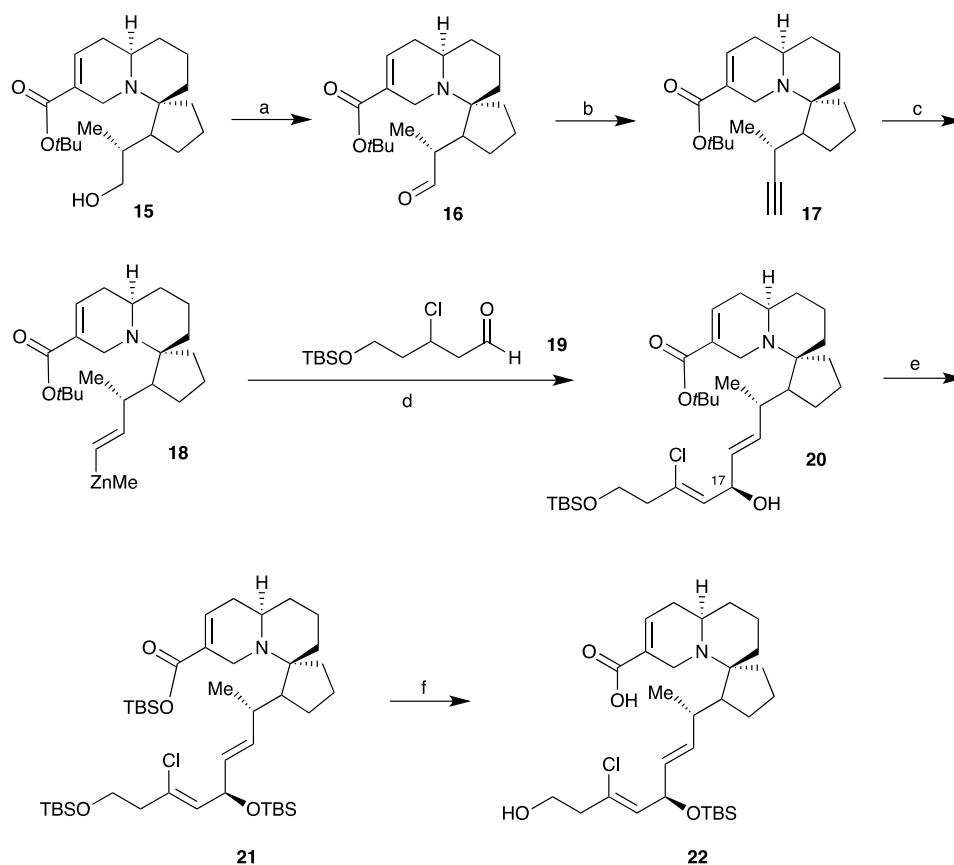
The protected spiroquinolizidine core **14** was synthesised from known compound, 'Meyers-lactam' **6** in 12 steps.⁴⁰ The last step involved a selective deprotection tried in two ways, one removed the silyl ester to afford a primary alcohol, and the other removed the *tert*-butyl group, releasing the corresponding acid. The deprotected alcohol **15** was reacted further.³⁸



Scheme 2. The route from Meyers Lactam towards the spiroquinolizidine core. a) allyltrimethylsilane, TiCl_4 , CH_2Cl_2 , -78°C to r.t.; b) Na , NH_3 , THF , EtOH , -78°C ; c) Boc_2O , DMAP , THF ; d) (i) LiHMDS , THF , -40°C ; (ii) MeI , -78°C to 0°C ; e) LiOH , THF , H_2O ; f) (i) EtOCOCl , Et_3N , THF ; (ii) NaBH_4 , MeOH ; g) TBDPSCl , Et_3N , DMAP , CH_2Cl_2 ; h) (i) 9-BBN, THF ; (ii) $\text{Pd}(\text{dppf})\text{Cl}_2$, Ph_3As , Cs_2CO_3 , DMF , H_2O ; i) (i) TFA , CH_2Cl_2 ; (ii) H_2O , K_2CO_3 ; j) $t\text{-BuOAc}$, LiHMDS , THF , -50°C to r.t.; k) i) CH_2O , EtOH , $(\text{Me}_3\text{Si})_2\text{NLi}$, THF , 0 ii) $\text{CP}_2\text{Zr}(\text{H})\text{Cl}$, r.t., HF .pyridine, THF .⁴⁰

The challenging oxidation of **15** finally produced the corresponding aldehyde **16**, when reacted crude, followed by a Serferth-Gilbert homologation to produce a terminal alkyne **17**. This was converted to a vinyl zinc species **18**, by hydrozirconation and transmetalation. Addition of **19** produced **20** in a 4:1 ratio of desired (17*R*)-diastereomer, which was taken forward without

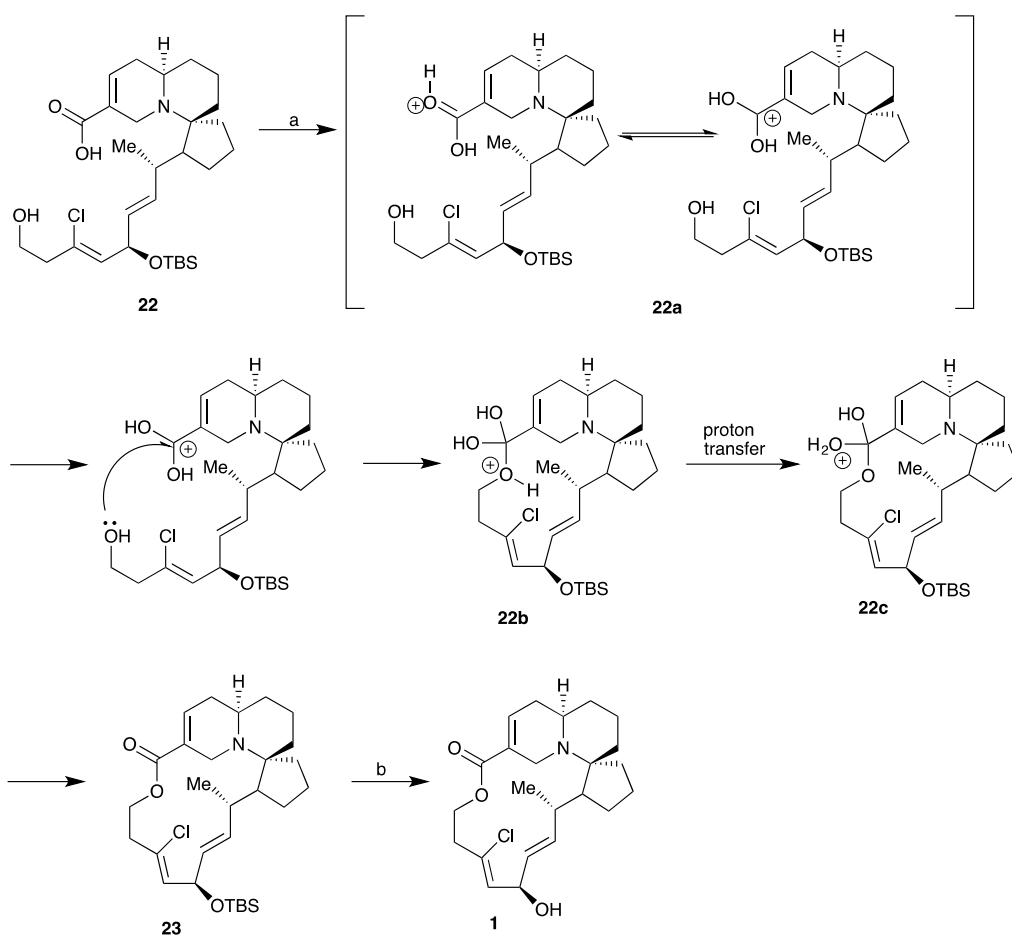
separation. Protecting group manipulation followed, by replacement of the *tert*-butyl ester with a silyl group, which consequently protected the hydroxyl group in the process. The two primary silyl groups were then removed, leaving the secondary silyl ester on **22** intact (Scheme 3).⁴⁰



Scheme 3. Synthetic route from the spiroquinolizidine core to the deprotected derivative. a) TPAP, NMO, MeCN, r.t.; b) $\text{N}_2\text{CHP}(\text{O})(\text{OMe})_2$, KOtBu , THF, -78°C ; c) (i) $[\text{Cp}_2\text{Zr}(\text{H})\text{Cl}]$, CH_2Cl_2 ; (ii) Zn_2Me , heptane, -65°C ; d) **19**, DIBAL, PhMe, CH_2Cl_2 , -78°C ; e) TBSOTf, 2,6 Lutidine, CH_2Cl_2 , -78°C to r.t.; f) NH_4F , MeOH, H_2O .³⁹

The ring closing step consisted of a Fischer esterification reaction under Keck macrolactonisation conditions,⁴¹ which involved the transfer of a proton from

DMAP.HCl to the acid. The result is a charged species, which can delocalise around the carbonyl carbon and hydroxyl group of the acid **22a**. The primary alcohol then attacks the carbonyl carbon and attaches forming **22b**, followed by a proton transfer generating a leaving group, **22c**. The carbonyl is reformed during dehydration **23**, after which the final silyl protecting group is removed to achieve **1**.³⁹



Scheme 4. The final steps in the first total synthesis of halichlorine. a) EDCI, DMAP, DMAP·HCl, CHCl₃, THF, Δ; b) HF-pyridine, pyridine, THF.³⁹

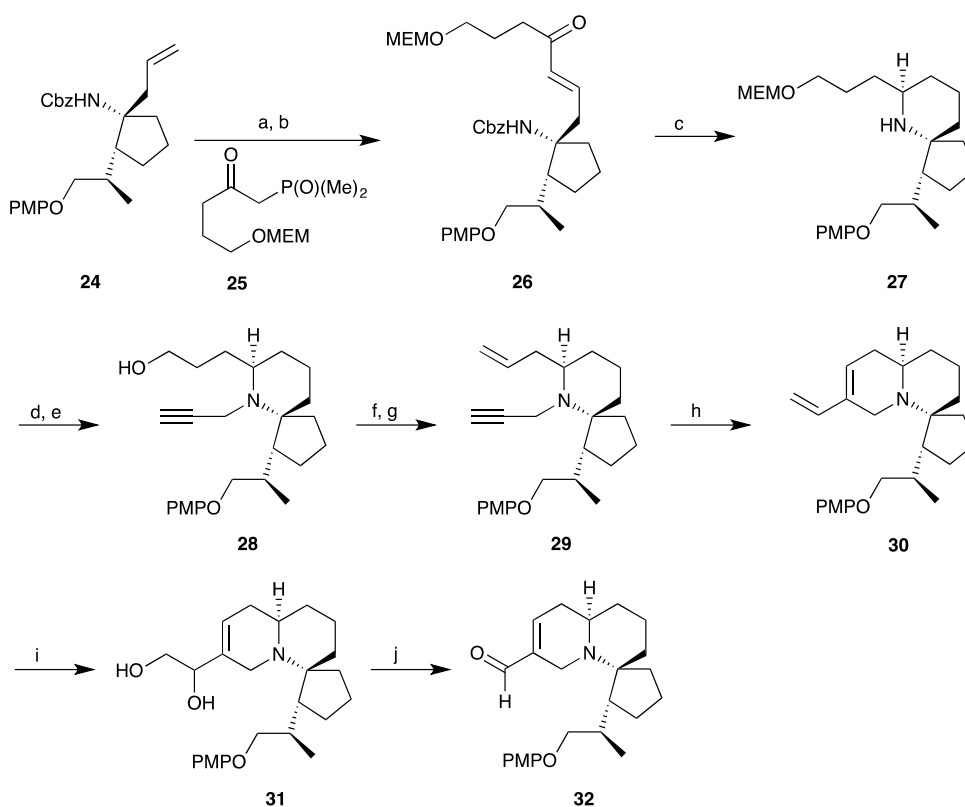
2.1.2 The Uemura Group

2.1.2.1 Synthesis of a Tricyclic Halichlorine Core

Halichlorine was discovered by the Uemura group, whilst on their quest for biologically active substances from marine organisms.¹ The isolated yield was $3.5 \times 10^{-7}\%$ (70.8 mg from 200 kg of wet sponge), with which they determined the structure and absolute stereochemistry of the compound.⁴² They were also the group who discovered its biological potential, including its ability to inhibit the induction of VCAM-1.¹

In 2004, the Uemura group published the synthesis of the halichlorine tricyclic core via an ene-yne metathesis-based strategy. They began with a cyclopentane derivative **24**, constructed during the synthesis of pinnaic acid,⁴³ which already contained functionality in the correct positions, oxidative cleavage of this terminal alkene to an aldehyde was followed by a Horner-Wadworth-Emmons reaction with phosphonate **25**, yielding **26**. Hydrogenation of **26** effected a series of reactions, including saturation of the double bond, removal of the carboxybenzyl protecting group and stereo-selective reduction of the cyclic imine intermediate. Reproducible results of the desired product were achieved by using a large amount of catalyst without the presence of acid. Introduction of a propargyl substituent to the sterically hindered nitrogen atom also proved challenging, this was finally successful when Proton Sponge™ was used, followed by the removal of the methoxyethoxymethyl (MEM) group to afford **28**. A 2-nitrophenylselenyl group was added onto the primary alcohol, followed by the oxidation and elimination of the selenium group to give the

terminal alkene on **29**. The ring closing ene-yne metathesis reaction was performed using 2nd generation Grubbs's Ru-catalyst under an ethylene atmosphere forming **30** in a good yield. Sharpless dihydroxylation of the terminal alkene in **30** afforded **31**, and the diol was finally oxidatively cleaved yielding the desired aldehyde and tricyclic halichlorine core **32**.⁴⁴



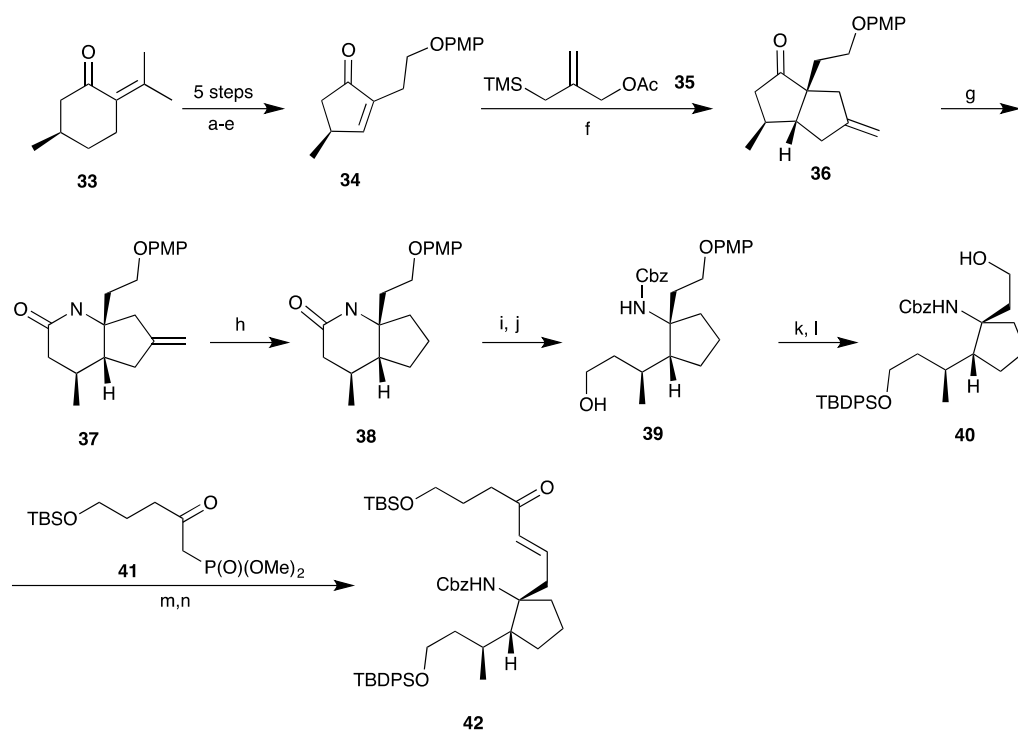
Scheme 5 a) O_3 , MeOH, ii. Me_2S ; b) LiCl, Et_3N , THF, phosphate **25**; c) H_2 , $Pd(OH)_2/C$, EtOH, 94%; d) propargyl bromide, proton sponge, MeCN, 60°C, 60%; e) PPTS, *t*-BuOH, reflux, 77%; f) 2-nitrophenyl selenocyanate, $(n-Bu)_3P$, THF, r.t., 98%; g) mCPBA, THF, r.t., 87%; h) 2nd generation Grubbs Ru-catalyst (11.7 mol %), ethylene atmosphere, toluene, 80°C, 72%; i) $K_2OsO_4 \cdot H_2O$, (DHQD)₂PHAL, $NaHCO_3$, $K_3[Fe(CN)_6]$, aq. *t*-BuOH, r.t., 52%; j) $NaIO_4$, MeOH, 0°C-r.t., 81%.⁴⁴

2.1.2.2 Enantioselective Total Synthesis of Halichlorine

In 2014, 10 years after the publication of the tricyclic core,⁴⁴ the Uemura group reported an enantioselective total synthesis of halichlorine and pinnaic acid.⁴⁵ Interestingly, they did not build on previous work towards halichlorine described above.

As pinnaic acid and halichlorine share the same structural backbone, the synthesis was designed to produce a common intermediate, in which both could be synthesised from. They combined efforts from the previous total syntheses of pinnaic acid and the early steps in the synthesis of the halichlorine core.^{43, 44, 46, 47}

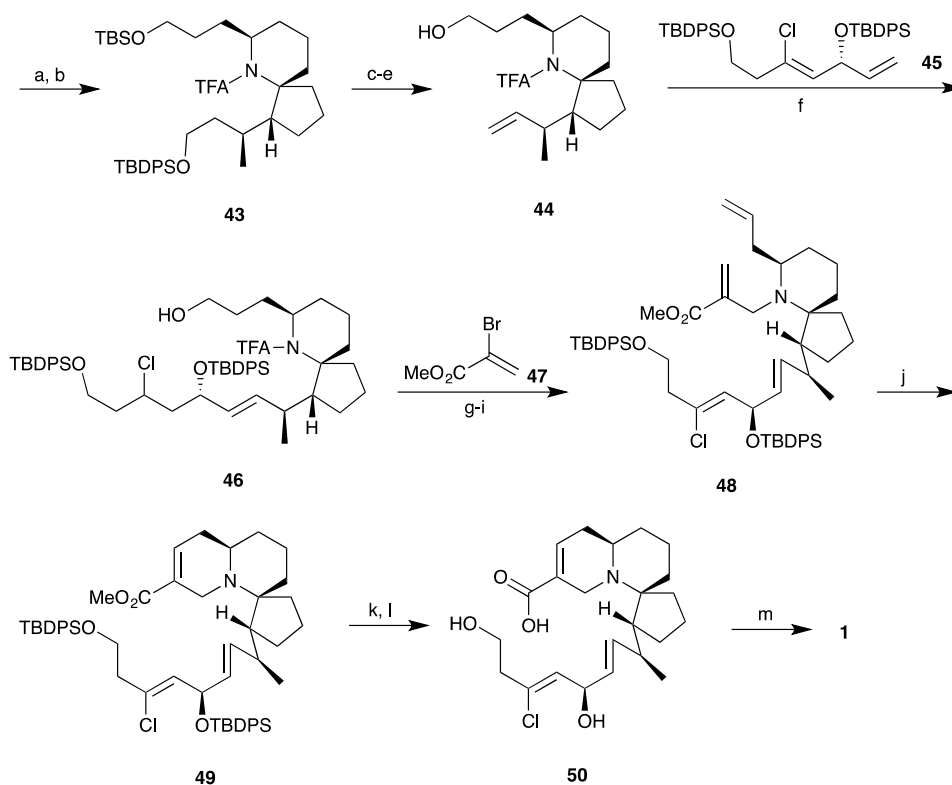
As with the 2007 asymmetric total synthesis of pinnaic acid, they began their efforts with commercially available (*R*)-(+)-pulegone **33**, with the first key intermediate being synthesised in 5 steps. With quantities of the key chiral cyclopentenone **34** in hand, a palladium catalysed [3+2] cyclisation with **35** gave the fused bicyclic compound **36**. Installation of the nitrogen atom proved challenging, after trying the Schmidt reaction and the Beckmann rearrangement, the hindered nitrogen reagent *o*-mesitylenesulphonylhydroxylamine (MSH) proved to be more successful, achieving **37** with a reproducible 85% yield. A one-pot ozonolysis-Clemmensen reduction gave **38**, which was followed by the protection of the nitrogen atom before the reductive ring opening with LiBH₄, giving **39**. Further protecting group manipulation gave **40**. Oxidation of the free hydroxyl group was followed by a Horner-Wadsworth Emmons reaction with **41** to afford spiro-cyclic precursor **42** as the single trans isomer (Scheme 6).⁴⁵



Scheme 6. Steps towards the spirocyclic core shared with pinnaic acid and halichlorine. a) O_3 , $0^\circ C$, HOAc, H_2O , EtOAc; b) AllylOH, H_2SO_4 (cat.), Dean-Stark, reflux, 89% (2 steps); c) K, AllylOH, PhMe, reflux, *p*-2-(iodoethyl)-methoxyphenyl, reflux; d) HCl, acetone, r.t.; e) $Pd(OAc)_2$ (5 mol %), MeCN, $90^\circ C$, 49% (3 steps); f) **35**, $Pd(OAc)_2$, $(iPrO)_3P$, THF, reflux, 80%; g) MSH, CH_2Cl_2 , r.t., silica gel, 85%; h) O_3 , *i*PrOH, CH_2Cl_2 , $-78^\circ C$ then, Zn, TMSCl, $-78^\circ C - 0^\circ C$, (one pot) 72%; i) NaH, CbzCl, THF, reflux, 87%; $NaBH_4$, LiBr, THF, $50^\circ C$; j) TBDPSCI, DMAP, Et_3N , CH_2Cl_2 , r.t.; k) CAN, MeCN, H_2O , $0^\circ C$, 79% (2 steps); l) $SO_3 \cdot py$, Et_3N , DMSO, r.t.; m) **41**, Et_3N , LiCl, THF, $30^\circ C$, quant. (2 steps).⁴⁵

Compound **42** undergoes an impressive one pot four step cyclisation, triggered by hydrogenation, proving to be a very efficient and powerful way to produce the piperidine ring present in both **1** and **2**. It consists of four consecutive transformations: 1) saturation of the alkene, 2) removal of the Cbz protecting group, 3) intramolecular cyclisation of the imine/enamine formation, 4)

stereoselective reduction of the imine/enamine intermediate. The amino group in the spirocycle was protected to give **43**, followed by the selective deprotection of the TBDPS group and a Grieco elimination, after which the MOM group was removed yielding the terminal alkene in **43**. Cross metathesis of **44** with **45** proceeded smoothly achieving **46**. Grieco elimination of the remaining hydroxyl group gave the corresponding terminal alkene, followed by the removal of the TFA group, and addition of **47**. This provided **48** with the ability to undergo ring closing metathesis using second generation Grubb's catalyst. Deprotection of the TBDPS groups on **49**, and hydrolysis of the methyl ester allowed Shiina macrolactonisation of **50** to complete the total synthesis of **1**.⁴⁵



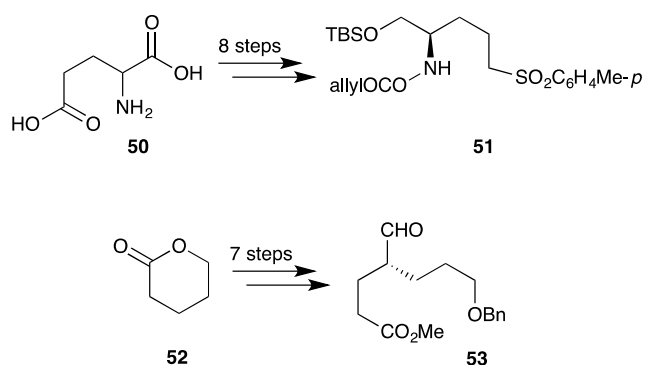
Scheme 7. The final steps towards the enantioselective total synthesis of halichlorine. a) H_2 , Pd(OH) $_2$ /C (20 mol %), HOAc, EtOH, r.t.; b) TFAA, *i*Pr $_2$ Net, CH $_2$ Cl $_2$, 0°C, 80% (2 steps); c) TBAF, THF, 0°C; d) *o*-NO $_2$ PhSeCN, nBu $_3$ P, THF, r.t., then mCPBA, r.t., (99%); e) PPTS, *t*BuOH, 90°C, 86%; f) **45**, Hoveyda-Grubb's II catalyst (28 mol %), PhMe, static vacuum, 60°C, 72%; g) *o*-NO $_2$ PhSeCN, nBu $_3$ P, THF, r.t., then H $_2$ O $_2$, r.t., 84% (2 steps); h) NaBH $_4$, EtOH, 30°C; i) **47**, K $_2$ CO $_3$, MeCN, 60°C, 84% (2 steps); j) Grubb's II catalyst (10 mol %), CH $_2$ Cl $_2$, reflux; k) HF•py, r.t., 93%; l) NaOH, THF, MeOH, H $_2$ O, 50°C; m) MNBA, DMAP, THF, r.t., 56% (2 steps).⁴⁵

2.1.3 The Clive Group

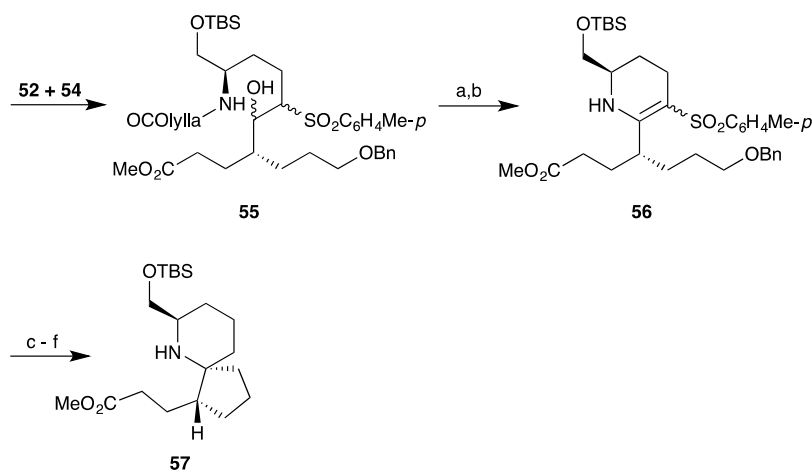
2.1.3 Synthesis of Spirobicyclic core Structures

The Clive group began their studies by focusing on the spirobicyclic core of **1** and **2**. In 1999 and 2004, the Clive group reported two methods in producing very similar cyclic core structures, using radical cyclisation.^{48, 49}

The earlier paper comprised of two segments being synthesised from D-Glutamic acid **51** and valerolactone **53** (scheme 8a). Deprotonation of **52** followed by the slow addition of aldehyde **54** produced a diastereoisomeric mixture of **55**. Oxidation of the hydroxyl group, followed by the removal of the allyloxycarbonyl group allowed the formation of the enamine. The benzyl protecting group was removed, allowing the replacement of the proton with a bromide, this then radically cyclised and finalised with a desulphonylation to achieve **57**.⁴⁸

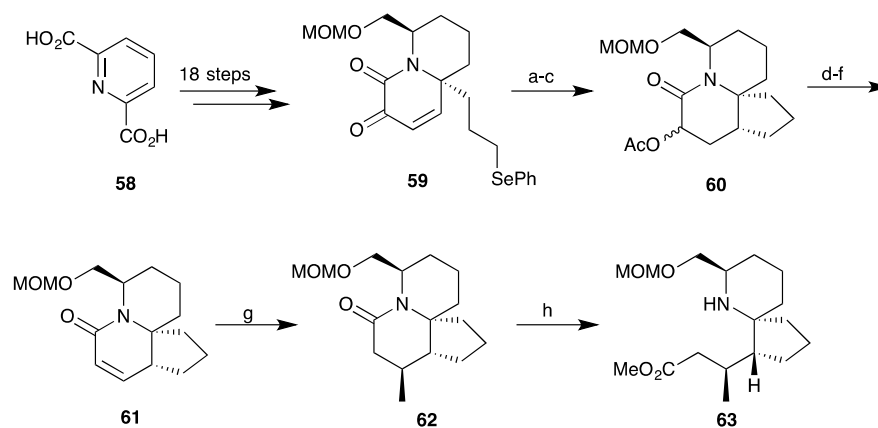


Scheme 8a. The two segments synthesised for Clive's route to a spirocyclic core.



Scheme 8b. Clive's first synthesis of a spirocyclic core of **1** and **2**. a) Dess-Martin reagent, CH_2Cl_2 , 90%; b) $(\text{PH}_3\text{P})_4\text{Pd}$, dimedone, THF, 88%; c) Pd-C, H_2 , MeOH-EtOAc, 90% d) Ph_3P , 2,6-lutidine, CBr_4 , MeCN, 82%; e) Bu_3SnH , AIBN, PhMe, 75°C , 57%; f) $\text{Na}(\text{Hg})$, MeOH, Na_2HPO_4 , 75%.

In 2004, the Clive group published a second paper showing an alternative method to synthesise a very similar azaspiro[4.5]decane core. This time they began with pyridine 2,6 dicarboxylic acid **58** and produced intermediate **59** in a lengthy 18 step synthesis. After experiencing some difficulties in the radical cyclisation of **59**, the enone was reduced which allowed the cyclisation to proceed giving **60**, followed by the removal of the acetoxy group. After installation of the required methyl group, the lactam was opened with Meerwein's reagent affording **63**.⁴⁹



Scheme 9. Clive's second syntheses towards a spirocyclic core. a) NaBH_4 , $\text{CeCl}_3 \cdot 7\text{H}_2\text{O}$, MeOH , -45°C , 40 min, 85%; b) Ac_2O , pyridine, 12 h, 99%; c) Bu_3SnH (addition over 10 h), AIBN, PhH , 80°C , reflux further 3 h, 67%; d) MeONa , MeOH , 4 h; e) MeSO_2Cl , Et_3N , THF ; f) DBU, PhMe , reflux, 48 h, 69% over 2 steps; g) Me_2CuLi , Me_3SiCl , Et_3N , THF , -78°C (2 h) to 25°C (1 h), 81%; h) Me_3OBF_4 , 2,6-di-*tert*-butylpyridine, CH_2Cl_2 , 4.5 h, aq. Na_2CO_3 , 71%.⁵⁰

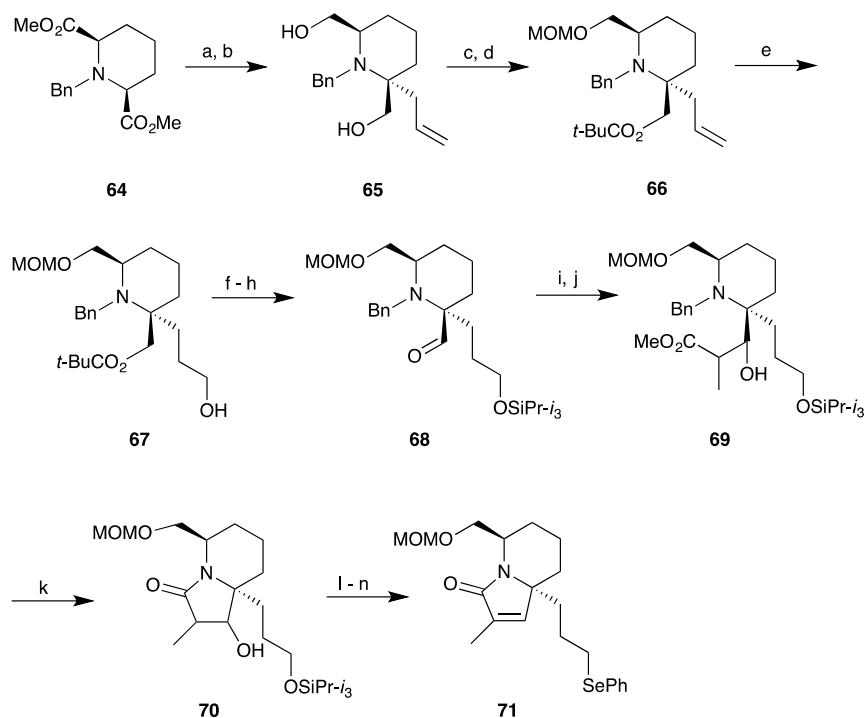
This core structure was followed soon after with another spirocyclic amine.

Further reading into Clive's partial syntheses can be found here.^{32, 38, 50, 51}

2.1.4 Clive's Total Synthesis of Halichlorine

Following the several partial syntheses of **1** and **2**, the Clive group focussed their efforts on a total synthesis of **1**. They looked to employ a completely new route to the one's previously published, who's syntheses relate to Danishefsky's routes. After extensive exploratory studies, they constructed their synthesis to form an asymmetric spiro-centre early, and built around it.⁵²

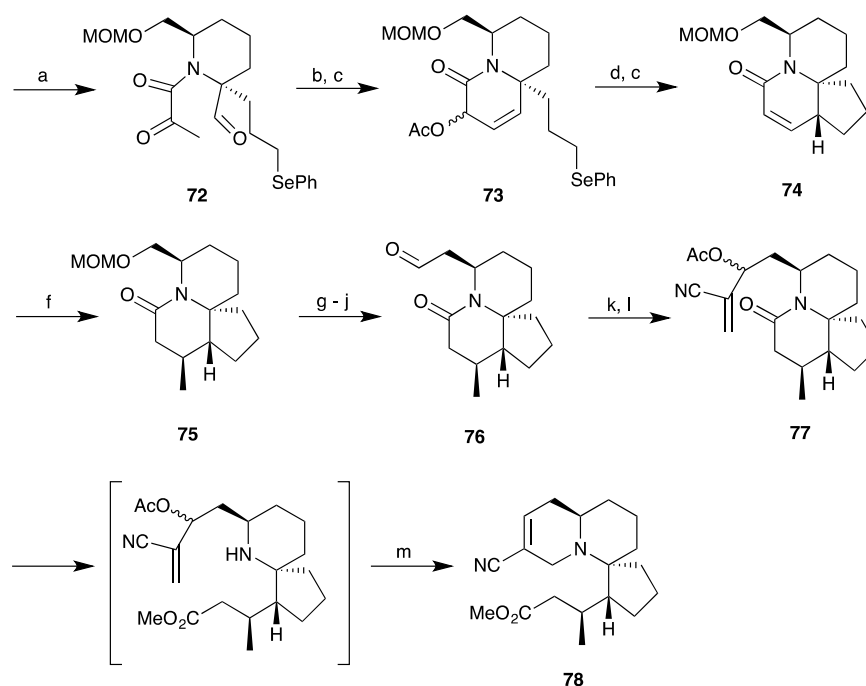
They began with the diester **64**, allylation and reduction of the diesters afforded **65**. Selective protections of the hydroxyl groups **66** allowed hydroboration of the allyl **67**. Protecting group manipulation of the corresponding hydroxyl group and removal of the pivaloyl group allowed the formation of an aldehyde **68** by Swern oxidation. Aldol condensation of **68**, was followed by the removal of the benzyl group yielding **69** in a diastereoisomeric mixture. Heating in PhMe formed the rigid bicyclic lactam **70**. Dehydration of the hydroxyl group, followed by removal and replacement of the silyl group with first a bromide, which was proved to provide the wrong stereochemistry for the vital pendent methyl group on **1**, when radical cyclisation occurred, was later changed for a phenylseleno group **71**.⁵²



Scheme 10. The first steps towards Clive's total synthesis of halichlorine. a) chiral base, BuLi, THF, allyl bromide, 65%; b) LiAlH₄, THF, 0°C to r.t., 71%; c) *t*-BuCOCl, *i*-Pr₂NEt, DMAP, CH₂Cl₂, -10°C, 67%; d) MOMCl, *i*-Pr₂NEt, DMAP, CH₂Cl₂, 0°C to r.t., 95%; e) 9-BBN, THF, 0°C to r.t.; 30% H₂O₂, MeOH, NaOH, 0°C to r.t., 99%; f) *i*-Pr₃SiOSO₂CF₃, *i*-Pr₂NEt, CH₂Cl₂, 0°C, 99%; g) DIBAL-H, CH₂Cl₂, Et₂O, -78, 89%; h) Swern, 93%; i) LDA, MeO₂CCH₂CH₃, THF, -78°C; j) 10% Pd-C, 1,4-cyclohexadiene, EtOAc, 58°C, 94%; k) PhMe, reflux, 48 h, 89%; l) MsCl, Et₃N, THF, 0°C to r.t.; DBU, reflux, 88%; m) Bu₄NF, THF, 93%; n) PhSeCN, Bu₃P, THF, 97%.⁵²

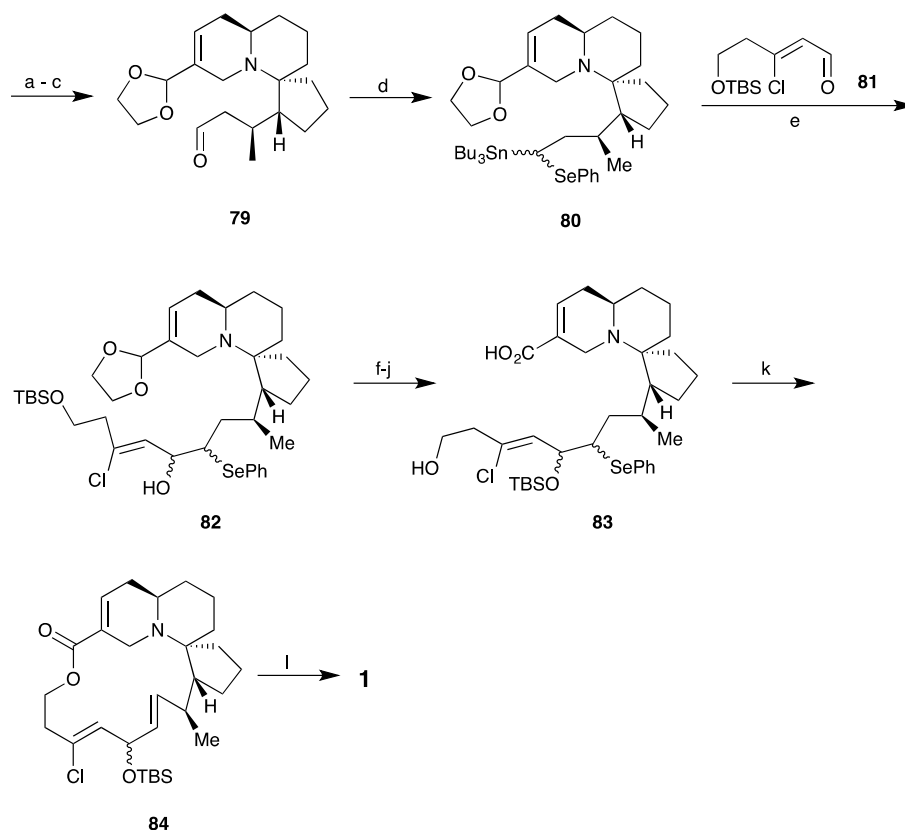
Ozonolysis of **71** opened up the bicyclic ring. Upon treatment with DBU, **72** underwent consecutive intramolecular aldol condensation and dehydration to afford **73**. The enone was reduced before radical cyclisation of the selenium protected pendent. This produced a number of compounds including the corresponding acetate in both diastereoisomers, as well as an enone **74**. All the acetate was converted to **74**, before the introduction of the methyl group **75**.⁵²

Installation of the final ring proceeded by removal of the MOM group, oxidation to the corresponding aldehyde followed by Wittig olefination and acid hydrolysis to afford **76**. **76** was subjected to a Baylis-Hillman reaction, to give an alcohol, which was immediately converted to the acetate **77**. These previously formed lactam was opened to give a methyl ester, and also experienced spontaneous intramolecular cyclisation yielding **78**.



Scheme 11. Installation of the spirocyclic rings. a) O_3 , CH_2Cl_2 , $-78^\circ C$; $(MeO)_3P$, $-78^\circ C$ to r.t., 84%; b) DBU, THF, $0^\circ C$ to r.t., 80%; $NaBH_4$, $CeCl_3 \cdot 7H_2O$, MeOH, $-45^\circ C$, 90%; Ac_2O , pyridine, 98%; d) Bu_3SnH , AIBN, PhH, $80^\circ C$, e) Bu_3P , $o-O_2NC_6H_4SeCN$, THF, H_2O_2 , 96%; f) Me_2CuLi , Me_3SiCl , HMPA, THF, $-78^\circ C$ to r.t., 96%; g) Me_3SiBr , CH_2Cl_2 , $-10^\circ C$, 86%; h) Pr_4NRuO_4 , NMO, CH_2Cl_2 , 84%; i) $MeOCH_2PPh_3Cl$, $t-BuOK$, THF, $0^\circ C$; j) CSA, MeCN-water, 92%; k) acrylonitrile, DABCO, $Sc(OTf)_3$, 5 days; l) $AcCl$, pyridine, CH_2Cl_2 , $0^\circ C$ to r.t., 89%; m) Me_3OBF_4 , CH_2Cl_2 ; aq. Na_2CO_3 , MeCN.⁵²

Now that the spiro-bicyclic system was in place, the side chain was extended in preparation for macrocyclisation. The nitrile was reduced to an aldehyde before being protected. This allowed for selective oxidation of the alcohol **79**, which was quickly converted to selenides **80**, before addition of the known chloro- aldehyde **81**. The selenium was removed forming a double bond, before protecting group manipulation of **82** protected the hydroxyl group and released the aldehyde, which was oxidised to the corresponding acid. Selective deprotection of the primary silyloxy group released the hydroxyl group **83**, which underwent macrocyclisation to achieve **84**, as shown in Danishefsky's synthesis.⁴⁰ Finally, the remaining silyl group was removed affording **1** (Scheme 12).⁵²



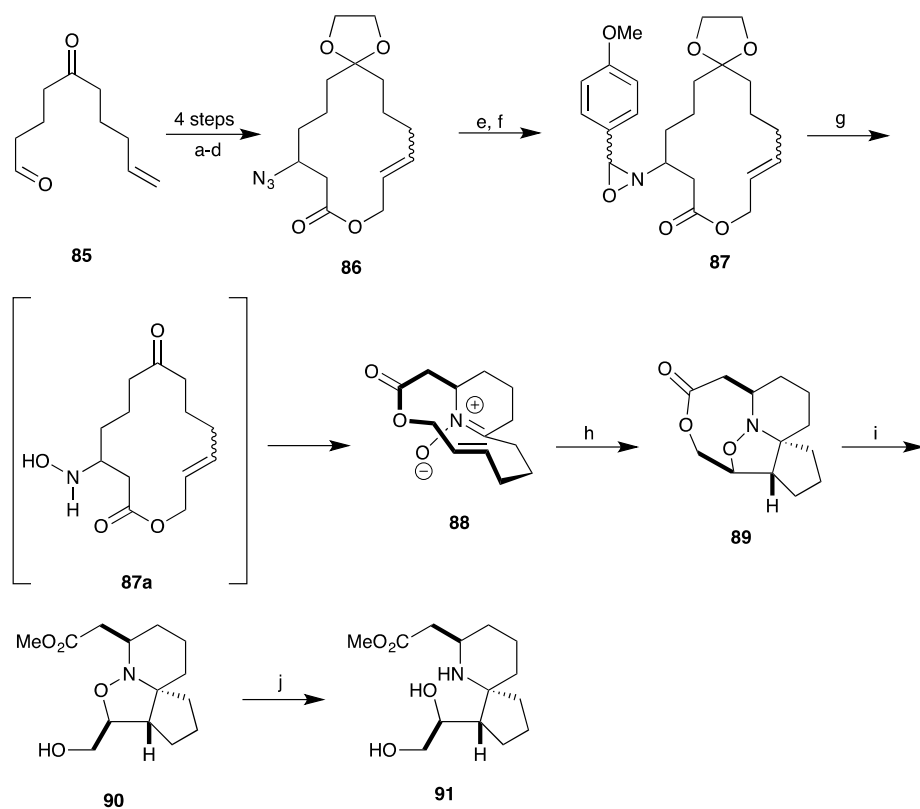
Scheme 12. The final steps towards the total synthesis of halichlorine. a) DIBAL-H, CH₂Cl₂, THF, PhMe, -78°C, 72%; b) Me₃SiOSO₂CF₃, 1'2-bis(trimethylsiloxy)ethane, CH₂Cl₂, 76%; c) Pr₄NRuO₄, NMO, CH₂Cl₂, 88%; d) Bu₃SnLi, THF, -78°C; then Bu₃PPhSeCN, THF, pyr, 61%; e) **81**, BuLi, THF, -78°C; f) NaHCO₃, NaIO₄, MeOH; g) *t*-BuMe₂SiCl, ImH, DMF, 36%; h) Me₃SiOTf, 2,6-lutidine, CH₂Cl₂, 81%; i) Pinnick oxidation, 75%; j) NH₄F, water-MeOH, 40°C, 20 h, 81%; k) DMAP, DMAP•HCl, EDCl, CHCl₃, reflux, 58%; l) HF-Pyr, THF, 54%.⁵²

2.2 Partial Syntheses of Halichlorine using Nitron Chemistry

2.2.1 The White Group

The White group based their efforts towards the core of **1** and **2** using a transannular nitron cycloaddition. This unique class of intramolecular reaction differs by containing both the dipole and the alkene within a ring, allowing a high degree of stereocontrol. One requirement of this reaction is that the macrocycle must be large enough to permit flexibility to allow the functional groups to meet, but not too large that the N-oxide passes through the plane of the ring. Upon meeting these conditions, the reaction will proceed yielding a single stereocentre.⁵³

The synthesis began by formation of the macrocycle. Using a keto aldehyde **85**, an oxaziridine **86** was formed in 4 steps. Treatment of **87** with *p*-toluenesulfonic acid resulted in simultaneous hydrolysis of the ketal forming the hydroxylamine intermediates, which spontaneously cyclised forming the nitron **88**. Upon heating a single crystalline product was afforded **89**, before methanolysis gave **90** and reductive cleavage of the isoxazolidine afforded the spirocyclic amine **91**.^{38, 53}

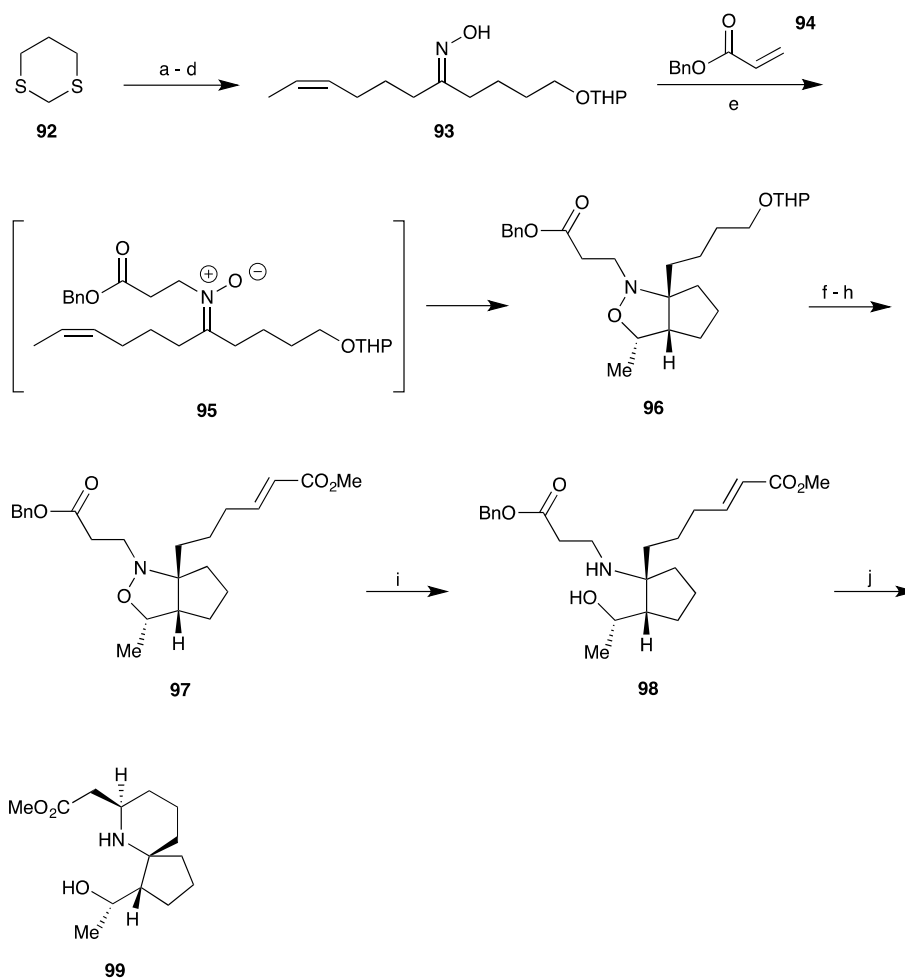


Scheme 13. White's partial synthesis of halichlorine. a) $\text{Ph}_3\text{CHCO}_2\text{CH}_2\text{CHCH}_2$, CH_2Cl_2 ; b) HN_3 , Et_3N , PhH , reflux; c) $(\text{CH}_2\text{OSiMe}_3)_2$, Me_3SiOTf , CH_2Cl_2 , -78°C ; d) Grubbs I, CH_2Cl_2 ; e) Ph_3P , *p*- $\text{MeOC}_6\text{H}_4\text{CHO}$, reflux; f) mCPBA, -78°C to r.t.; g) TsOH , MeOH ; h) PhMe , reflux; i) K_2CO_3 , MeOH , reflux; j) Sml_2 , THF .⁵³

2.2.2 The Zhao Group

The Zhao Group used intramolecular cycloaddition reactions of nitrones previously developed by Grigg and co-workers, as they are usually regio- and stereospecific.^{54, 55} Employing this method, they managed to produce a spirocyclic structure, and unlike the White group, with the alkene already situated within the macrocycle, the Zhao nitron was only connected to the alkene at one terminus.

They began their synthesis with sequential alkylation of 1,3-dithiane **92** to yield a dialkylated dithiane. Hydrolysis released the ketonic carbonyl, which was treated with hydroxylamine hydrochloride to afford oxime **93**. Upon heating with benzyl acrylate **94**, nitron intermediate **95** was formed, before cyclisation to **96**. Removal of the THP protecting group, followed by Swern oxidation and Wittig homologation gave the corresponding enonate **97**. Cleavage of the N-O bond yielded **98**, which upon heating cyclised intramolecularly to achieve the desired product **99** (scheme 14).^{38, 54}



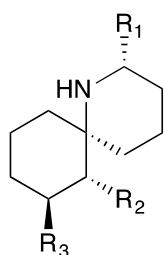
Scheme 14. Zhao's partial synthesis utilising nitron chemistry. a) $\text{Cl}(\text{CH}_2)_4\text{OTHP}$, BuLi, THF, 85%; b) $\text{CH}_3\text{CH}(\text{CH}_2)_3\text{I}$, BuLi, THF, HMPA, 87%; c) NCS, AgNO_3 , MeCN-water, 97%; d) $\text{H}_2\text{NOH}\cdot\text{HCl}$, AcONa, MeCN, 99%; e) benzyl acrylate **94**, xylene, 140°C , 92%; f) $\text{TsOH}\cdot\text{H}_2\text{O}$, MeOH 93%; g) Swern, 97%; h) $\text{PH}_3\text{PCHCO}_2\text{Me}$, CH_2Cl_2 , 93%; i) Zn, AcOH-water, 55°C , 94%; j) $o\text{-Cl}_2\text{C}_6\text{H}_4$, reflux, 84%.³⁸

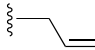

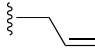
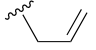
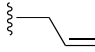

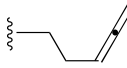
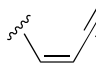
2.3 Synthetic Studies towards Histrionicotoxin

The histrionicotoxins (HTX) are a family of alkaloids, members of which were first isolated in 1971 by the Daly group.⁵⁶ Since that time, other members have been discovered, taking the HTX family to 15 plus derivatives.⁵⁷ **Table 1** shows the HTX core structure, with the HTX substrates shown in the first entry. The following entries the various combinations isolated. The review by Stockman shows a extensive research on the HTX derivatives.⁵⁷

Table 1. The histrionicotoxin family of alkaloids.

	R1	R2	R3
100			OH
101			OH
102			OH
103			OH
104			OH
105			OH
106			OH
107			OH
108			OH
109			OH
110			OH



111			OH
112			H
113			H
114			H

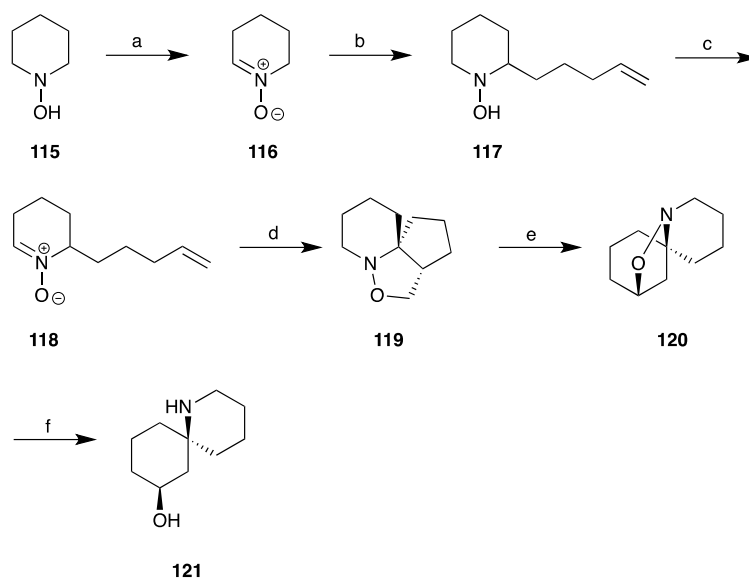
HTX can be isolated from the skin of Dendrobatidae, poisonous dart frogs, which have shown to store the poison, which is secreted onto the surface of the skin as a defence mechanism. Studies have shown that frogs raised in captivity they do not produce such alkaloids, indicating the source to be dietary.⁵⁸

HTX are of synthetic interest due to their biological activity and unique structure. They have shown to have various effects on both mammalian and amphibian nerve-muscle preparations by selectively binding to the acetylcholine receptors, which interrupt the transmission neuromuscular impulses.⁵⁹

There have been many synthetic approaches adopted in the total syntheses of HTX variants,⁵⁷ comprehensively reviewed by Stockman. This review will only look at those syntheses of relevance to the nitronone-based approach studied in this thesis.

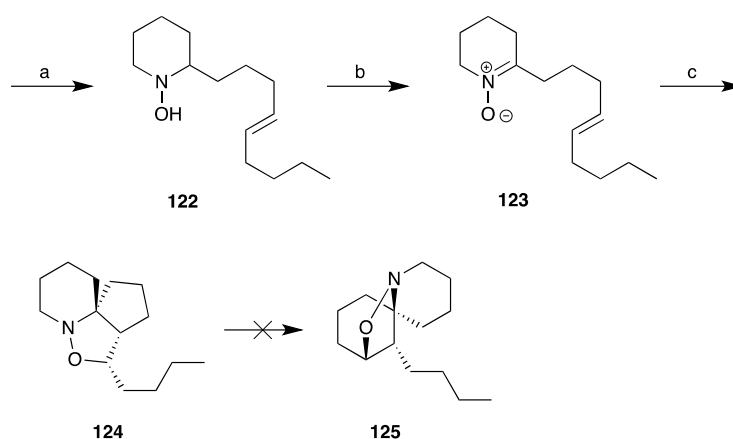
2.3.1 The Gossinger Group

In 1975, the Gossinger group reported their efforts towards HTX utilising nitron chemistry. They began with piperidinol **115**, which was synthesised from 1,5-dibromopentane in a double S_N2 cyclisation. Oxidation to nitron **116** was achieved using HgO , followed by a nucleophilic addition of 4-pentenylmagnesium bromide to **116**. Oxidation of **117** with HgO gave the nitron **118**, which in refluxing toluene underwent intramolecular 1,3-dipolar cyclisation to give the kinetic cyclo-adduct **119**. This was converted to the thermodynamic product **120**, by heating to $195^\circ C$ in a sealed tube. Raney nickel hydrogenation opened up the ring to yield HTX **121** (scheme 15).^{57, 60}



Scheme 15. Synthesis of HTX core structure by the Gossinger group. a) HgO , $CHCl_3$, $0^\circ C$ to r.t.; b) $BrMg(CH_2)_3CH=CH_2$, Et_2O , reflux; c) HgO , Et_2O , $0^\circ C$ to r.t.; d) toluene, reflux; e) toluene, $195^\circ C$; f) H_2 , Raney Ni, $EtOH$.

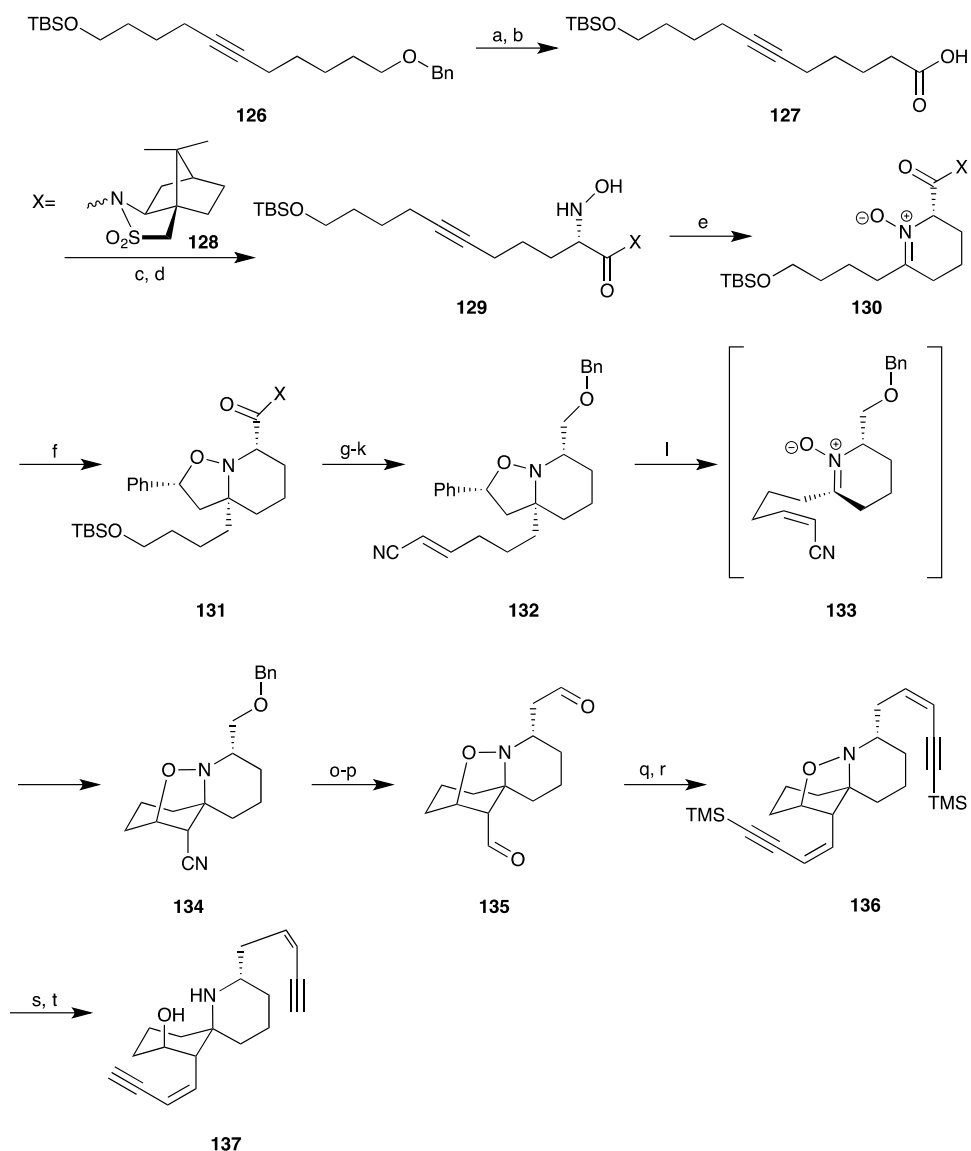
With **121** successfully synthesised, The Gossinger group then tried to produce a more substituted member of the HTX family using the same methodology, the nucleophilic addition was performed using non-4-enylmagnesium bromide to give **122**. Oxidation formed the corresponding nitron **123**, followed by the intramolecular cyclisation which resulted in a 6,5,5-kinetic adduct **124**, with a butyl chain. Unfortunately, this compound could not be converted to the desired thermodynamic product **125**, which maybe a result of the steric hindrance caused by the butyl chain.⁶⁰



Scheme 16. Synthetic efforts towards a HTX structure. a) $\text{BrMg}(\text{CH}_2)_3\text{CH}=\text{CH}(\text{CH}_2)_3\text{CH}_3$, Et_2O , reflux; b) HgO , Et_2O , 0°C to r.t.; c) toluene, sealed tube, reflux.

2.3.2 The Holmes Group

In 1999, the Holmes Group reported their route to an enantioselective total synthesis of (-)-HTX283A, also utilising the functionality of the nitron.⁶¹ They began their efforts with a known acetylenic diol **126**. Debenzylation allowed oxidation to the acid **127**, followed by the addition of (1*R*)-(+)-2,10-camphorsultam **128**, which was used as a chiral auxiliary to achieve the desired stereoselectivity. Installation of the hydroxylamine **129** was therefore achieved diastereoselectively. Intramolecular cyclisation between the hydroxylamine and the alkyne gave nitron **130**, which was swiftly followed by an intermolecular cyclisation with styrene to yield isoxazolidine **131** as a single regio- and stereoisomer. The chiral auxiliary was removed, followed by protecting group manipulation, oxidation of the hydroxyl group to an aldehyde and conversion to a nitrile **132**. Heating in a sealed vessel at 190°C, caused a retro-[3+2] cycloaddition, decomposition of the five membered heterocycle, releasing the styrene moiety, and forming a key nitron intermediate **133**, before intramolecular cyclisation to the thermodynamic tricyclic adduct **134**. With the ring structure to the HTX core now in place, the Holme's group converted the benzyl ester pendant to a nitrile, followed by reduction of both nitriles to bis-aldehyde **135**. The aldehyde groups were converted to enyne chains through a modified Stork-Wittig procedure, which involves an enamine alkylation before the installation of the alkyne. The final stages include the reductive ring opening and removal of the TMS groups to yield HTX **137**.^{57, 61}

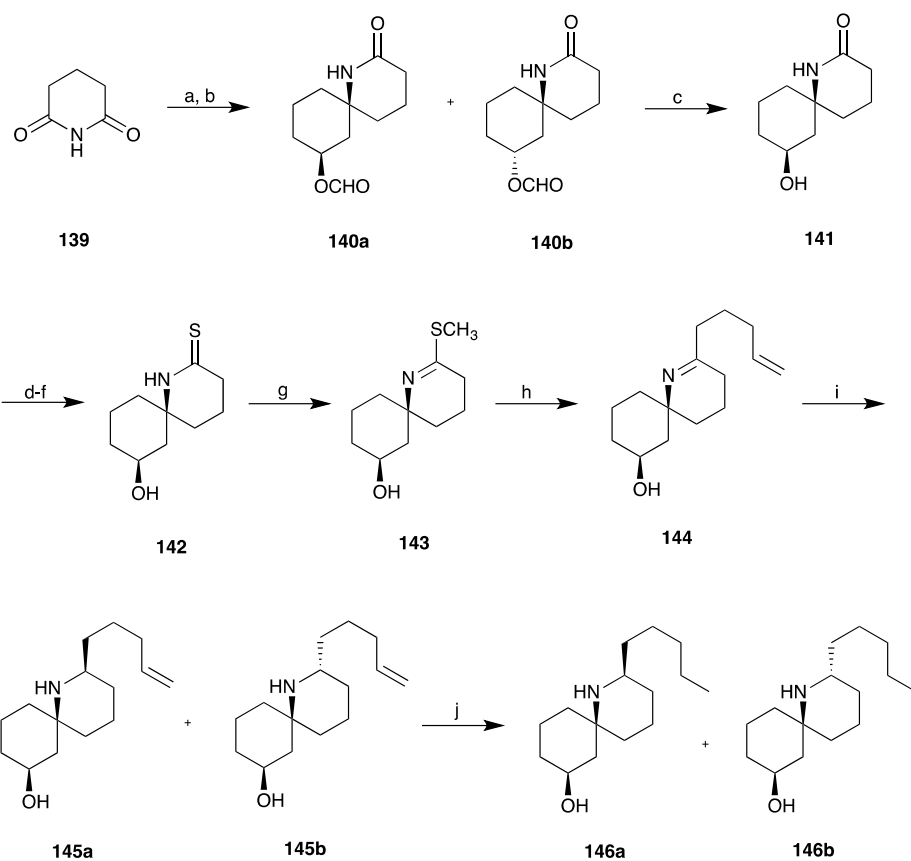


Scheme 17. Holme's enantioselective total synthesis of (-)-HTX283A. a) $\text{BCl}_3 \cdot \text{DMS}$, CH_2Cl_2 , 97%; b) Jones' reagent, acetone, 98%; c) NEt_3 , pivaloyl chloride, 0°C then (1*R*)-(+)-10,2-camphorsultam **128**, $n\text{-BuLi}$, THF, -78°C , 84%; d) $\text{NaN}(\text{TMS})_2$, 1-chloro-1-nitrosocyclohexane, THF, then HCl (aq), 70%; e) toluene, 80°C , 6 h; f) styrene, 75°C , 85% (2 steps); g) LiAlH_4 , THF, 0°C ; h) NaH , BnBr , THF 90% (2 steps); i) HF , CH_3CN , 91%; j) TPAP , NMO , 4 \AA sieves, 98%; k) $\text{Me}_3\text{SiCH}_2\text{CN}$, $n\text{-BuLi}$, THF, -78°C , $\text{B(O}^i\text{Pr)}_3$, 87% (E:Z 10:90 increasing to 8:92 with HMPA); l) toluene, sealed tube, 190°C , 3.5 h, 80%; m) $\text{BCl}_3 \cdot \text{DMS}$, CH_2Cl_2 , 99%; n) methanesulfonyl chloride, NEt_3 , DMAP , CH_2Cl_2 , 100%; o) NaCN , DMSO , 4 \AA sieves, 55°C , 85%; p) DIBAL-H , toluene,

-78°C, 100%; q) KN(TMS)₂, [Ph₃PCH₂I]⁺I⁻, THF, -78°C, 95%; r) Pd(PPh₃)₄, CuI, Et₂NH, MeSi-CCH, 92%; s) Zn, AcOH, 30 min, 98%; t) K₂CO₃, MeOH, 94%.

2.3.3 The Brossi Group

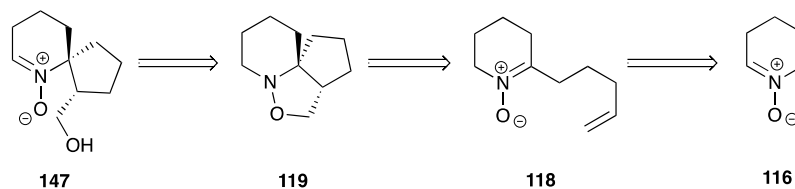
In 1985, the Brossi group reported an efficient route to a 6,6-spirocyclic core structure, through the use of lactams. While this approach does not utilise nitrene chemistry it is of some relevance to the work towards the HTX core structure described in this thesis, which focuses on C-2 functionalised analogues. The synthesis began with addition of pent-4-enylmagnesium bromide onto glutarimide **139**, providing a cyclic iminium species which underwent intramolecular cyclisation with the alkene portion of the introduced pentenyl side chain forming isomeric spirocyclic mixtures **140a**, **140b**, which could be separated, after many synthetic investigations the Brossi group found that after further reactions on **140a** and **140b** the diastereoisomers could no longer be separated, they therefore resorted back to **140a**. They first reduced the aldehyde to **141**, before functional group manipulation, firstly through a thiolactam **142**, to a methylthio group **143** to a ketimine **144**, which was reduced to give diastereoisomeric mixture **145a** and **145b**. Reduction of the terminal alkene yielded pentyl derivatives **146a** and **146b**.⁶²



Scheme 18. Bossi's route to a HTX derivative.⁶² a) $\text{CH}_2=\text{CH}(\text{CH}_2)_3\text{MgBr}$, THF, 40-60°C; b) HCOOH, 25°C; c) KOH/EtOH/H₂O; d) Ac₂O, PyH, 25°C; e) P₂S₅, benzene, reflux; f) MeONa, EtOH, reflux; g) MeI, CH₂Cl₂, 25°C; h) $\text{CH}_2=\text{CH}(\text{CH}_2)_3\text{MgBr}$, MgCl₂, CH₂Cl₂, reflux; i) NaBH₄, MeOH, -70°C; j) H₂, Pd/C, EtOH, 25°C.

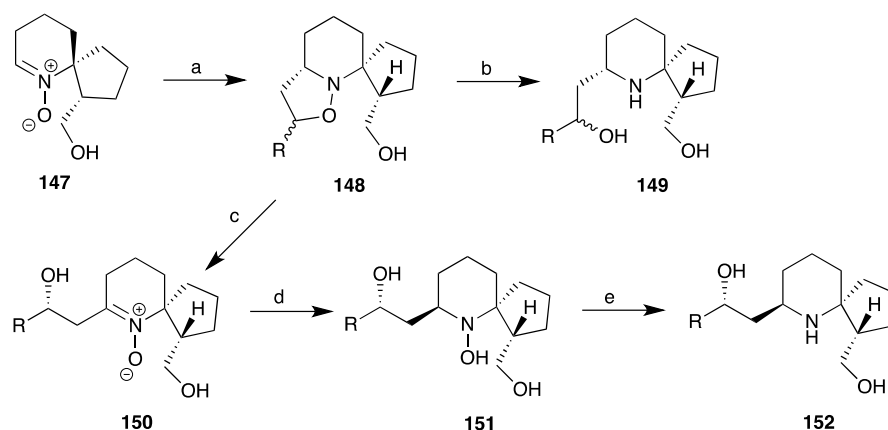
2.3 Previous Syntheses by the Caprio group

The Caprio group have concentrated their efforts on the core structure of both **1** and **2** utilising nitron chemistry. Based on the synthetic route of Gössinger *et al.* (Scheme 15),⁶⁰ who produced the tricyclic compound from piperidinol, a spironitron core structure was synthesised (Scheme 19). In this strategy spironitron **147** is retroanalysed back to tricyclic isoxazolidine **119**, which in turn is obtained by intramolecular cycloaddition of alkene tethered nitron **118**. The alkene tether is introduced by Grignard addition onto nitron **116**.



Scheme 19. Retrosynthetic analysis of spironitron **147**.

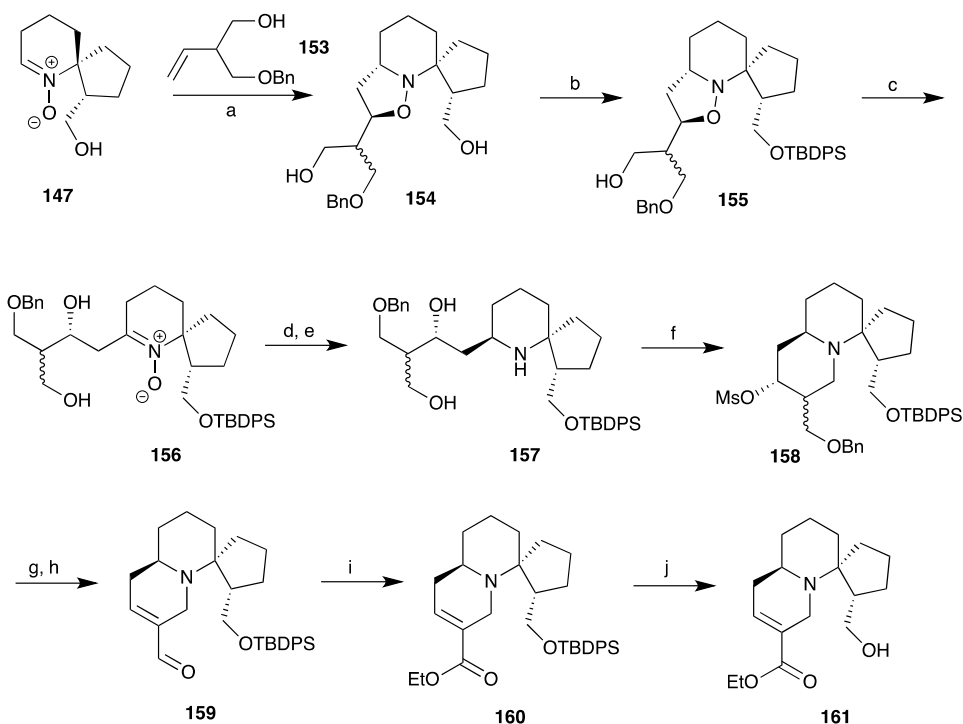
Using **147**, a study of 1,3-dipolar cycloadditions was performed, using both electron rich and electron deficient alkene substrates, which gave a range of isoxazolidines **148** as single stereoisomers. Reductive ring opening conditions were then optimised which produced a small range of spiro-amines **149**. As the undesired stereoisomer was achieved, the reduced adducts were transformed to the desired stereoisomers by an oxidation/reduction sequence **152** (Scheme 20).



Scheme 20. Caprio's 1,3-dipolar cycloaddition, reductive ring opening studies. a) **147**, dipolarophile, electron deficient dipolarophiles were heated, PhMe/ EtOH/CH₂Cl₂, 64-94%; b) Zinc dust, AcOH-water 1:1, reflux, 3 h, 76-81%; c) mCPBA, CH₂Cl₂, 0°C, 1 h, 85%; d) NaBH₄, MeOH, 0°C, 20 min, 90%; e) 20% TiCl₃(aq), H₂O, MeOH, r.t., 3 h, 92%.⁶³

Following the preliminary stereoisomeric and optimisation studies, they next constructed the core structures of both pinnaic acid and halichlorine. Synthesis of the halichlorine core began using the nitron intermediate **147**. 1,3-dipolar cycloaddition with dipolarophile **153**, gave **154** as an inseparable diastereomeric mixture. Selective silyl protection yielded **155**, before **156** was achieved through oxidative ring opening and reduction as previously optimised. Cyclisation with mesyl chloride gave a mixture of diastereoisomers **158**, which was followed by removal of the benzyl protecting group allowing oxidation to the corresponding aldehyde to proceed. Further oxidation and esterification gave **160**. Finally, removal of the silyl group gave the target core structure **161**

Scheme 21.



Scheme 21. Synthetic route towards a halichlorine core structure. a) **153**, PhMe, 210°C, MW, 2 h, 78%; b) TBDPSCI, DMAP, Et₃N, CH₂Cl₂, 0°C to r.t., 1 h, 93%; c) mCPBA, CH₂Cl₂, 0°C to r.t., 1 h, 93%; d) NaBH₄, MeOH, 0°C to r.t, 30 min, 89%; e) cat. In, Zn, EtOH-NH₄Cl_(aq) (2:1), reflux, 4 h, 100%; f) 2 equiv. MsCl, Et₃N, CH₂Cl₂, 0°C to reflux, 6 h, 99%; g) LiDDB, THF, 0°C to r.t., 89%; h) Dess-Martin periodinane, 0°C to r.t., 1 h, 80%; i) 1. NaClO₂, NaH₂PO₄, 2-methyl-2-butene, ^tBuOH, 0°C, 24 h, 74%; 2. DCC, EtOH, DMAP, CH₂Cl₂, 0°C to r.t., 24 h, 65%; j) TREAT•HF, Et₃N, MeCN, reflux, 4 h, 94%.

Chapter 3. Synthetic Studies

3.1 The History of Nitrones

Nitrones have the general formula of $X-CH=NO-Y$.⁶⁴ The unique functionality of nitrones makes them extraordinarily useful substrates and one of the most efficient multifunctional compounds, therefore making them the centre of extensive research into their actions as both radical spin traps and 1,3-dipoles.

The use of nitrones as radical spin traps was first reported in 1969, by Janzen and Gerlock. Spin traps are used to detect and identify short-lived free radicals by forming a more stable adduct which can be detected by electron paramagnetic resonance (EPR).⁶⁵ α -Phenyl *N*-tertiary-butyl nitrone (PBN, **162**) was used in Janzen and Gerlock's study, and is still one of the most popular radical spin traps, along side 5,5-dimethyl-1-pyrroline-*N*-oxide **163** (figure 3).

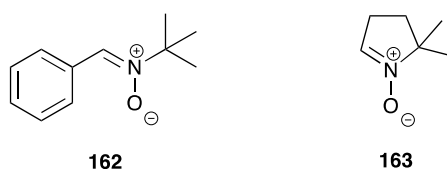


Figure 3. The structures of the most studied and widely used nitron spin traps.

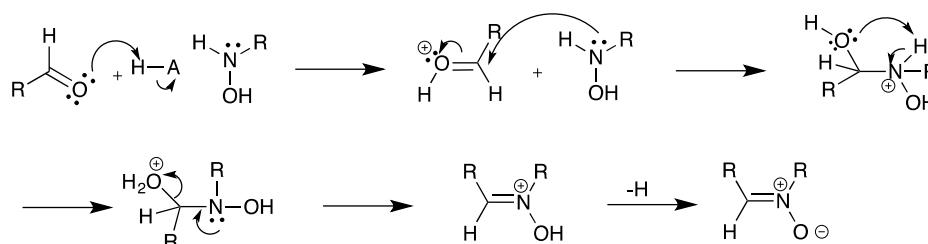
Early research implicated that nitrones were useful for trapping free radicals in chemical systems, which later led to their application as spin trap reagents in biochemical systems, consequently leading to the thought that they play an active role in anti-ageing.^{64, 66, 67} The free radical process in biological systems

has shown to be much more complex than originally conceived. By trapping the free radicals, oxidative damage to the brain is reduced, thus exhibiting neuro-protective activity.⁶⁸ PBN has shown to have general anti-inflammatory properties, with a PBN derivative making it to clinical trials as a potential protective drug for strokes.⁶⁹

3.2 Preparation of Nitrones

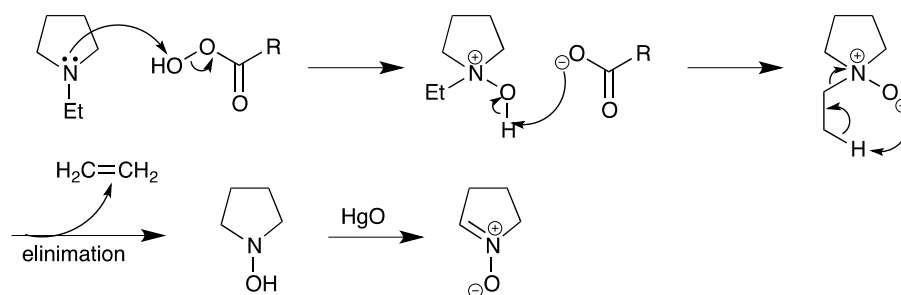
There are a number of methods employed in the synthesis of both acyclic and cyclic nitrones, with most reactions centring on the oxidation of imines, amines and hydroxylamines.

A common route to acyclic nitrones involves the condensation reaction of a hydroxylamine with an aldehyde or ketone, which forms a nitrone through an iminium ion intermediate (Scheme 22).⁷⁰ *N,N*-disubstituted hydroxylamines also form nitrones by utilising a wide range of reagents including metallic compounds and organic oxidants.



Scheme 22. The mechanism of action for a condensation reaction, forming a nitrone.

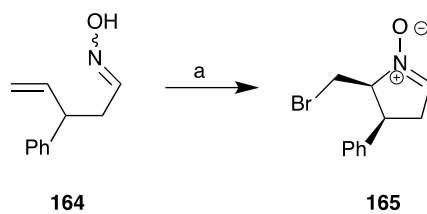
Acyclic and cyclic nitrones can be synthesised from simple tertiary amines. Oxidation and elimination forms a hydroxylamine, followed by further oxidation with oxidants such as mercuric oxide to produce the corresponding nitrone (Scheme 23).⁷⁰



Scheme 23. A mechanism for a common way to synthesise cyclic nitrones.

Indeed, there are a range of reagents useful in the oxidation of hydroxylamines or amines to nitrones. The former transformation can be achieved with mercuric oxide,⁶⁰ manganese dioxide,⁷¹ gold nanoparticles,⁷² triphenylbismuth carbonate,⁷³ sodium hypochlorite,⁷⁴ iodine, tert-butyl hydroperoxide, ceric ammonium nitrate,⁷⁵ hypervalent iodine compounds⁷⁶ and even by electrochemical oxidation.⁷⁷ A wide range of methods have been developed for the conversion of secondary amines to nitrones including alkyl hydroperoxide in the presence of titanium catalysts,⁷⁸ sodium tungstate/hydrogen peroxide,⁷⁹ oxone,⁸⁰ methyltrioxorhenium/hydrogen peroxide,⁸¹ urea-hydrogen peroxide complex,⁸² molecular oxygen in the presence of picryl hydrazide with tungsten oxide/alumina,⁸³ and trichloroacetonitrile/hydrogen peroxide.⁸⁴

There have been reported efforts in the synthesis of cyclic nitrones from alkylation of oximes and bromocyclisation of oximes for example **164-165**, although reported yields are low (scheme 24).⁸⁵



Scheme 24. A bromocyclisation to achieve a cyclic nitrone. a) Br₂, NaHCO₃, 0°C to r.t., 23%.⁸⁵

3.3 Reactions of Nitrones

The nitron structure consists of a four electron system, which is shared across three atoms, with two π electrons coming from the double bond and two coming from a lone pair off the oxygen. Although it is implied that the positive charge resides on the nitrogen, delocalisation between the nitron and α -carbon results in a 1,3 dipolar structure (figure 4).⁸⁶

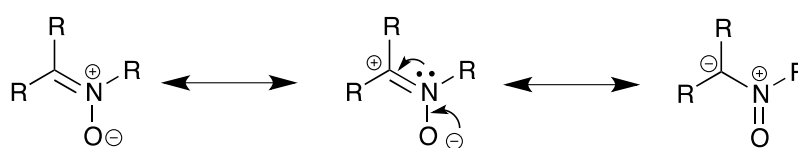


Figure 4. The delocalisation of electrons in the 1,3 dipole of a nitron.

Studies performed on the nitron models have reported some interesting properties. Of the nitron **166** and oxime **167** studied (Figure 4), the study showed that the nitron has a shorter N-O bond, 1.284Å, in comparison to 1.408Å of the oxime. It also exhibits a longer C=N bond length of 1.309Å versus the 1.260Å in the oxime.⁸⁶ This indicates partial double bond characteristics in the nitron and also supports the delocalisation theory show in figure 5.

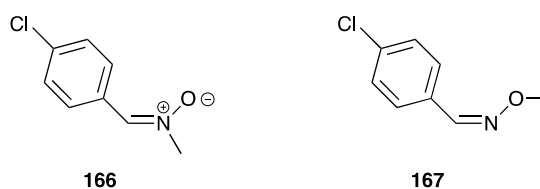


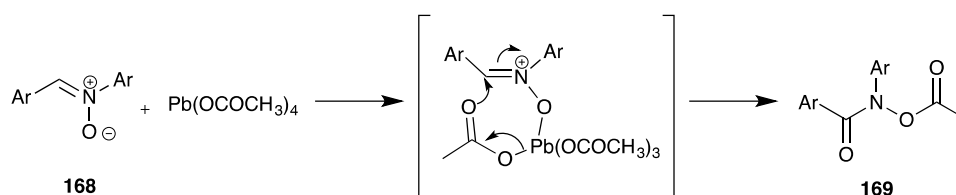
Figure 5. The nitron **166** and oxime **167** studied.⁸⁶

Since the discovery of the nitron, many research groups have investigated the capabilities of this functional group, some of which will be highlight below. For a more in depth review please refer to the review by Eli Breuer.⁸⁶

3.3.1 Oxidation of Nitrones

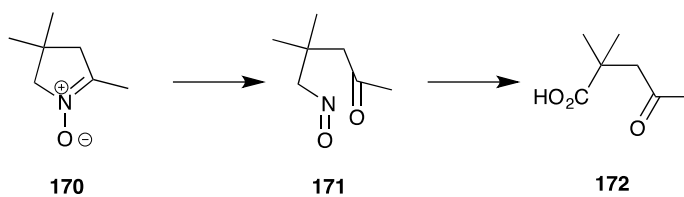
The influence of varying oxidising agents on nitrones has been examined. Oxidants such as lead tetraacetate (LTA); Iron (III) salts; periodates; ozone; and selenium dioxide are just a few which have been reported to successfully oxidise various acyclic and cyclic nitrones.

LTA has shown to oxidise nitrones with various groups attached including ketonitrones, arylaldonitrones and triphenyl nitron. The example below shows the formation of *N*-acetoxy-*N*-acylamine **169** from an arylaldonitron **168** through a pentacoordinated lead derivative intermediate Scheme 25.



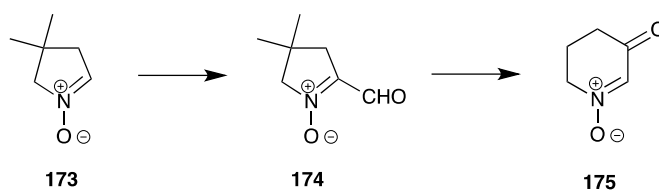
Scheme 25. Oxidation of an arylaldonitron using LTA.

Iron complexes such as ferric chloride and potassium ferricyanide have been reported as successful oxidising agents of aldo- and ketonitrones. The aldonitrones produced hydroxamic acids, whereas the ketonitrones such as **170** can be oxidised first to nitrosoketones **171** then to acids devoid of the nitrogen **172** Scheme 26.



Scheme 26. An example of oxidising a ketonitrone.

Selenium dioxide oxidises a methyl or methylene group to the α -position of the nitron. It has also been reported that oxidation of a pyrroline *N*-oxide **173** leads to a six membered ketonitrone **175** by rearrangement of the initially formed aldehyde **174** Scheme 27.⁸⁷

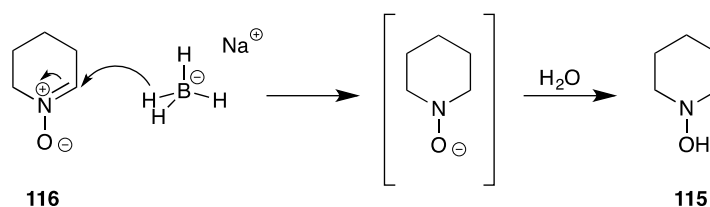


Scheme 27. Oxidation and rearrangement of a ketonitrone.

3.3.2 Reductions of Nitrones

Reduction of a nitron can either form an imine or a hydroxylamine, depending on the reducing agent used.

Hydride reducing agents such as sodium borohydride or lithium aluminium hydride reduce nitrones to the hydroxylamines as shown in scheme 28. The reaction proceeds by attack of a hydride at the electrophilic α -carbon, followed by hydrolysis. It has been reported that even under vigorous conditions, it doesn't reduce any further.

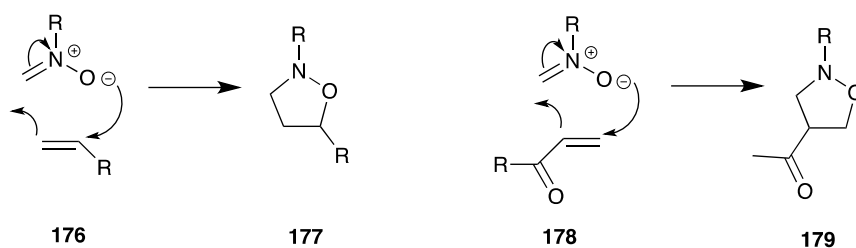


Scheme 28. Reduction using sodium borohydride to produce a hydroxylamine.

Zinc dust in acetic acid is just one of many methods employed to remove the oxygen. It occurs through a single electron transfer, and utilises fairly mild conditions, although this method is not compatible with acid-sensitive compounds.

3.3.3 The 1,3 Dipolar Cycloaddition

The four π -electron component of the nitron allows the formation of five membered rings through a single-step concerted cycloaddition reaction. The [4+2] cycloaddition occurs in the presence of a two-electron component, the dipolarophile, such as a simple alkene.



Scheme 29. The mechanism for the [4+2] cycloaddition.

The 1,3 dipolar cycloaddition can be described by frontier molecular orbitals (FMO) theory, and the orbital interactions can be classified into 3 different types depending on their relative FMO energies between the dipole and the dipolarophile. Type I focuses on an interaction between the $\text{HOMO}_{\text{dipole}}$ and $\text{LUMO}_{\text{alkene}}$, implying that an electron withdrawing group is present on the dipolarophile; in type II the dipole and alkene have similar FMO energies, which makes both interactions important; type III are controlled by interactions between the $\text{LUMO}_{\text{dipole}}$ and $\text{HOMO}_{\text{alkene}}$, which would be indicative of an electron donating group present on the dipolarophile.

The unique functionality of the nitrene means it is both electrophilic and nucleophilic, meaning both its HOMO and LUMO interactions are important, it is therefore characterised as a type II interaction (figure 6).

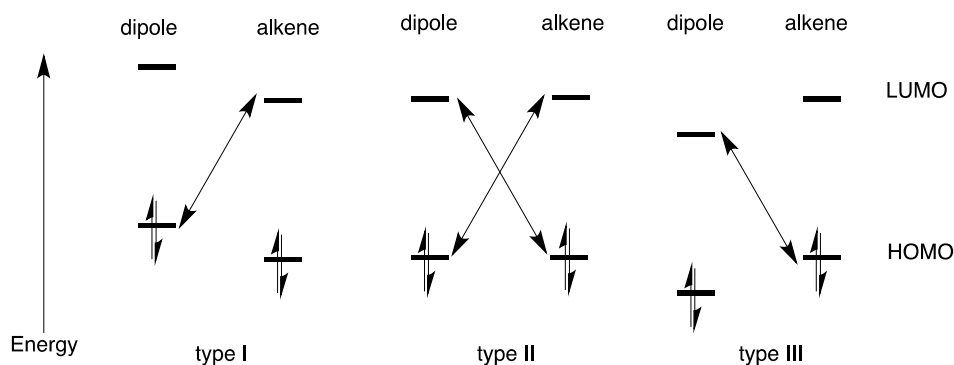


Figure 6. A frontier molecular orbital diagram showing the various types of HOMO-LUMO interaction in the 1,3-dipolar cycloaddition.

The FMO approach helps us to visualise the possible outcomes for the p-orbital interactions, and can also be useful in predicting the relative reactivity of dipole/dipolarophile pairs. Figure 7 shows the FMO for a typical 1,3 dipolar cycloaddition. It can be seen, following the explanation of the type II interaction, that both the $\text{HOMO}_{\text{dipole}} - \text{LUMO}_{\text{alkene}}$ and $\text{HOMO}_{\text{alkene}} - \text{LUMO}_{\text{dipole}}$ give rise to bonding overlap of orbitals and are thus symmetry allowed.

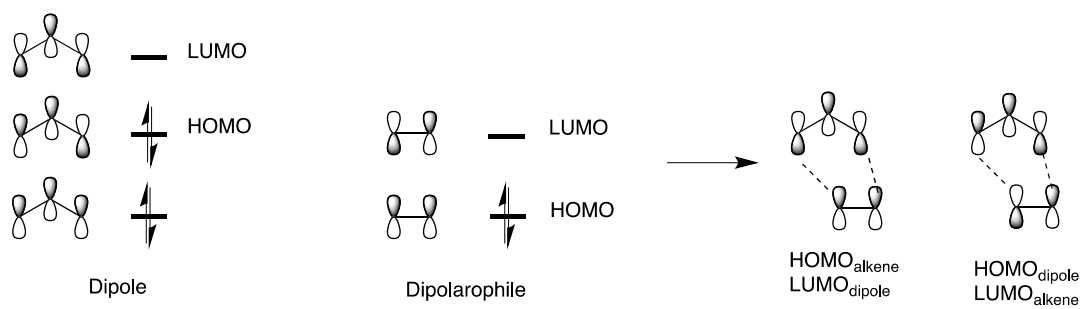


Figure 7. Shows the FMO for the dipole and dipolarophile, leading to two possible transition states, depending on the electronegativity of the dipolarophile.

3.3.3.1 Stereochemistry of the cycloaddition.

The stereochemistry of cycloadditions, including the Diels-Alder reaction and 1,3-dipolar cycloadditions can be readily predicted from a knowledge of the geometrical isomerism of diene/dipole and alkene partners which makes these reactions especially powerful in the preparation of products with multiple chiral centres.

A Diels Alder cycloaddition is stereospecific, meaning that the geometrical isomerism of substrates is “locked” into the relative stereochemistry of the products. For instance, reaction of the diene and ethene below gives rise to one of two products:

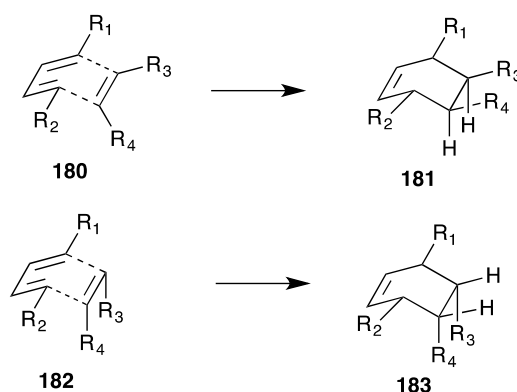


Figure 8. Showing the differences in the endo and exo reaction, which illustrates why the exo product is favoured.

The *cis*-relationship between R₃ and R₄ arises from the *cis*-stereochemistry of the dienophile substrate. Similarly, the relative stereochemistry between R₁ and R₂ is predetermined by the stereochemistry of the diene. The relative stereochemistry between R₁/R₂ and R₃/R₄ can also be predicted by the

favourability of an *endo* over and *exo* transition state in this reaction. In an *endo* approach (the R3/R4 approach), from “underneath” the diene, the approach is favoured by secondary π -orbital interactions between R3/R4 and π -orbitals of the diene (figure 9).

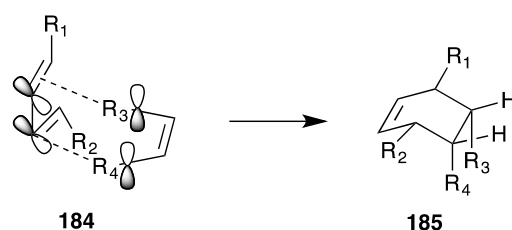


Figure 9. A representation of an *endo* orbital interaction in a Diels Alder cycloaddition.

The alternate, *exo*-approach is favoured by a reduction in steric effects seen in the *endo*-mode of approach but the secondary orbital effect dominates in the Diels-Alder process.

The 1,3 dipolar cycloaddition is also stereoselective. Specifically with the nitronone as the dipolarophile, which contains no secondary π orbitals for stabilisation, *exo*-products predominate. However, the stereochemistry of the dipolarophile is retained on conversion to products as in the Diels-Alder reaction (figure 10).

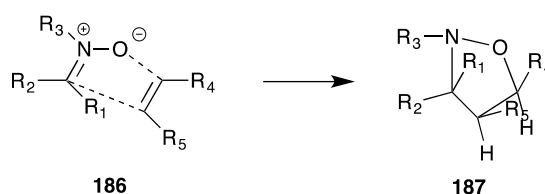
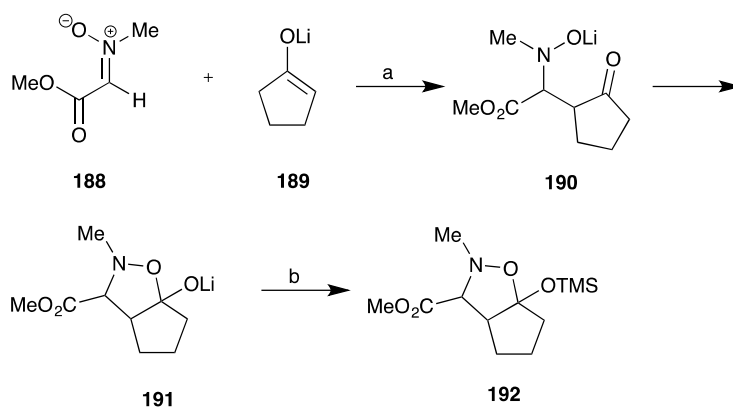


Figure 10. The stereoselective bond formation in a 1,3 dipolar cycloaddition.

3.3.4 Nucleophilic Addition to Nitrones

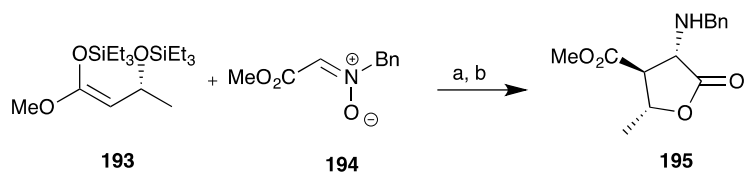
Nitrones react readily with nucleophiles to give N,N-disubstituted hydroxylamines. A wide variety of nucleophilic reagents have shown to add successfully to a number of nitron structures, including Grignard reagents; metalated oximes; sulfones; pyrroles; silylketene acetals etc, although organometallic additions are the most widely reported.⁸⁸

The addition to nitron **188**, impressively, also proceeds with enolates **189**, although in this case it is common for the hydroxylamine product **190**, to undergo a spontaneous intramolecular cyclisation resulting in a substituted isoxazolidine **191** (scheme 30).⁸⁹



Scheme 30. Shows the nucleophilic addition of a lithium enolate, before the spontaneous intramolecular cyclisation. a) THF, -78°C (10 min) then -40°C; b) TMSCl, TEA, -40°C, 19% over two steps.⁸⁹

Stereocontrolled reactions can be achieved using chiral additives, this had also been explored with regards to addition to nitrones. Using silylketene acetal **193**, a stereochemically pure pentonalide **195** was achieved.^{88, 90}



Scheme 31. Shows the stereocontrolled addition of a chiral nucleophile.⁹⁰ a) ZnI₂ (cat.), CH₂Cl₂, -70°C, 0.5 h b) Zn, AcOH, 60°C, 0.5 h.

3.4 Project Aim's

The ultimate aim of the project was to synthesise a biologically active derivative of halichlorine, based on pinnaic acid and halichlorine's shared 6-azaspiro[4.5]decane core. In order to achieve this goal, it was planned to exploit nitron chemistry, using a key nitron intermediate previously designed by the Caprio group, and apply novel synthetic methodology to produce a library of compounds. Biological assays will be performed on each derivative to determine if they exhibit any biological activity.

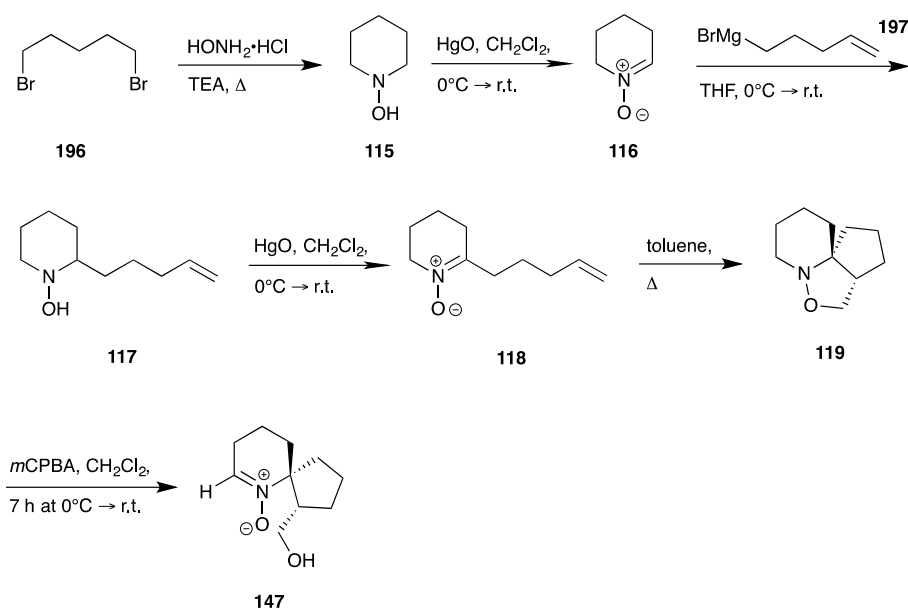
Due to the complexity of halichlorine, it is a challenge to produce quantitative amounts for pharmacological evaluation. Therefore, it is hoped that the more simple derivatives, which are far more accessible will possess some of the biological properties of its parent compound.

The results of these biological screenings may provide an insight as to which functional groups are involved in the bio-interaction, which would allow for a more specific library of derivatives to be produced in the future.

Chapter 4 Additions to [6,5,5]-Spirotrione

4.1 Synthesis of the Spirotrione

To begin this project, quantities of the spirotrione **147** were produced. The synthetic route utilised studies by the Gossinger group (Section 2.3.1),⁶⁰ to prepare tricyclic **119**. An oxidative ring opening of this isoxazolidine, previously developed by the Caprio group, then provides spirotrione **147**, (scheme 32).



Scheme 32. The synthetic route used to produce quantities of the spirotrione **147**.

The route to tricyclic isoxazolidine **119** proceeds from tetrahydropyridine *N*-oxide **116**. Thus, addition of a pentenyl fragment followed by oxidation to nitronium **118** is followed by an intramolecular 1,3-dipolar cycloaddition provides **119** as a single diastereomer with the desired relative stereochemistry for the synthesis of halichlorine/pinnaic acid.

Once produced, the Caprio group functionalised spironitrone **147**, via 1,3 dipolar cycloadditions, with success, though in no systematic manner, as discussed in section 2.3.

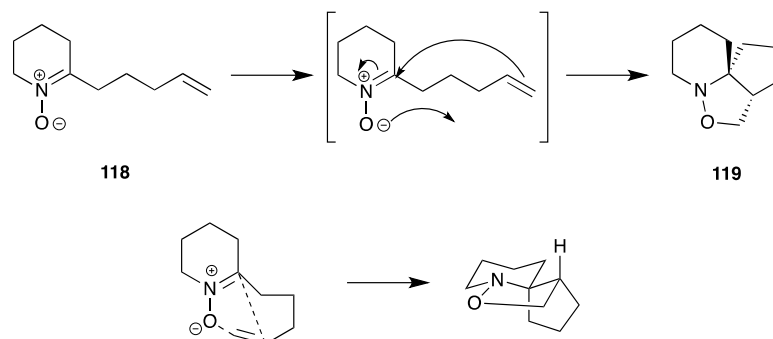
This current project aimed to bio-evaluate a range of easily accessible spirocyclic scaffolds, based on the structures of pinnaic acid and halichlorine. To date, only a very limited study into the addition of Grignard reagents to **147** have been examined, thus we decided to focus our studies in this area to generate a wide range of simple spirocyclic analogues using Grignard reagents. It was planned to add a range of ever bulkier alkyl Grignard species from methyl to hexylmagnesium bromide and including phenyl, benzyl, pentenyl and allyl derivatives.

The synthesis of nitrogen **147** began with a double S_N2 on dibromide **196** using hydroxylamine hydrochloride, which neatly cyclised to **115** obtained as a clear oil after column chromatography, which solidified upon cooling. Oxidation of **115** followed, using mercuric oxide in CH_2Cl_2 . This reaction was monitored by TLC until all the starting material shifted to the baseline in ethyl acetate:methanol (9.5:0.5), indicating oxidation to a much more polar species. After filtration and concentration, the nitrone was taken further without purification, owing to the known instability of this compound. Using freshly prepared pentenylmagnesium bromide under inert conditions, which was added via cannula to a cooled solution of **116** in THF provided pentenyl adduct **117**. To maximise product yield it was found important to quench the reaction with a small amount of aqueous ammonium chloride and remove the THF prior

to further work-up. Analysis of the $^1\text{H-NMR}$ spectrum of product clearly confirmed formation of the desired product by the absence of an α -proton at approximately 7.3 ppm present in a nitron and two peaks at 4.8-4.9 and 5.7-5.8 ppm assigned to the alkene functional group of the pentenyl chain.

Purified **117** then underwent the same oxidation conditions to a second nitron **118**, which was also used crude. In this oxidation, two nitrones can be produced but the desired, more substituted target predominates. This is again taken through without purification owing to instability issues.

Formation of **119** proceeds through an intramolecular 1,3 dipolar cycloaddition, which was achieved by heating under reflux in toluene, yielding a kinetic [6,5,5] cyclo-adduct product (scheme 33).

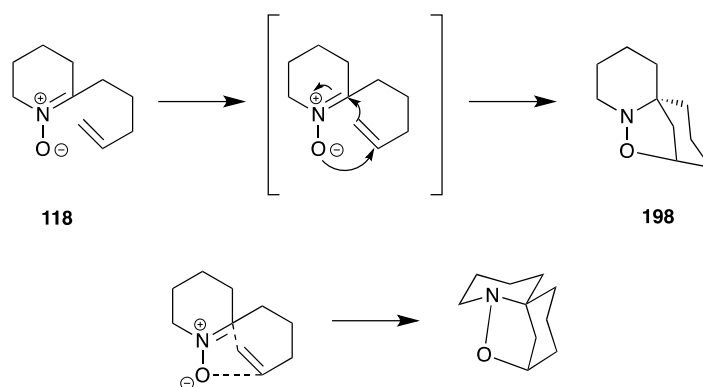


Scheme 33. Mechanism of action for the formation of the kinetic [6,5,5] cyclo-adduct **119**.

Analysis of the $^1\text{H-NMR}$ spectrum clearly shows no peak for the α -proton, as well as the loss of the two alkene peaks. The peaks furthest downfield belong

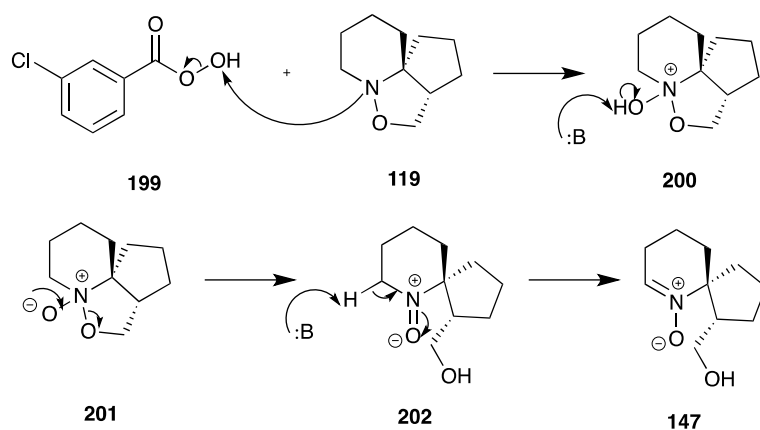
to α -protons to the oxygen, at 4.2 and 3.4 ppm, indicating the desired product was formed.

The thermodynamic [6,6,5] cyclo-adduct can be formed by applying more heat and increased pressure. We have developed a convenient procedure for this transformation using a microwave reactor. This strategy provides a basis for the synthesis of the core structure of histrionicotoxin and will form the basis of discussion in chapter 5.



Scheme 34. Thermodynamic product in the 1,3 dipolar cycloaddition of **118**.

The final step towards spironitrone **147** involved a challenging oxidative cleavage of the weak N-O bond using *meta*-chloroperbenzoic acid (*m*CPBA) **199**. Nucleophilic attack of the hydroxyl group on *m*CPBA occurs to give *N*-hydroxy derivative. Removal of a proton followed by opening of the isoxazolidine ring allows the formation of a nitrosonium species. Deprotonation then forms the nitrone functionality in **147**.



Scheme 35. Mechanism for the oxidative ring opening of **119**.

The reaction is very sensitive to the rate of addition of oxidant and reaction concentration. If this rate is too high then a number of other, possibly partially oxidised products are formed. Thus, success was only achieved using a 7 hour drop-wise addition of oxidant as a solution in dichloromethane at 0°C and the procedure was thus only successful, and reproducible, on a large scale (above 3g) when such a rate of addition can be easily maintained to low concentration of tricycle **119**. The spironitrone, however, is stable to column chromatography, presumably owing to its bulk, and was purified using CH₂Cl₂:methanol (9.5:0.5) as the eluent without much difficulty.

From the ¹H-NMR spectrum it was easily determined that the nitron was present due to a triplet pertaining to α-proton 7. The protons on '1, adjacent to the oxygen, have also shifted together to form a multiplet at 3.6 ppm integrating to two protons, whereas in isoxazolidine **119** they are split, and appear as a triplet and a multiplet at 4.2 and 3.4 ppm respectively.

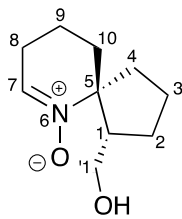
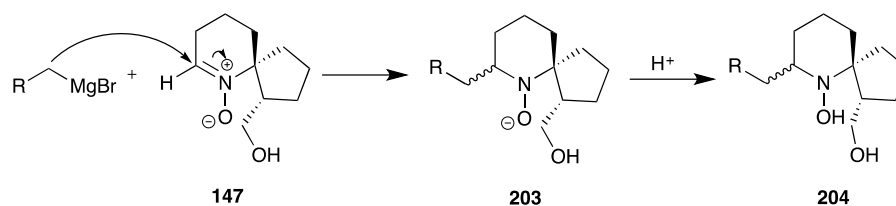


Figure 11. Spiroitrone **147**.

4.2 Nucleophilic Additions to the Spironitrone

Whilst challenging, the oxidation of **119** to **147** could be routinely performed on a 3-4g scale, and indeed performs better on a large scale. With quantities of the spironitrone in hand, the next step was the addition of the Grignard species to create a library of spirocyclic analogues. Some of the Grignard reagents were commercially available, and the rest were prepared freshly when required. The reaction conditions remained the same throughout, irrespective of the Grignard species employed, using inert conditions and addition at 0°C, with the only difference being a change in solvent (either diethyl ether or THF) when solubility of the resulting magnesium alkoxide salt initially transferred became an issue (scheme 36).



Scheme 36. The mechanism of action for the nucleophilic additions to spironitrone **147**.

Upon addition of the Grignard reagent, ($\text{RMgBr} = \text{Me, Et, Pr, Pentyl, Ph, Bn}$) analysis using thin layer chromatography of the reaction mixture quenched with saturated aqueous NH_4Cl , displayed new bright permanganate-active product spots, with an R_F much higher than the R_F of the nitronitrone, which indicated conversion of a nitronitrone to a less polar hydroxylamine. Unfortunately, upon

purification by flash column chromatography, separation of these spots proved challenging. This is possibly due to the presence of adduct diastereoisomers eluting directly after one another, although only single diastereoisomers have been isolated in these studies. In order to resolve this issue, the substituted hydroxylamines were instead reduced without isolation. Purification of these compounds by column chromatography was significantly easier than the free amine using CH₂Cl₂: methanol (9:1) as the eluent, and only one spot was evident on TLC.

NMR studies were then carried out on each of the substrates to confirm the desired product had been formed, and to determine stereochemistry. Analysis of the methyl-adduct **205** displayed the characteristic peaks you would expect to find on a ¹H-NMR of these adducts. For instance, the spectrum of the methyl adduct displayed a doublet at 1.2 ppm integrating for three protons indicative of a methyl group to the desired position on the spirocyclic ring. Additionally a proton, α-to the nitrogen atom was observed to resonate at 3.42-3.5 ppm, as well as the protons on C'1 split at 3.5-3.6 ppm and 3.7-3.8 ppm, (figure 12).

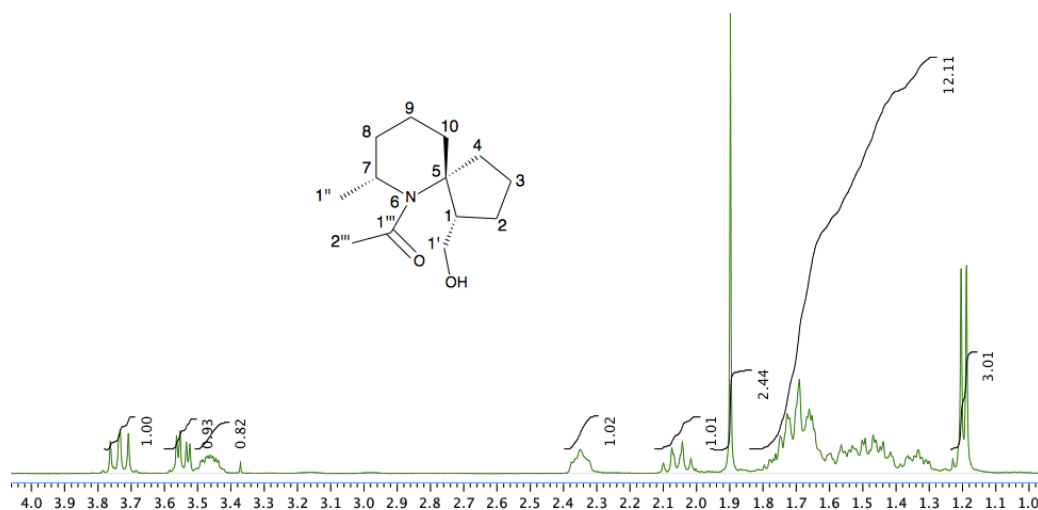


Figure 12. $^1\text{H-NMR}$ of the *N*-acetylated methyl adduct **205**.

The spectra of other alkylated products ($\text{R} = \text{Et}, \text{Pr}$ etc) all displayed a characteristic triplet at 0.8-0.9 ppm, indicating incorporation of an alkyl chain.

Intriguingly, on closer inspection of all NMR spectra of these adducts, a singlet, integrating for three protons, was observed at 1.9 ppm. This peak was not always easily discernable as it often appeared overlaid onto the envelope of hydrocarbon-like proton resonances between 1.1 and 2.0 ppm. This observation led us to postulate that *N*-acetylation has occurred *in-situ* – a theory that was backed up by high resolution mass spectral analysis of each adduct- to provide a range of *N*-protected substrates (figure 13).

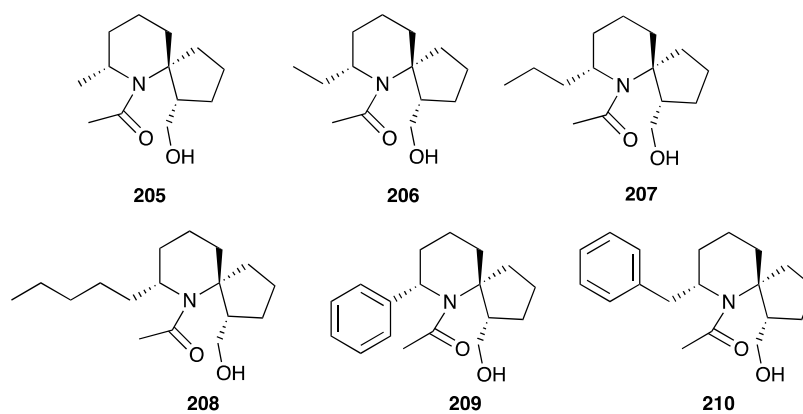


Figure 13. Structures of N-acetylated reduced compounds **205-210**.

Although unexpected and not the desired derivatives of choice, these six compounds may still be of biological interest. The additional N-acetyl group, may merely act as a prodrug, by aiding with the administration/solubility of the compound, as well as potentially reducing drug toxicity, or facilitate in delivering the drug to a specific area. These compounds were also far easier to purify, making them more manageable to reproduce.

4.2.1 Stereochemistry of the acetylated cycloadducts

The relative stereochemistry of addition was determined by analysis of the 2D-NOESY spectra obtained for each adduct. The adduct can adopt either of two conformers with the newly introduced R-group in an axial or equatorial position. Examination of the structure of each possible conformer, arising from attack of a Grignard reagent on the opposite face as the hydroxymethyl group (**a**, **a'**) (figure 14), indicates that equatorial oriented conformer (**a**) is most likely lower in energy owing to steric hindrance likely to occur in conformer (**a'**) between the alkyl chain and protons on C4. Introduction of the R-group on the same side as the hydroxymethyl group gives rise to two additional conformers (**b**, **b'**). Here, **b'** is most likely lower in energy due to steric hindrance between R/ CH₂OH in conformer **b**.

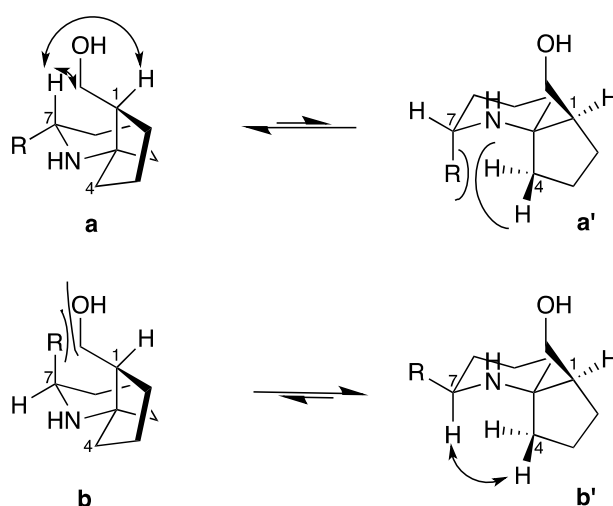
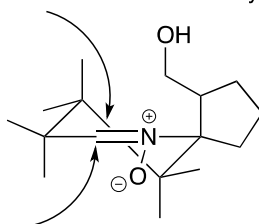


Figure 14. Possible conformers generated from a nucleophilic addition of a Grignard species to nitron **147**.

Comparison of the two preferred conformers above indicates that observation of NOESY cross peaks between the proton α -to the nitrogen at C7 and the hydroxymethyl protons (C'1), indicates attack from the opposite face the hydroxymethyl moiety, while cross peaks between protons on C4 and C7 indicate attack on the same face as the hydroxymethyl (figure 15).

attack from the same face as the hydroxymethyl group

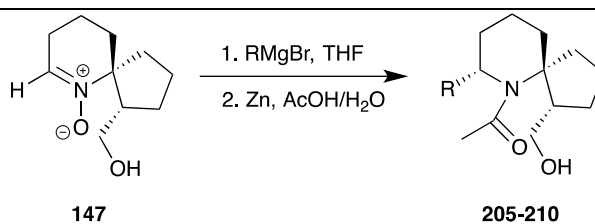


attack from the opposite face

Figure 15. The different sides of attack leading to conformers a, a'; and b, b'.

Analysis of the NOESY spectra of N-acetylated methyl adduct **205** clearly indicated a correlation between H7 and H1 strongly suggesting the formation of conformer a. This coincides with the stereochemistry gained from previous work published by the Caprio group throughout the series of cycloadditions.⁶³

Table 2. Reductions of the spirocyclic adducts with zinc powder, with the addition of an acetate group.



Entry	R group	Acetate adducts	Yield (%) ¹
1	Methyl	205	44
2	Ethyl	206	38
3	Propyl	207	47
4	Pentyl	208	40
5	Benzyl	209	61
6	Phenyl	210	42

¹Yield over 3 steps.

4.3 Indium-Mediated Reductive Method

In order to resolve the issue of the addition of an acetate during reduction of hydroxylamines yielded via Grignard addition to nitrene **147**, an alternative reductive method was proposed. Indium powder as the reductant was chosen as literature shows this reagent conveniently reducing hydroxylamines to amines under mild conditions.^{63 91}

Following the method developed by the Goti group,⁹¹ a convenient nucleophilic addition of the Grignard species, followed by an indium-mediated reduction in a one pot process was carried out. Under inert conditions, the Grignard species were added via syringe to the cooled solution of either diethyl ether or THF. Again, a range of alkyl, aryl and alkenyl Grignard reagents were examined. After warming to room temperature and allowing to stir for 12 hours, the reaction mixture was quenched with saturated aqueous NH₄Cl: ethanol (1:2) and stoichiometric amounts of indium powder, this was heated under reflux for 5 hours. Upon completion quantities of saturated aqueous NH₄Cl were added before extraction with diethyl ether. The reduced products formed very streaky spots on TLC, owing to the formation of a free amine. Nevertheless, the compounds were purified by flash column chromatography using CH₂Cl₂: methanol (9:1) as the eluent. The adducts were difficult to fully purify, probably due to how much they streaked down the column, but a range of adducts that was aimed for was achieved, (figure 16). With these results in hand, NMR spectral analysis was conducted to confirm structure and stereochemistry.

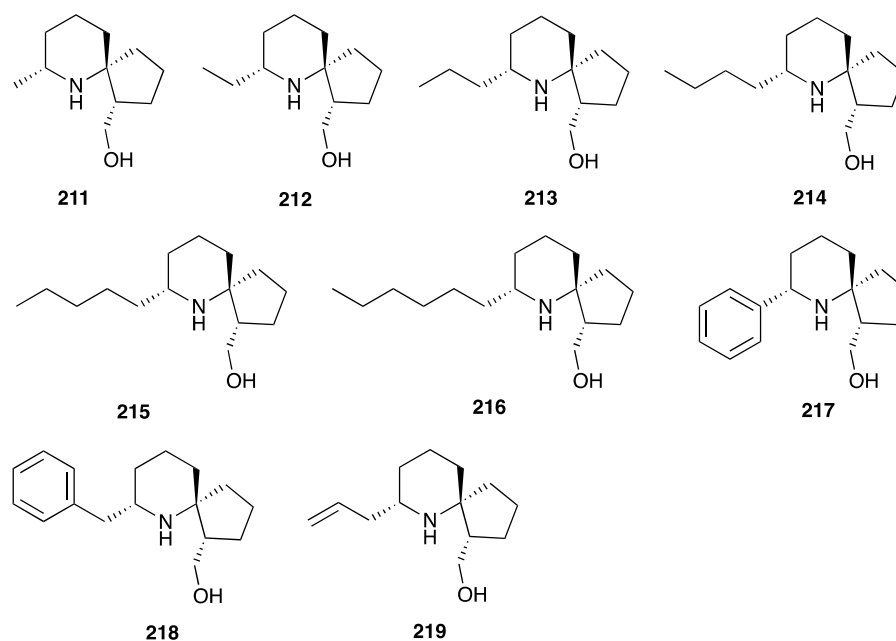


Figure 16. Spirocyclic amines synthesised via Grignard addition/ indium reduction one pot method.

As per the previous adducts, formed via Grignard addition using Zn/AcOH methodology. NMR spectra readily confirmed the formation of the desired adducts. A doublet at 1.4 ppm, revealed addition of a methyl group to give adduct **211** while the presence of easily discernable triplets at 0.85 ppm indicated addition of increasingly sizeable alkyl chains to yield adducts **212-216**. The presence of absorbance's in the aromatic region between 7.2 and 7.4 ppm confirmed the addition of phenyl rings to give **217/218** while two peaks in the NMR spectrum of compound **219** at 5.0 and 5.7 ppm confirmed addition of an allyl moiety.

The use of NOESY spectra to determine relative stereochemistry here was complicated as the important proton resonances for C7/C1/C1' often overlapped. In contrast to the N-acetyl adducts the two hydroxymethyl protons

at C1' split into two signals at around 3.5 and 4.0 ppm with the later overlapping with the C7 proton resonance, which also signals at 3.5 ppm (figure 17a). Thus NOESY cross peaks between either C7/C1 or C1'/C1 (both resonating at 3.5 ppm/ 2.45 ppm) could not be unambiguously identified.

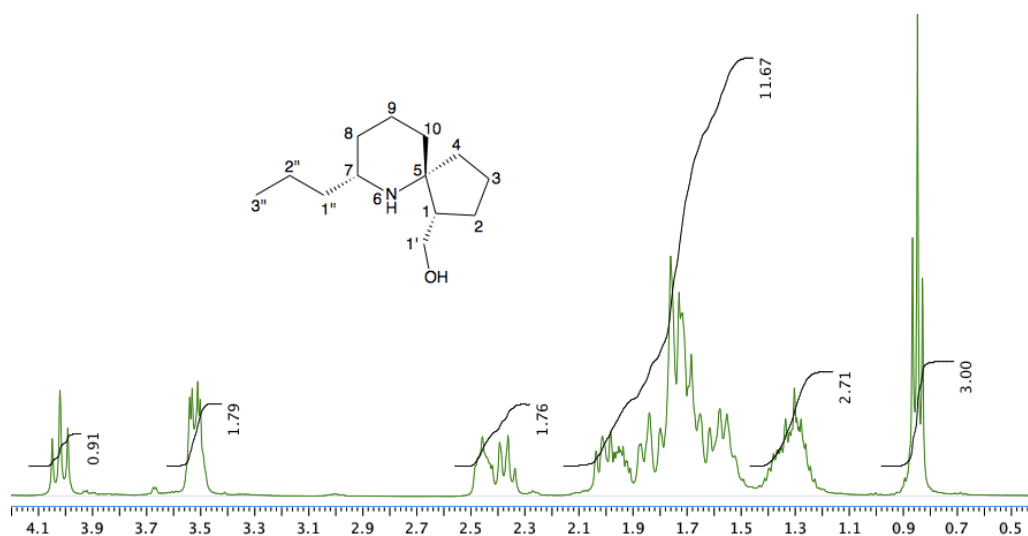


Figure 17a. ¹H-NMR spectrum of the propyl adduct **213**.

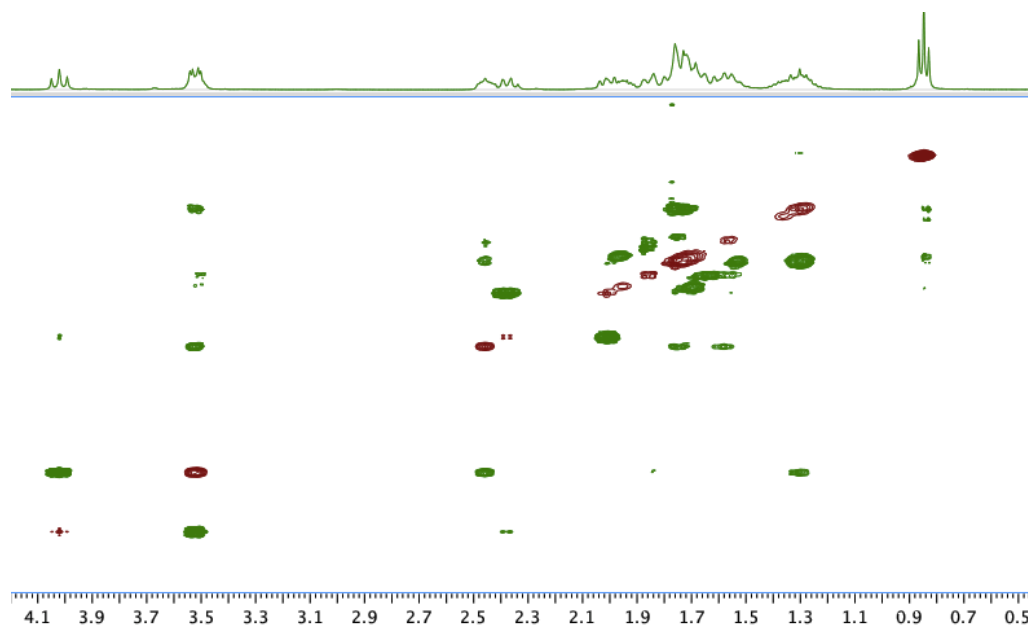
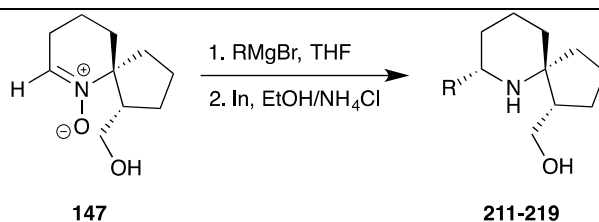


Figure 17b. NOESY spectrum of the propyl adduct **213**, showing the cross peaks for overlapping peaks C1'/C7.

Taking into consideration the stereochemistry of compounds of a similar structure, where the orientation of the R-group on C7 prefers attaching on the opposite face to the hydroxymethyl group, it is logical to assume that these have adopted the same orientation.

Table 3. Grignard addition/ indium reduction onto nitron **147**.



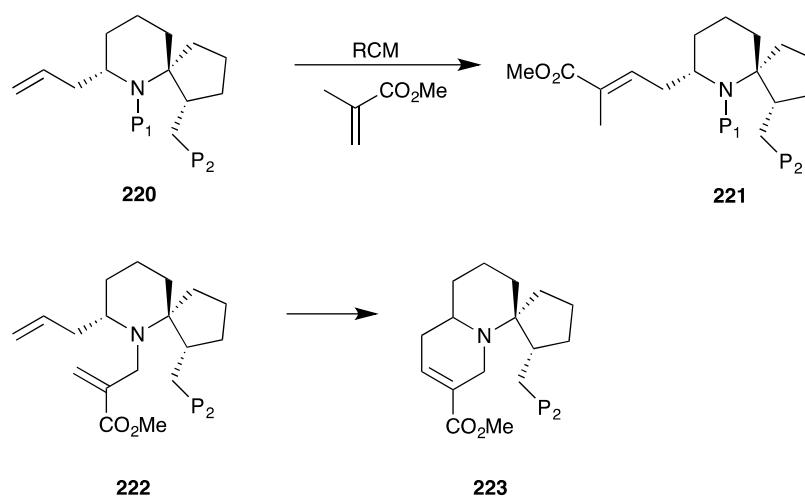
Entry	R group	Cycloadducts	Yield ¹ (%)
1	Methyl	211	42
2	Ethyl	212	27 ²
3	Propyl	213	29
4	Butyl	214	43
5	Pentyl	215	44
6	Hexyl	216	34
7	Benzyl	217	32
8	Phenyl	218	67
9	Allyl	219	55 ³

¹Yield over 2 steps; ²NMR contained impurities; ³ Mixture of diastereoisomers.

The results of the additions are summarised in Table 3. In general yields are slightly lower than those obtained for addition/reduction/acetylation probably owing to the difficulty in purifying these polar amines. However, it should be borne in mind that three transformations are achieved in one pot and all products are obtained as single diastereomers with three chiral centres. Furthermore, sufficient quantities were obtained for some detailed biological evaluations described in chapter 7.

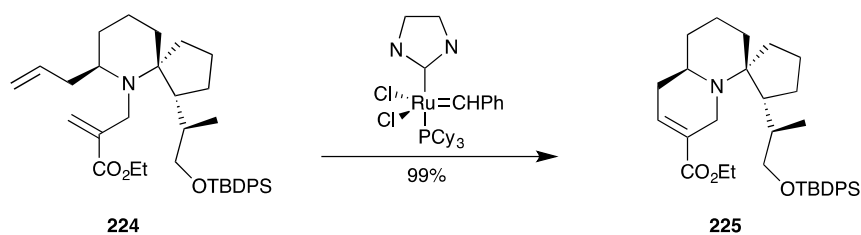
4.4 Further studies into the allyl-adduct

The allyl adduct **220**, with its useful terminal alkene group, potentially provides access to a host of useful analogues. In particular, analogues closely matching the core structure of pinnaic acid/halichlorine could be accessed by RCM of compounds **221** and **222**, readily derived from this compound.



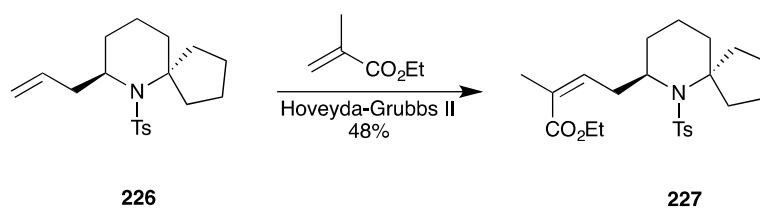
Scheme 37. Proposed synthesis of the Pinnaic acid core structure from allyl adduct **220**.

Indeed, a similar strategy has been previously adopted to access these core structures. For instance, diene **224** underwent RCM to provide tricycle **225** in near quantitative yield.⁹²



Scheme 38. RCM-based synthesis of the Halichlorine core structure.⁹³

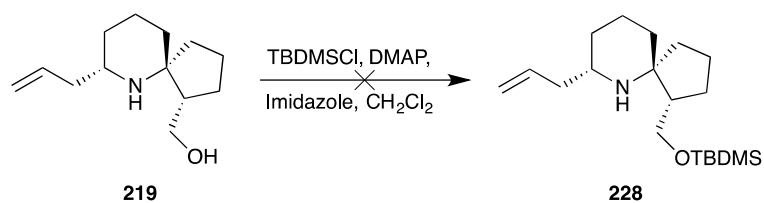
Additionally, the core of pinnaic acid **227** was accessed by cross metathesis of *N*-protected, allylated spirocycle **226**.⁹⁴



Scheme 39. RCM-based synthesis of the Pinnaic acid core structure.⁹³

Unfortunately, while all other Grignard adducts were isolated as single diastereomers, the allyl adduct was obtained as a diastereomeric mixture which could not be separated on column chromatography. These were separated as the *N*-hydroxy derivatives obtained by omitting the reduction step after addition of the Grignard reagent. This was achieved albeit with great difficulty, as the spots sat directly above one another, (RF values of 0.67 and

0.73. A single diastereomer was obtained cleanly in 3% yield. NOESY studies indicated that this exhibited undesired relative stereochemistry arising from addition of the allyl group from the “bottom” face as seen during addition of other Grignard reagents. Unfortunately, the other diastereomer could not be obtained cleanly. It was attempted to protect this compound as a silyl ether **228**, as a prelude to functionalising towards the pinnaic acid/halichlorine core as outlined above. Unfortunately, this proved unsuccessful, with analysis of ^1H and ^{13}C NMR spectra exhibiting evidence of the protecting group, but additional peaks were also present. Accurate mass of this sample did not detect the desired mass.



Scheme 40. Studies into protection of the hydroxyl group.

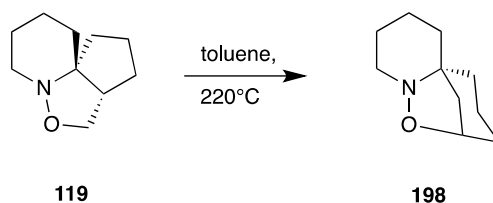
Chapter 5 Additions to 6,6-Spironitrone

This chapter focuses on investigations into the synthesis of the histrionicotoxin core structure and analogues. As outlined in section 2.3, this natural product is isolated from the skin of poisonous tropical frogs of the *Dendrobates* species. Histrionicotoxins are known to be noncompetitive inhibitors of neuromuscular, ganglionic and nicotinic acetylcholine receptors.⁵⁷ Inhibitors of such neuron receptor proteins will inhibit the main function of the receptors, being transmission of signals at neuromuscular junctions and in the central and peripheral nervous systems.⁹⁵

The unusual neurological effects these compounds possess makes them of interest to the biochemist, with various research groups exploring the biological capabilities and structural variations such as the Holmes group and the group of Stockman.^{57, 61}

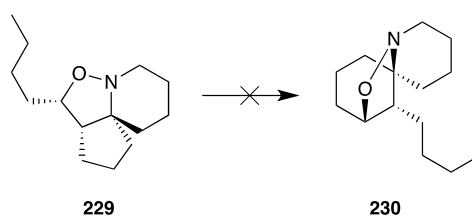
Despite this interest, the HTX core structure has proven quite resistant to the development of suitably flexible synthetic approaches that can generate libraries of analogues. For instance there are very few analogues at the C2 position of this molecule. Given the obvious structural similarity between the 6,5-azaspirodecane core of pinnaic acids/halichlorine and histrionicotoxins, we envisioned application of our approach to the former to access HTX-like molecules with a variety of substituents at the C2 position. The group of Gossinger discovered that cycloadduct **119** utilised by us towards halichlorine could be converted to the isomeric 6,6-isoxazolidine by heating in toluene in a

sealed tube at 220°C. Indeed, the 6,5-adduct **119** is the kinetic product of this internal cycloaddition while the 6,6-adduct **198** is the thermodynamic adduct (scheme 41).



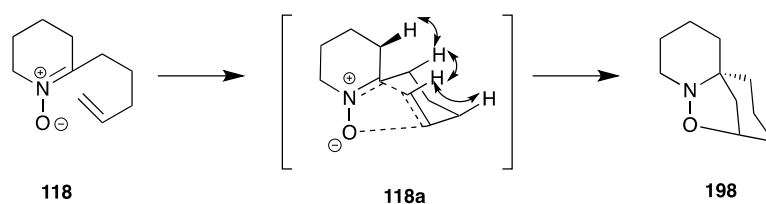
Scheme 41. Conversion of kinetic product **119** to thermodynamic product **198**.

Unfortunately, in order to access the thermodynamic adduct, the reactions conditions have to be quite forceful, and conversions of substituted cycloadducts such as the attempted conversion of **229** to **230**, which does not proceed (scheme 42).⁶⁰



Scheme 42. The attempted conversion of kinetic product **229** to thermodynamic product **230**.

The relatively high activation energy towards the [6.6.5]-tricyclic can be attributed to destabilising 1,3-diaxial interactions in the transition state, scheme 43. This has been further investigated further by Holmes *et al.*, who applied computer modelling to this problem, which revealed that there is a relatively poor overlap between the requisite dipole/ alkene orbitals involved in the reaction due to poor alignment of the reacting groups.



Scheme 43. A predicted transition state during the formation of the [6,6,5]-tricyclic **198**, showing the destabilising 1,3-diaxial interactions.

5.1 Synthesis of the 6,6-Spirotrone

Using the methodology previously outlined by the Gossinger group,⁶⁰ and the information by Holmes,⁶¹ we postulated that we could access quantities of the [6,6,5]-tricyclic adduct through applying more energy to achieve the more stable thermodynamic product.

We envisioned that the potentially hazardous thermodynamic cycloaddition, affected in a sealed tube, could be more conveniently, and much more safely, achieved with a microwave reactor which utilises thick glass walled, pressure-capped, reaction vessels. Here the reaction is performed within the instrumentation, which protects the experimentalist from any hazards due to the development of high pressures and reaction can be routinely performed at pressures up to 30 bar. Indeed, heating a toluene solution of cycloadduct **119** at 220°C and a pressure of 4 bar lead to the formation of a product spot on tlc with a RF close to the original cycloadduct. However, despite running the reaction over prolonged periods, up to 2.5 hours, the reaction only proceeded to about 50-60%, although the kinetic tricycle was easily collected and recycled. Nevertheless, both components were readily separated by column chromatography and NMR analysis of the newly formed compound indicated it was the desired 6,6-spiroadduct.

Analysis of the ¹H-NMR spectrum shows clear distinctions between the 6,5-cycloadduct and the 6,6-cycloadduct. The main change being the α -proton to

the oxygen, where in the 6,5-cycloadduct there are two peaks integrating to these protons, there is now only one. Evidence from the DEPT 135 also confirms that C8 is a methine, rather than a methylene carbon.

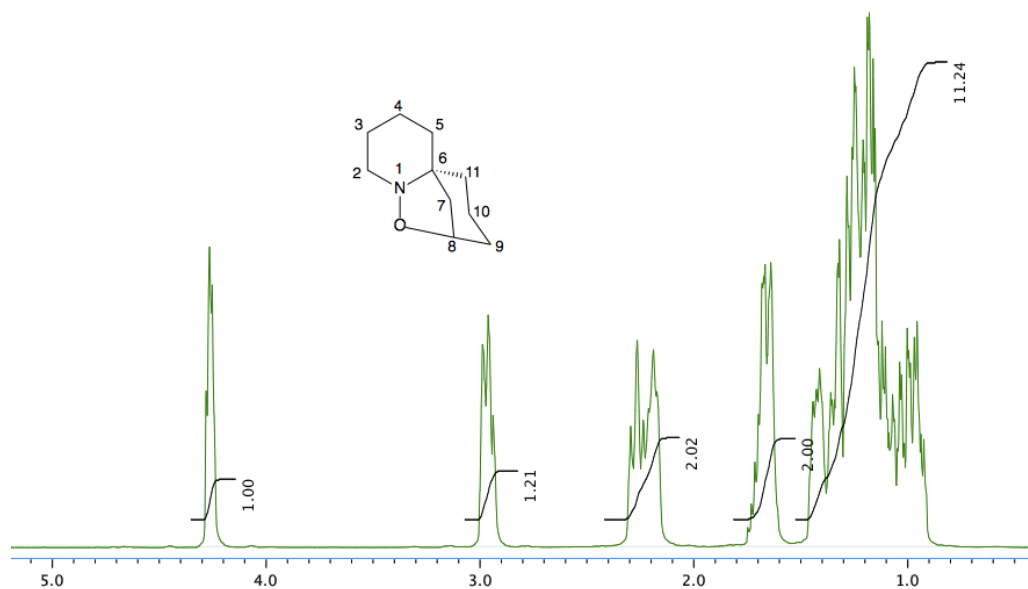
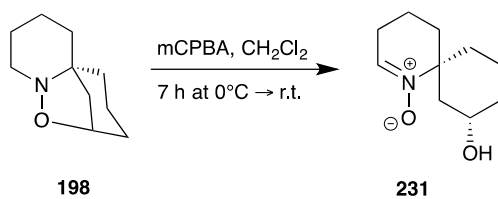


Figure 18. ¹H-NMR spectrum of the [6,6,5]-cycloadduct **165** product.

With quantities of the 6,6-cycloadduct **198** in hand, conversion to the nitron derivative **231** was performed, applying our previously developed oxidative ring opening methodology (scheme 44). The reaction proceeded without much difficulty, utilising slow addition of a mCPBA solution followed by flash column chromatography using eluent 9.5:0.5, CH₂Cl₂:MeOH as eluent gave a 6,6-spiro nitron in a 60% yield.



Scheme 44. Conversion of [6,6,5]-cycloadduct **198** to spironitrone **231**.

Analysis of the $^1\text{H-NMR}$ spectrum and comparison between the 6,5-spironitrone again shows a difference in integration for the α -proton to the hydroxyl group at 3.85 ppm, the distinctive nitrone triplet can also be seen at 7.1 ppm.

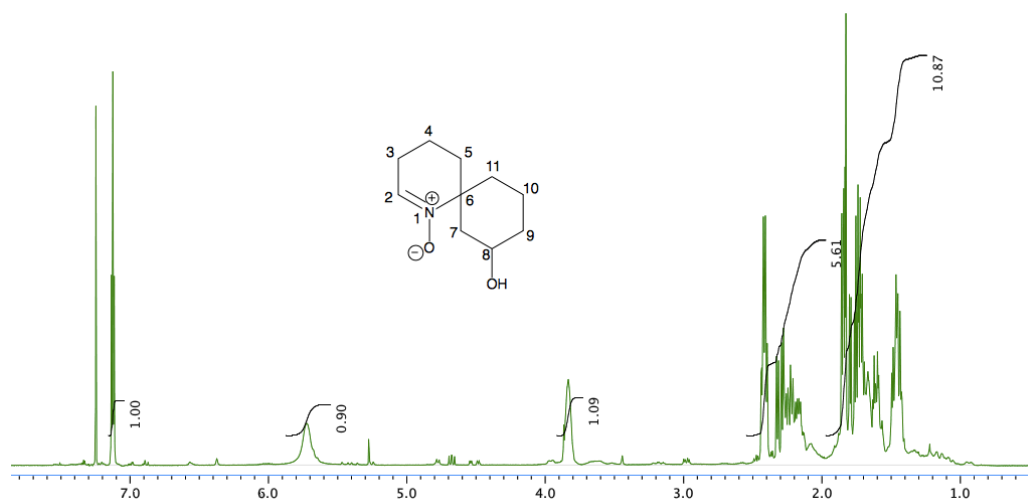


Figure 19. $^1\text{H-NMR}$ spectrum of the 6,6-spironitrone **231**.

5.2 Cycloadditions to the 6,6-Spironitrone

We envisioned that cycloadditions to the 6,6-spironitrone **231**, could be carried out in the same manner as the 6,5-spironitrone,⁶³ without great difficulty. It was planned to conduct a small number of cycloadditions using various substrates with terminal alkenes, both electron rich and electron poor substituents. A list of substrates attempted are tabulated below.

Table 4. Cycloadditions onto spirocyclic nitrone **231**.

231 **232-236**

Entry	R ₁	R ₂	Solvent	Temp (°C)	Cycloadduct	Yield (%)
1	Ph	H	PhMe	110	232	25
2	COCH ₃	H	EtOH	40	233	41
3	COCH ₃	H	PhMe	110	233	0
4	H	CO ₂ CH ₃	PhMe	110	234	46
5	CO ₂ CH ₃	CO ₂ CH ₃	PhMe	110	235	0
6	CN	H	CH ₂ Cl ₂	25	236	0
7	CN	H	EtOH	40	236	0
8	CN	H	PhMe	110	236	0

These cycloadditions proved more challenging than originally perceived. Whilst monitoring the reactions by TLC, the loss of starting material was seen, with the appearance of numerous new spots. The general work up for these cycloadditions involved removal of the solvent before purification by flash column chromatography. This was difficult, and analysis of the different fractions collected by $^1\text{H-NMR}$ suggests the formation of diastereoisomers.

A number of these cycloadditions (entries 3, 5-8) resulted in the formation of very complex product mixtures, especially the addition of acrylonitrile, which, after trying various reaction conditions didn't produce the desired results. However, three of these (entries 1, 2 and 4) were successful. The formation of the desired cycloadduct could be readily discerned by analysis of the relevant $^1\text{H NMR}$ spectra. Spectra of cycloadduct **232** exhibited a key absorbance at 5.06 ppm assigned to the proton at C3 along with aromatic signals between 7.19 and 7.37 while the $^1\text{H NMR}$ spectrum of cycloadduct **233** possesses key signals between 5.11-5.39 assigned to C2' and additionally, a singlet at 3.70 ppm, arising from the presence of the newly introduced methyl group associated with the acetate at C3". The spectrum of the cycloadduct arising from addition of methyl acrylate, **234**, was complicated possibly due to the presence of inseparable diastereoisomers as a number of peaks are doubled up. Nevertheless, mass spectral analysis of this product indicated that the reaction produced the desired product.

Unfortunately, NMR studies have been unable to definitively assign relative stereochemistry, as key protons overlap in the $^1\text{H-NMR}$ spectra. Diagnostic

NOESY spectrum cross peaks can be predicted by examination of cycloadduct conformers, which are more complex for the cycloadditions than those in section 4.2.1.

Figure 20 displays the possible conformers arising from cycloaddition from the “top” face, the same side as the hydroxyl group. Each conformer arises by flipping of the chair conformations of each 6-membered ring in turn. Conformers **a** and **b** are expected to be minor conformers due to steric hindrance between C3 and C3' on conformer **a** and C2 and C2' on conformer **b**, while conformers **c** and **d** are thus major conformers expected, and thus, upon analysis of the NOESY, you should find correlations between protons on C2 and C11.

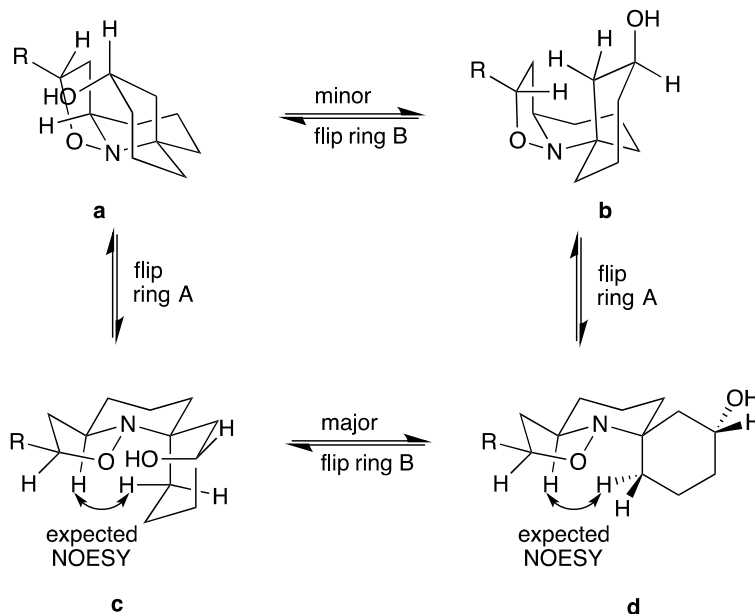


Figure 20. The possible conformers of a cycloaddition if attack occurs from the top face.

Alternatively, attack from the bottom, opposite to the hydroxyl group gives conformers **a** and **b** major conformers, where correlations should be observed between C2 and C4', figure 21. Conformers **c** and **d** would be minor conformers, again, due to steric hindrance between the 5-membered ring on the isolazidine and the hydroxycyclohexane ring.

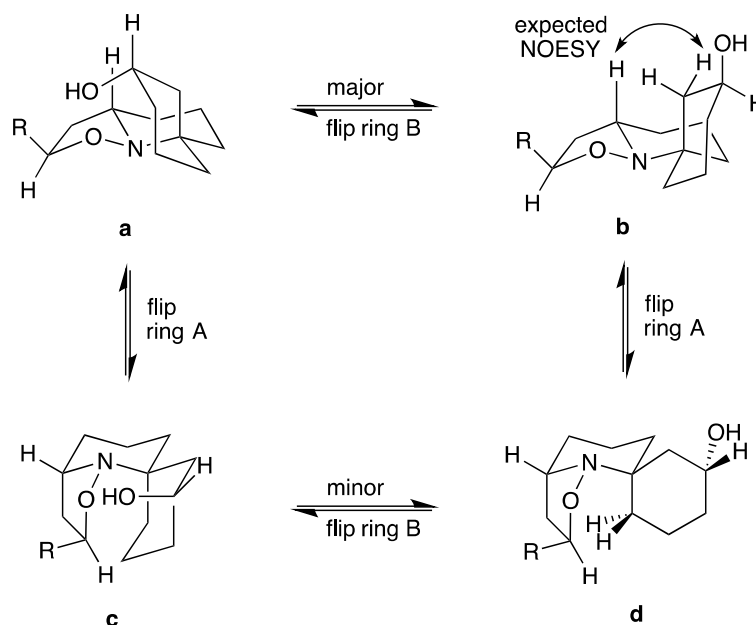


Figure 21. The possible conformers of a cycloaddition if attack occurs from the bottom face.

Unfortunately, upon analysis of the $^1\text{H-NMR}$ and NOESY spectra, it was discovered that protons on both C2 and C4' reside under the same multiplet, and therefore we cannot use NOESY to unambiguously determine stereochemistry for these structures at the present time. Upon referring to previous cycloadditions to the 6,5-spironitrone, we can reasonably assume that the exo isomer would result but we are unable to determine relative stereochemistry at C3' at present, figure 22.

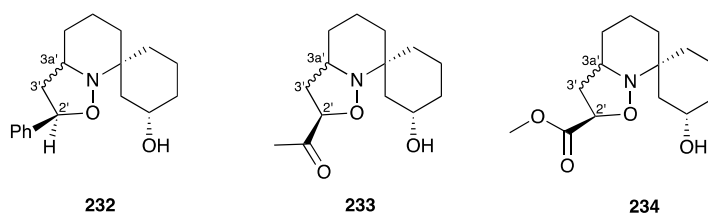
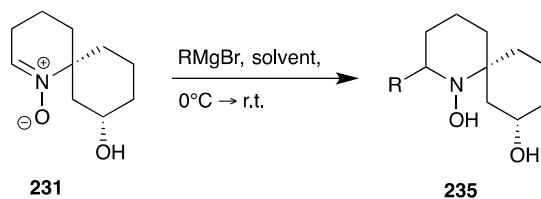


Figure 22. Shows the expected stereochemistry for the series of cycloadditions, with the unassigned conformation of C2''.

5.3 Grignard Additions to the 6,6-Spironitronone

With small quantities of the 6,6-spironitronone in hand, the next aim was to produce a small library of alkyl derivatives through the addition of Grignard reagents to spironitronone **231**.



Scheme 45. Addition of Grignard reagents onto spironitronone **231**.

It was envisioned that the reactions would proceed in a similar fashion, with comparable levels of success, to the previous nucleophilic additions to the 6,5-spironitronone (section 4.2), unfortunately this was not the case. The only previous example of the synthesis of mono, C -2 functionalised derivatives of histrionicotoxin (Section 2.3.3) reveals that an alkyl chain, in this case a pentenyl chain, has been previously added.⁶²

The reactions conditions were as previous, under inert conditions throughout, trialling both diethyl ether and tetrahydrofuran as solvents. TLC analysis showed a number of product spots, but upon purification by flash column chromatography, entries 1, 3-6 (table 5) formed complex mixtures. During attempted addition of a propyl group (Entry 1), analysis of both ¹H and ¹³C NMR spectra indicated a reduced spirocycle had formed, with no alkyl chain present.

This may have arose from reduction of the spirocyclic nitronne, indicating that no addition of Grignard reagent took place.

Unfortunately, we were only successful in attaching the hexyl group onto the 6,6-spiro nitronne. This may have been partially due to the small scale these reactions were conducted on (approximately 60 mg).

The ^1H NMR spectrum did closely match that obtained by Gessner and co-workers for pentenyl-substituted azaspirocycle **146b**, (figure 23). The proton spectrum for this compound exhibited peaks at 3.98 ppm for H-8 and at 2.85 ppm for H-2. While the ^1H -NMR spectrum for **240** exhibits peaks at 3.70 ppm assigned to H-8 and 2.88 ppm assigned to H-2. Mass spectral analysis also confirmed a product with the desired molecular mass had been isolated.

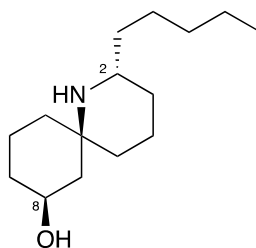
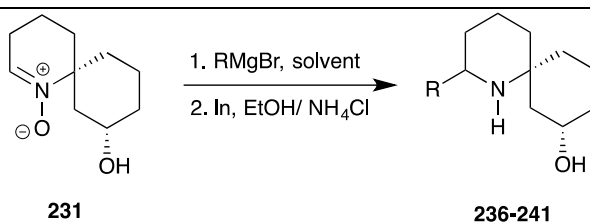


Figure 23. The pentyl adduct **146b** synthesised by the Brossi group.⁶²

Table 5. Shows the reaction conditions for the attempted nucleophilic additions onto the 6,6-spiro-nitrone **231**.



Entry	R group	Solvent	Cycloadduct	Yield ¹ (%)
1	Propyl	Diethyl ether	236	0
2	Butyl	Diethyl ether	237	0
3	Pentyl	Diethyl ether	238	0
4	Pentyl	THF	239	0
5	Hexyl	Diethyl ether	240	23
6	Hexyl	THF	241	0

¹ Yield over two steps.

We can try and predict the stereochemistry of these cycloadducts by investigating the possible conformers of the nitrone and hence the presence of any exposed faces to cycloaddition. The nitrone has four possible conformers, as it has two rings and each of these rings can be flipped. It is therefore easy to ascertain that there are four possible product conformations. Inspection of these conformers, should provide an indication of expected relative stereochemistry of addition (figure 24).

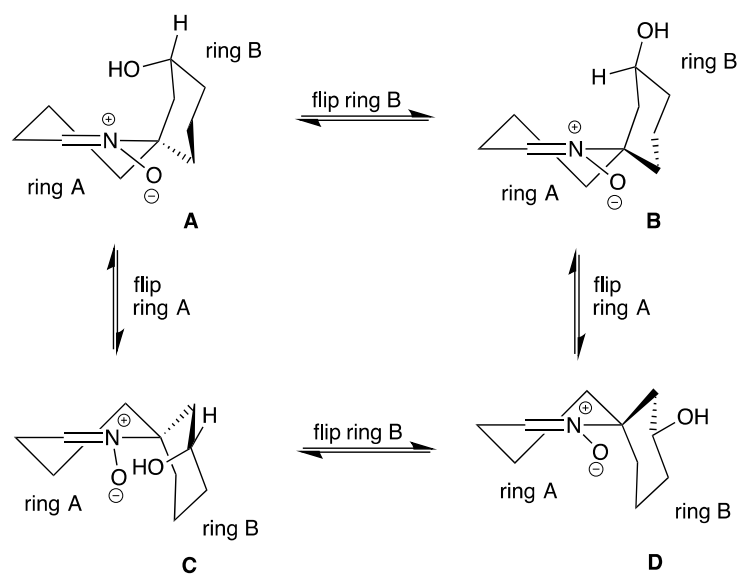


Figure 24. The possible conformers of spirocyclic nitronium **231**.

Unfortunately, there are no obvious candidates for high or low energy conformers amongst A-D and hence it is difficult to predict the diastereofacial preferences of dipolarophiles or Grignard reagents by simple inspection of these conformers.

Furthermore, due to the low amounts obtained, we were unable to obtain an adequate NOESY spectrum to confirm stereochemistry. Due to the likeness of the ^1H - NMR spectrum, we could reasonably assume the same stereochemistry has been obtained.

Chapter 6 Alternative Routes to Access Spirocyclic Structures

Functionalisation of 6,5-spironitronone **147** provides excellent access to a range of C2-analogues of halichlorine/pinnaic acid. However, the relative stereochemistry of products obtained is not that observed in the natural products and this strategy is less than flexible as nitronone **147** must be functionalised directly only providing access to hydroxymethyl-substituted products. Owing to problems encountered in the stereoselectivity of addition of alkenes and Grignard reagents to hydroxymethylnitronone **147** we became interested in attempting preparation of O-protected nitronone **242** and **243**, (figure 25).

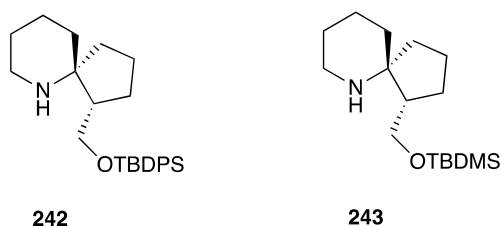


Figure 25. The bulky silyl protection groups of interest.

The presence of a bulky silylether may cause adoption of an alternate nitronone conformer where the “bottom” face is occluded leading to formation of products with relative stereochemistry matching that of the natural products (figure 26).

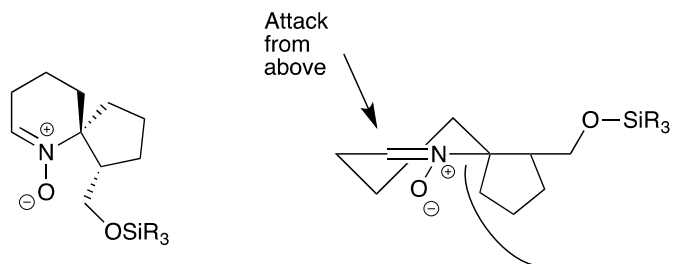
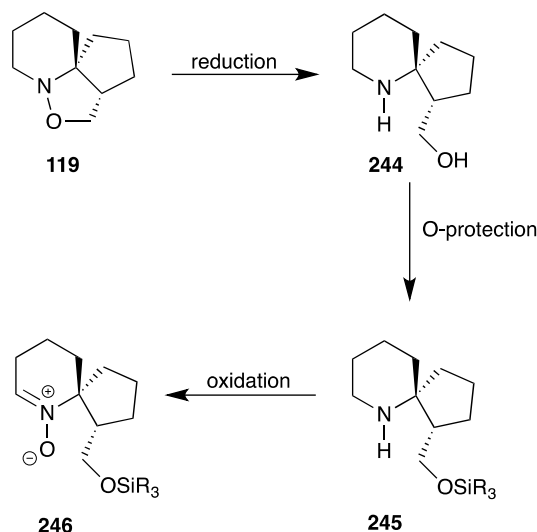


Figure 26. The expected conformer of a silyl-protected 6,5-spiro-nitrone.

6.1 Alternative Methods to Ring Open the Isoxazolidine

It was envisaged that the 6,5-spironitrone could be accessed by reductive cleavage of **119** followed by O-protection followed by direct oxidation of the amine to the nitron (scheme 46).



Scheme 46. Shows the proposed route to accessing an O-protected spironitrone.

The tricycle **119** was reductively ring opened using zinc and acetic acid, producing **244** in a good yield. Unfortunately, it was later discovered that like the allyl reductions, the zinc/ acetic acid method seemed to, on occasion add an acetate group onto the nitrogen (section 4.2). Reductive ring opening of **119** using indium powder was tried, although this was unsuccessful.

The next step in our synthetic route required protection of the free OH as a silyl ether, (table 6). Silylation as either a TBDMS or TBDPS ether was trialled under

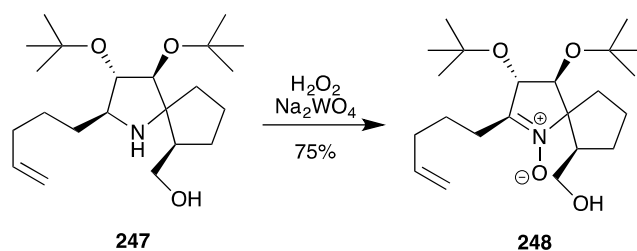
a variety of conditions. Protection of the hydroxyl group occurred without issue, and were purified without much difficulty.

Table 6. Protection of the C1-hydroxy group as a silyl ether.

$$\text{244} \xrightarrow[\text{DMAP, CH}_2\text{Cl}_2]{\text{SiR}_3, \text{ base}} \text{242-243}$$

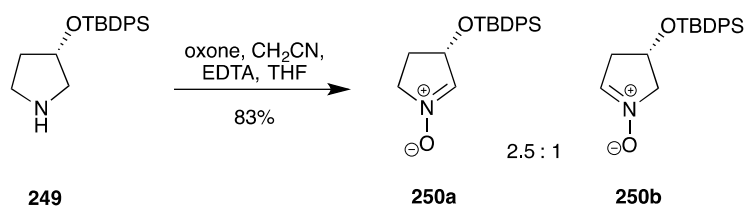
Entry	Protecting group	Base	Product	Yield
1	TBDPSCI	Imidazole	242	54
2	TBDPSCI	TEA	242	59
3	TBDMSCI	Imidazole	243	63
4	TBDMSCI	TEA	243	52

With quantities of **242** and **243**, studies to oxidise these to the corresponding nitron were investigated. A literature study on similar oxidations of amines to nitrones (reviewed in section 3.2) provided a number of possible methods to access the key nitron intermediate. Table 7 shows the numerous oxidation reagents used, as well as changes in the reaction conditions to help aid the oxidation, these included using sodium tungstate/ H_2O_2 ,^{79, 96} oxone⁹⁷ and titanium isopropoxide.⁸⁰ The peroxide/ sodium tungstate system has been used with success in the oxidation of spiro-amines close in structure to **242/243** (scheme 47).⁹⁸



Scheme 47. A successful oxidation using hydrogen peroxide and sodium tungstate.⁹⁸

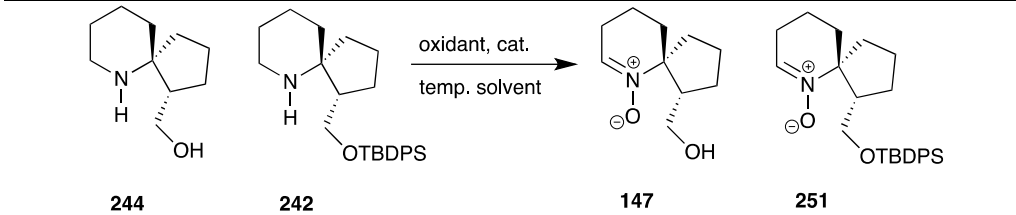
Oxone has also been used with success to oxidise relatively complex alkaloid skeletal, such as **249** to the corresponding nitrones **250a/250b**, (scheme 48).⁸⁰



Scheme 48. A successful oxidation using oxone and EDTA.

Unfortunately, both the tungstate-mediated oxidation and the oxone-based methodology proceeded without success. The most promising of these oxidations was the sodium tungstate and hydrogen peroxide method. The TLC's during the monitoring of this reaction displayed the UV active bright spot you would expect from the nitronium ion. Although this was performed on a 100 mg scale, so this may have contributed to the difficulties experienced in getting the desired product from this reaction.

Table 7. Reagents screened for oxidation of spirocyclic amines, with the hydroxyl group both TBDPS protected **242**, and deprotected **244** to nitrones.

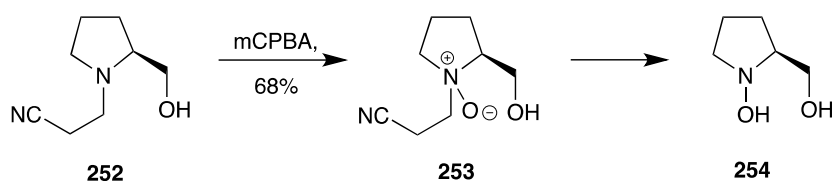


Entry	Amine	Oxidant	Catalyst	Solvent	Temp. (°C)	Nitrone ¹
1	244	Oxone	EDTA	MeCN	5	147
2	244	H ₂ O ₂	Na ₂ WO ₄ •2H ₂ O	MeOH	0	147
3	242	Oxone	EDTA	MeCN	5	251
4	242	Cumene H ₂ O ₂	Ti(O-Pr) ₄	CHCl ₃	0	251
5	242	H ₂ O ₂	Na ₂ WO ₄ •2H ₂ O	MeOH	0	251
6	242	H ₂ O ₂	Na ₂ WO ₄ •2H ₂ O	Acetone	25	251
7	242	H ₂ O ₂	Na ₂ WO ₄ •2H ₂ O/ TBAB/ K ₂ CO ₃	CH ₂ Cl ₂	0	251
8	242	H ₂ O ₂	Na ₂ WO ₄ •2H ₂ O/ Et ₄ NCl/ K ₂ CO ₃	CH ₂ Cl ₂	0	251

¹0% yield.

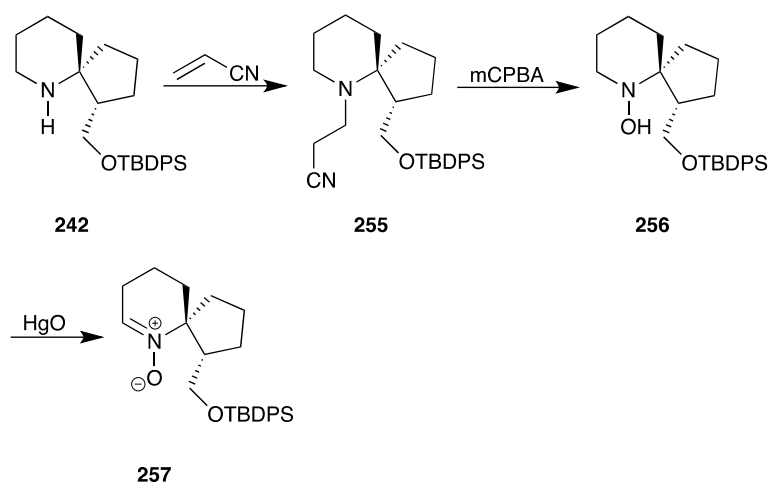
After unsuccessfully attempting to directly oxidize to the spironitrone **147** from **119** or **242** alternative methods were required. The group of O'Neil have developed a strategy to access *N*-hydroxy amines by Cope elimination of the *N*-oxides of β-cyanoethyl tertiary amines. Thus, cyanoethylamine **252** was oxidized with mCPBA to give the *N*-oxide **253** which underwent Cope-

elimination *in situ* to the hydroxylamine **254**. The latter process involves the thermal decomposition of an amine oxide, via a five-membered cyclic transition state (scheme 49).⁹⁹



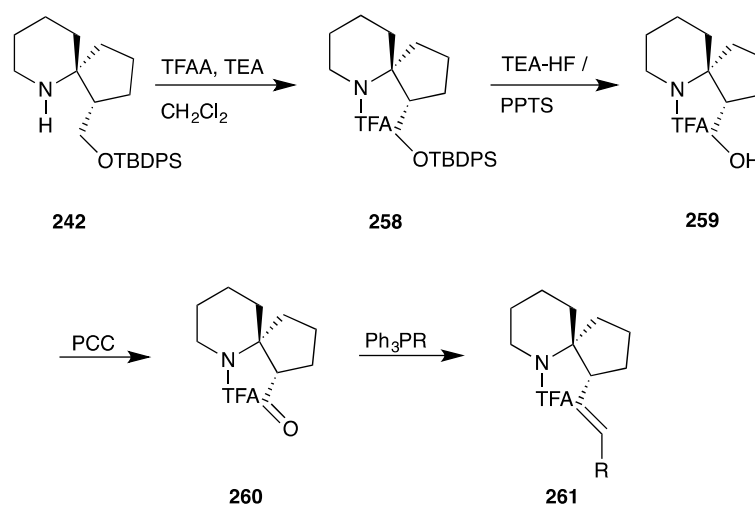
Scheme 49. The cope elimination method to access *N*-oxide intermediates.⁹⁹

The theory being that nucleophilic addition of a nitrile onto the free amine followed by oxidation would displace the nitrile group yielding the desired nitron, (scheme 50). Unfortunately, attempted additions of acrylonitrile to spiro-amine **242** were unsuccessful, which may have been due to steric reasons, with such a bulky protecting group attached.



Scheme 50. Synthesis of Spiro nitrones by Cope Rearrangement of *N*-oxo- β -cyanoethylamines

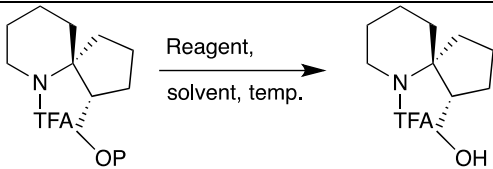
Alternatively, attention was moved to the studying the chemistry of the C1-hydroxy group. This functionalised pendant is a potentially useful tool to synthesise a range of C1-substituted pinnaic acid/halichlorine analogues. Theoretically, oxidation of the hydroxyl group to an aldehyde will then allow, through the use of Wittig reagents, a range of alkene derivatives (scheme 51).



Scheme 51. Proposed synthetic route towards extending the pendant chain.

The amine on **242** was protected with trifluoroacetic acid (TFAA) **258**, before the removal of the silyl protecting group. Unfortunately, this was far more challenging than theoretically predicted. The removal of the silylether was tried with both hydrofluoric acid and pyridinium p-toluenesulfonate (PPTS) without success, this was possibly due to steric factors hindering the release of the bulky protecting group. We therefore opted to attempt TFA-protection of the more labile TBS-ether **243** followed by deprotection. Unfortunately, this was unsuccessful (table 8).

Table 8. Reagents screened for deprotection of the silylethers on **207/208** to the free hydroxyl.



242/243 **263**

Entry	Silylether	Reagent	Equiv.	Solvent	Temp. (°C)
1	242	TEA-HF	10	MeCN	0 then 25
2	242	PPTS	10	CH ₂ Cl ₂	30
3	242	PPTS	30	CH ₂ Cl ₂	25

4	243	TEA-HF	10	MeCN	0 then 25
5	243	PPTS	10	CH ₂ Cl ₂	30
6	243	PPTS	30	CH ₂ Cl ₂	25

6.2 Di-alkenyl Additions to Access a Spirocyclic Core

We also became interested in synthesising unsubstituted spirocycles of general structure **264** which we postulated could be accessed by RCM of a bis-alkenyl precursors **265**. These compounds would allow investigation into the effects of C7-substitution on bioactivity without interfering effects from C1 functionality, (figure 27).

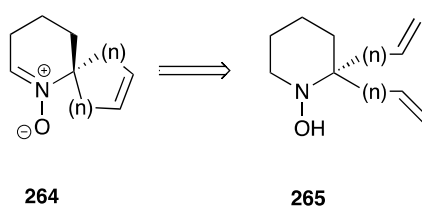
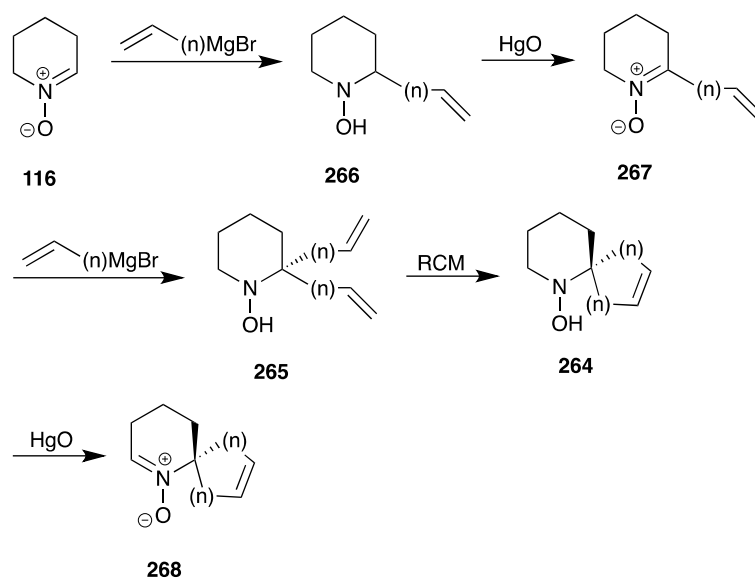


Figure 27. Retroanalysis of the intended RCM route.

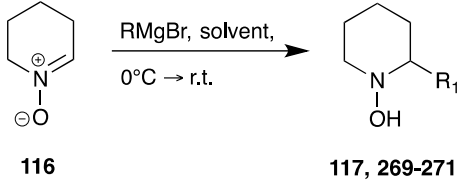
It was envisioned that utilising the previous method of a Grignard addition onto nitronone **117**, the hydroxylamine product **266**, could be synthesised by iterative Grignard addition/nitronone generation. Oxidation using mercury oxide could then provide the target nitronone systems **267**. This route could also provide convenient access to spirocycles **268**, in a variety of ring sizes including that seen in the HTX family of compounds (scheme 52).



Scheme 52. RCM-based synthetic route to various ring size spirocycles.

Firstly, a small range of Grignard additions to **116** were investigated. The product obtained from addition of a vinyl group was extremely difficult to purify, although mass spectral analysis indicated the correct compound was formed. Additions of allyl and butenyl groups proceeded with more success (table 9).

Table 9. Series of mono-additions to nitronone **116**.



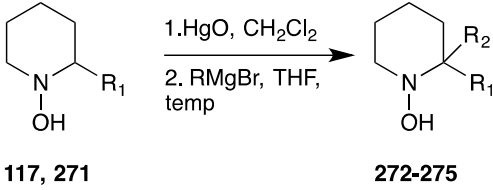
116 $\xrightarrow[0^\circ\text{C} \rightarrow \text{r.t.}]{\text{RMgBr, solvent}}$ **117, 269-271**

Entry	R ₁ MgBr	Solvent	Product	Yield (%)
1	Vinyl	Diethyl ether ¹	269	0
2	Vinyl	THF	269	18 ²
3	Allyl	Diethyl ether ²	270	0
4	Allyl	THF	270	23 ²
5	Butenyl	THF	271	37 ²
6	Pentenyl	THF	117	55 ²

¹Solubility issues; ²Contained impurities.

Next, the mono-adducts were converted back to a nitronone using the HgO-based method employed previously. This reaction was monitored by TLC, and when the spot had moved to the baseline, the reaction mixture was filtered through a pad of sodium sulphate and Celite and concentrated under reduced pressure. No attempt to purify these mono-substituted nitronones was made at this stage, owing to potential problems arising from degradation of these unstable molecules. Further functionalisation by addition of a second set of unsaturated Grignard reagents was then attempted. These included additions of vinyl- or allylmagnesium halides groups, (table 10).

Table 10. Series of Grignard additions onto mono-additions **101**, **231**.

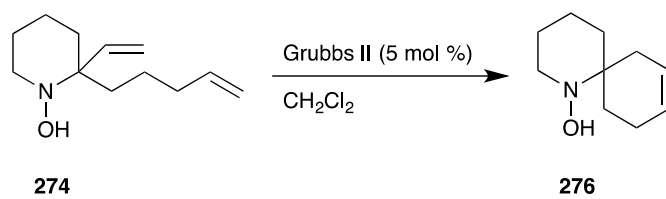


117, 271 **272-275**

Entry	Starting material	R ₂ MgBr	Temp.	Product	Yield (%)
1	271	Allyl	-78	272	21 ¹
2	271	Vinyl	0 then 25	273	30 ¹
3	117	Vinyl	0 then 25	274	41 ¹
4	117	Allyl	0 then 25	275	0

¹NMR spectra contained impurities.

NMR spectral analysis of these reactions did indicate complex mixtures and thus purification of these di-additions was difficult, and we were unfortunately unsuccessful in isolating products with very high levels of purity. Nevertheless, accurate mass data did indicate successful formation of the target dienes. This would also explain the complexity of the NMR analysis. RCM was attempted on **274** (scheme 53), which did display formation of a new compound on TLC, although comparison of ¹H- and ¹³C NMR between **274** and spirocycle **276**, revealed few visible differences. Once again accurate mass analysis did indicate that the desired spirocycle has formed.



Scheme 53. Attempted RCM of diene **274** to spirocycle **276**.

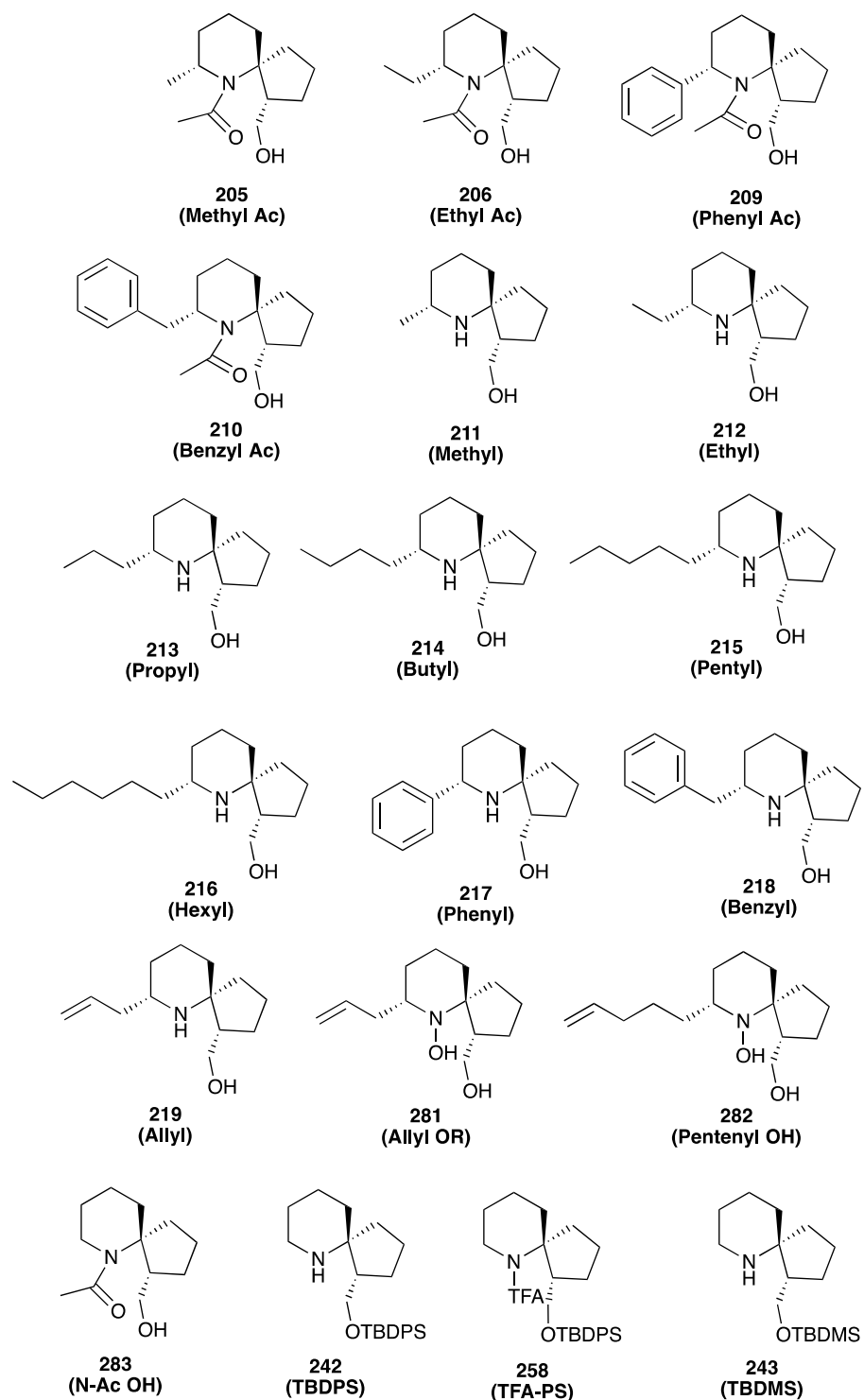
Chapter 7. Biological Studies

The aim of this section of work was to identify any biological activity for the easily accessible halichlorine analogues discussed in chapters 4-6. Two biological assays were conducted to determine if these molecules potentially possess any bioactivity.

A variety of 19 compounds were selected from the derivatives produced, summarised in scheme 54. The names have been abbreviated to reflect the structure of the analogue (for instance EthylAc signifies ethyl substitution at C-7 and presence of an *N*-acetyl group, i.e compound **206**). Stock solutions of each compound were prepared at 10^{-3} M, made up in DMSO. Serial dilutions in cell culture media from the stock gave working solutions of 10^{-4} M and 10^{-5} M that were tested in two biological *in vitro* assays to determine their effect on cell growth/viability and nitric oxide (NO) production.

Both assays were independently performed on both undifferentiated U937 cells and LPS activated U937 cells.

The findings were statistically analysed on SPSS, using an ANOVA test.



Scheme 54. A summary of the compounds tested in the biological assays, with the abbreviations used in the graphs.

7.1 Cell Culture

U937 cells were cultured using RPMI-1640 medium containing 25mM HEPES and L-glutamine supplemented with foetal bovine serum (FBS), and 1% penicillin. Cells were incubated in a humidified atmosphere of 5% CO₂ at 37°C, and all cell culture techniques were performed under adequate aseptic conditions to prevent contamination. The cell concentration was maintained below 1.5 x 10⁶ viable cells/ ml, by centrifugation and re-suspension in fresh medium every 2-3 days.

7.2 Growth and Viability Assays

This assay was conducted in order to determine if the growth or viability is affected upon coming into contact with the compounds. Using 96 well plates, six replicates of each molecule at both concentrations (10^{-4} M and 10^{-5} M), as well as six replicates of DMSO (vehicle) controls at the same concentrations as negative controls were performed, with the final cell concentration set to 0.5×10^6 viable cells/ ml.

Cell viability was assessed using trypan blue solution (0.4%), which stains dead cells blue. The viable cell counts were obtained using a Bio Rad TC20™ automated cell counter. Viable cell counts were taken from each of the six replicates, using an equal volume of cell suspension to trypan blue solution. The average replicate reading was compared to the average viable cell count taken from untreated cells.

The findings suggested that the ethyl adduct at 10^{-4} M and the benzyl at 10^{-4} M showed significant difference ($P < 0.05$) compared to the untreated cell growth, (Figure 28).

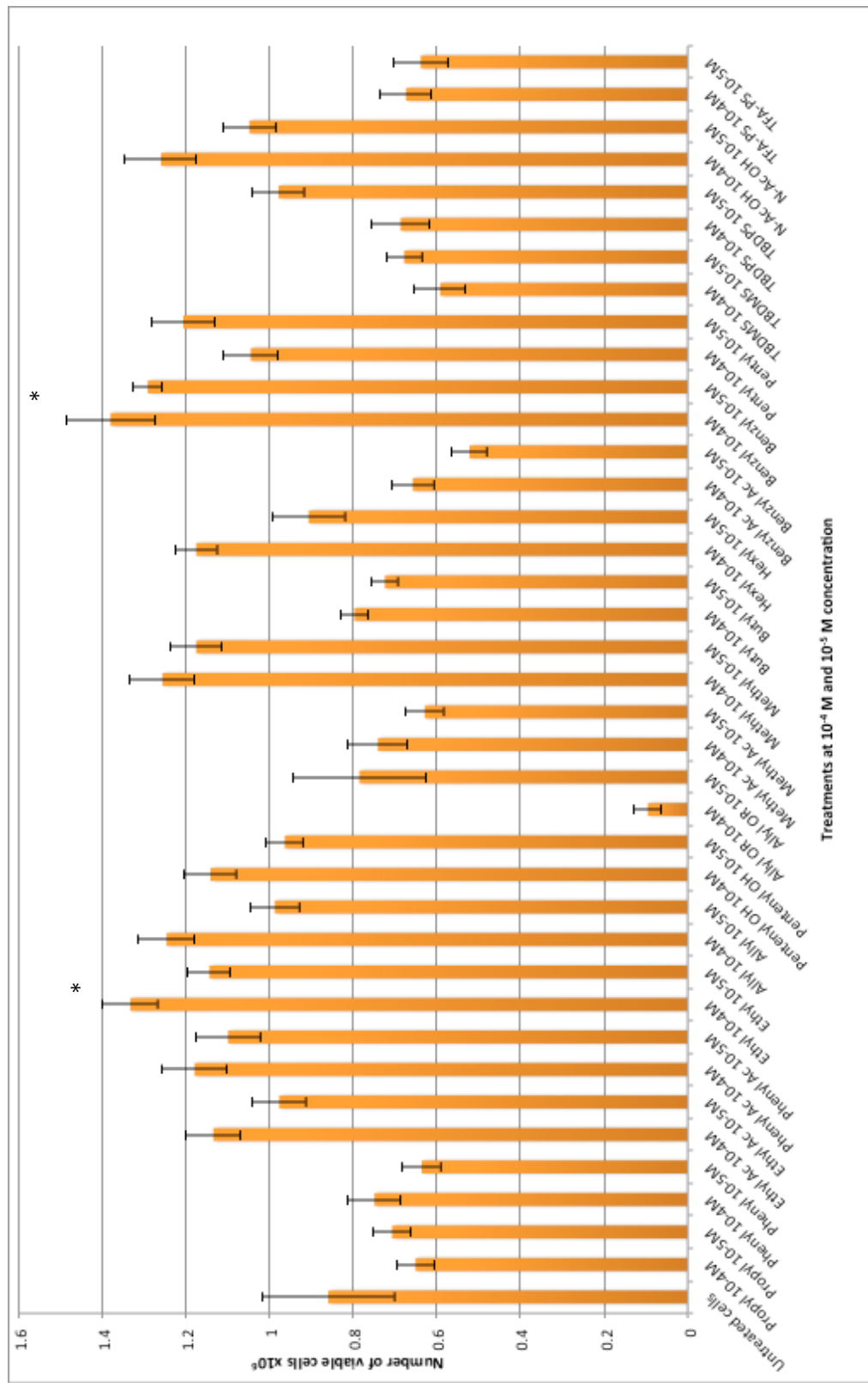


Figure 28. Effect of the molecules at 10^{-4} M and 10^{-5} M on undifferentiated U937 cells. * indicates a significant difference compared to the untreated cells ($P < 0.05$), calculated from 12 repeats.

After testing on undifferentiated cells, the same experiment was performed, but this time the cells were exposed to lipopolysaccharide (LPS) for 24 hours prior to the treatment with the compounds, which activated the cells and initiated an inflammatory type response. After 24 hours, the same derivatives were tested, again using a 96 well plate, with six replicates in all cases. The LPS activated final cell concentration was 0.5×10^6 viable cells/ml, (figure 29). Trypan blue solution and the same automated cell counter was used to collect the results.

Interestingly, these results exhibited different compound treatments to have a significant effect on cell growth/viability. The effective compounds included the *N*-acetylated ethyl-substituted analogue **206** at 10^{-4} M, the *N*-acetylated phenyl-substituted analogue **172**, at both concentrations, the allyl substituted adduct at 10^{-5} M **182**, the *N*-hydroxy pentenyl-substituted adduct at 10^{-4} M **236** and the pentyl-substituted adduct **178** at 10^{-4} M.

7.3 Nitric Oxide Assay

A nitric oxide (NO) assay was conducted on both undifferentiated U937 cells and LPS activated U937 cells. A Griess reagent was used to assess the production of NO. The Griess test is a colourmetric assay, which detects the presence of nitrite ions within a solution, the solution was prepared by addition of ultrapure water (10M Ω , which is considered nitrite free). The experiment was standardised using serial dilutions of sodium nitrite, from which, a standard curve was used to determine the concentrations of NO within the samples.

The assay was conducted on 96 well plates. The undifferentiated cells were treated with the same range of compounds used in the growth and viability assay, with a total cell concentration of 0.5×10^6 viable cells/ ml, and were incubated for 24 hours before the addition of the Griess reagent, followed by incubation for a further 15 minutes. The LPS-activated cells underwent the same procedure, after activation of the cells for 24 hours, and resuspension to the total cell concentration of 0.5×10^6 viable cells/ ml. The absorbance was read at 540 nm on a synergy HT plate reader after the 15 minute incubation.

7.3.1 Results of the NO assay

Analysis of the absorbances obtained from the assay followed. Firstly, the readings were blanked, using the average value obtained from the absorbance of just cell culture media. Next the absorbances were blanked again, this time for the negative control, which was the DMSO solutions at the corresponding concentrations (10^{-4} M and 10^{-5} M). The resulting values were then converted into concentrations, using the standard curve. Graphs were produced for the average concentrations, one for undifferentiated cells (figure 30), and one for LPs activated cells (figure 32).

Using the average viable cell counts from the growth and viability assay, the assay was standardised to determine NO production per million viable cells. Standardisation of these results gave a more robust interpretation of the anti-inflammatory capabilities of the compounds (figure 31 and 33).

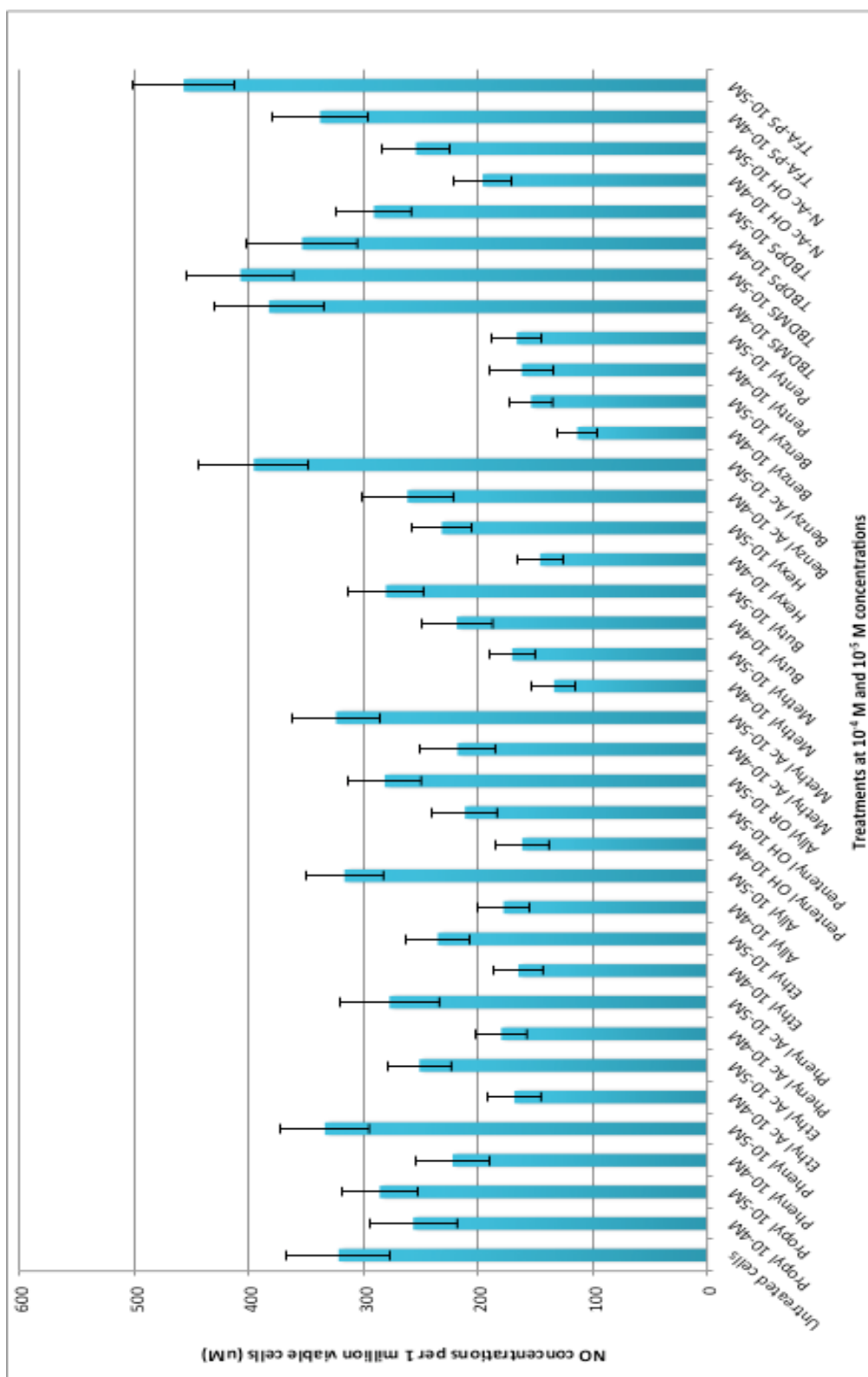


Figure 31. Average NO concentrations (µM) per million viable undifferentiated cells compared to the treated cells following treatment with molecules at 10⁻⁴ M and 10⁻⁵ M concentrations.

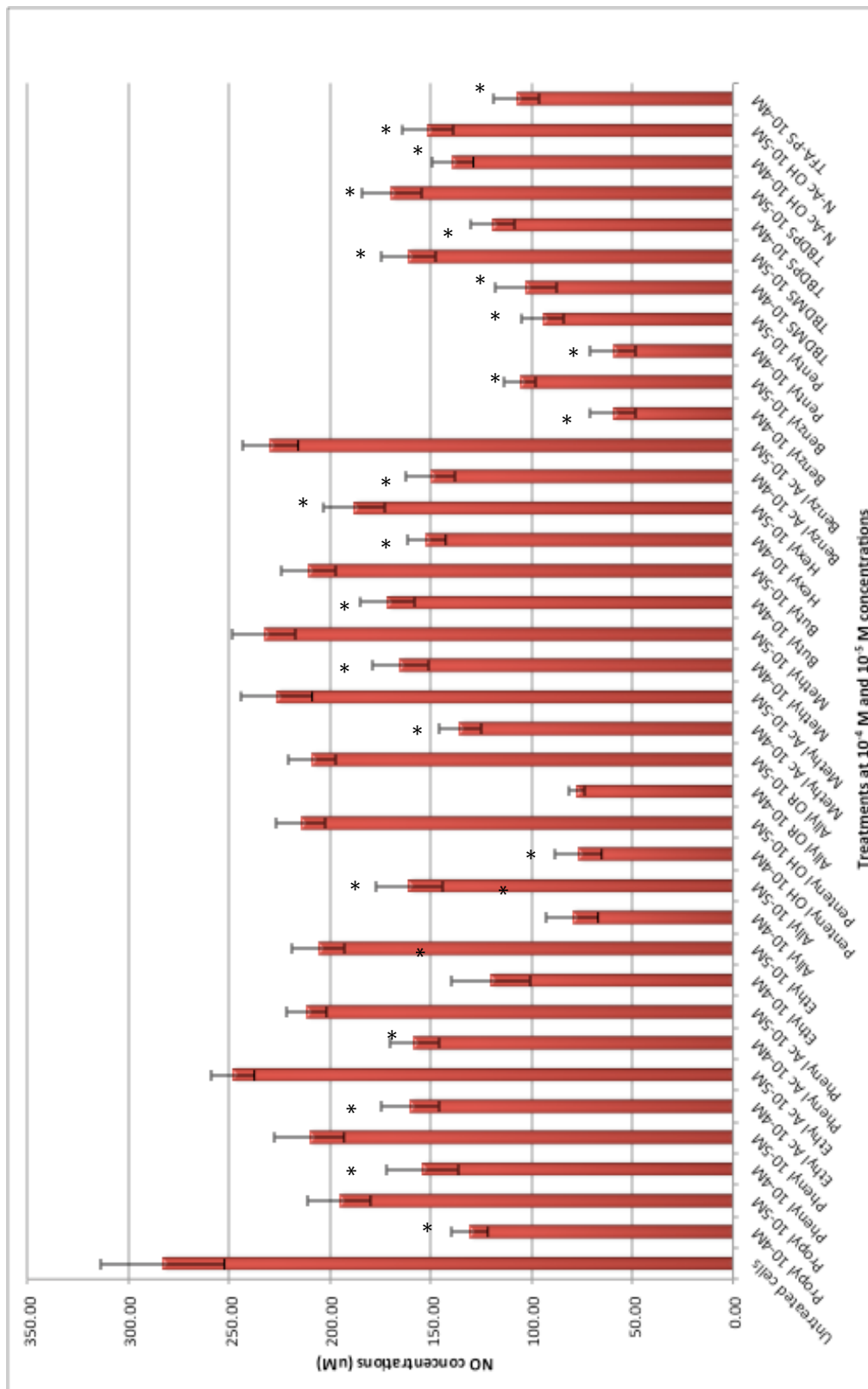


Figure 32. Average NO concentrations (μM LPS activated cells compared to the treated cells following treatments with molecules at 10^{-4} M and 10^{-5} M concentrations. * signifies a significant difference compared to the untreated cells ($P < 0.05$).

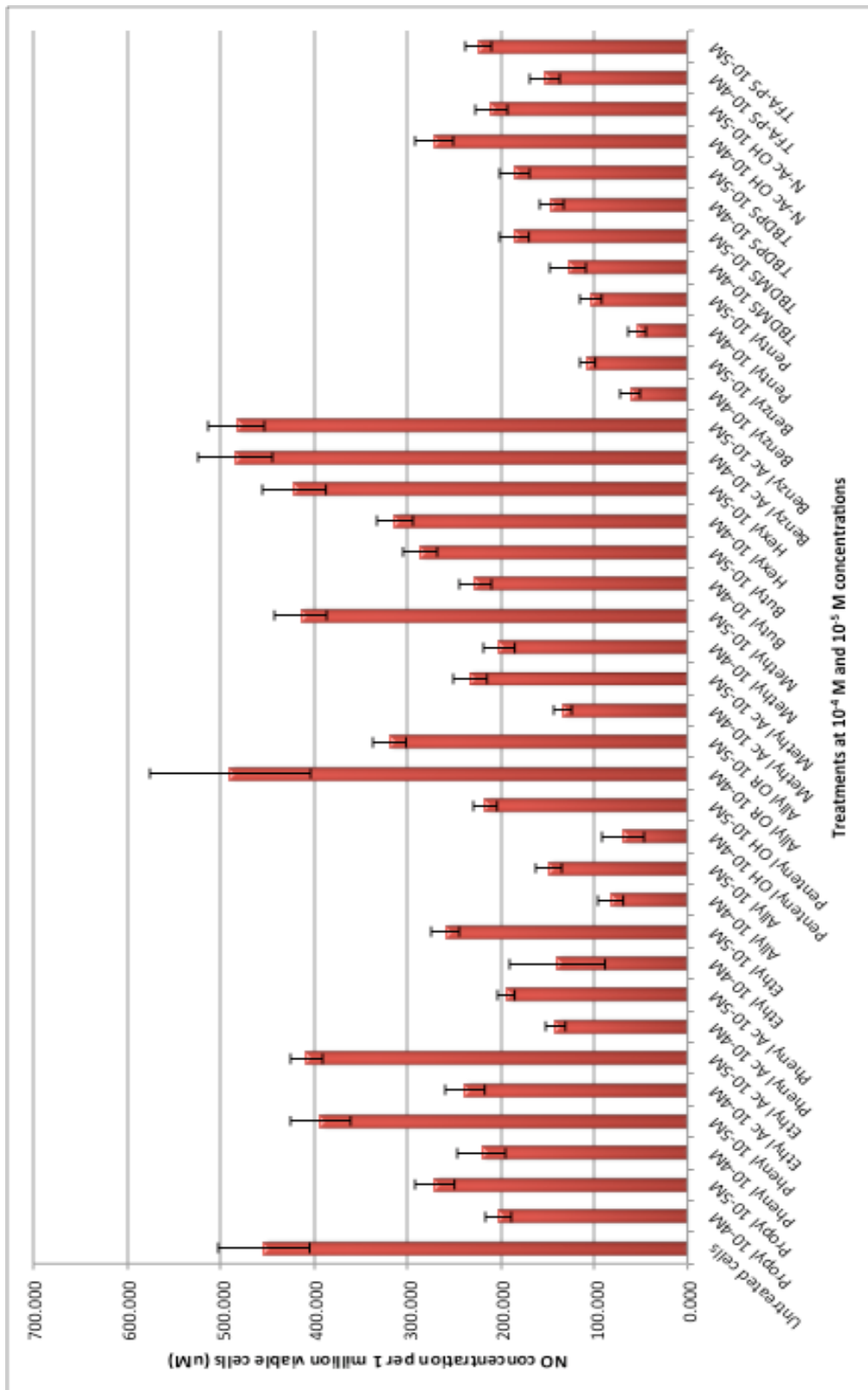


Figure 33. Average NO concentrations (µM) per million viable LPS activated cells compared to the treated cells following treatment with molecules at 10⁻⁴ M and 10⁻⁵ M concentrations.

7.4 Discussion

The results for the NO assays suggests that little NO activity occurs in the undifferentiated monocyte U937 cells, (figure 30), compared to the LPS activated NO assay, where a large proportion of the molecules used in the treatments expressed activity, especially at the higher concentration (figure 32).

Analysis of the 10^{-5} M concentration suggested that the more potent NO inhibitors seem to be the compounds containing the larger alkyl and aryl adducts attached to C7, in particular the allyl substituted adduct, the pentyl substituted adduct, the hexyl substituted adduct and the benzyl substituted adduct (figure 34). Further studies at a lower concentration would help to identify which of the molecules has the highest potency towards inhibition of nitric oxide.

The series of mono- and di-protections all displayed a significant difference to untreated cells at both concentrations, suggesting that the silyl ethers may possess some NO inhibition properties on their own.

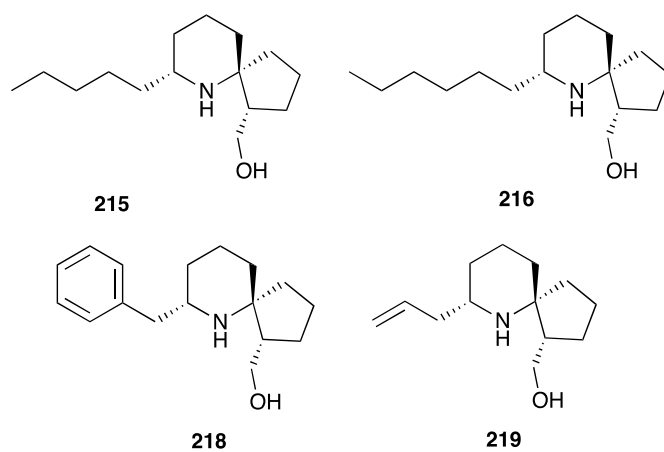


Figure 34. The molecules which shown a significant difference at both concentration in the NO assay with LPS activated cells, suggesting a higher potency.

Chapter 8. Summary and Future Work

8.1 Summary

The aims of the project were met, with a library of halichlorine derivatives synthesised, followed by biological studies on a range of these isolated compounds. The concise synthetic route towards the common key intermediate **147** was challenged by synthetic studies into alternate oxidative methods to gain access to **147** through a more convenient route determined alternative oxidants to be inadequate.

Many synthetic obstacles have been identified, including interferences from the hydroxyl group; reduction of the hydroxylamine to amines using zinc dust and acetic acid and selective deprotection.

The biological assays have provided evidence to suggest that this range of derivatives could possess anti-inflammatory properties. Further assays would help to provide a detailed description of the bioactivity, and contribute to determining which of the derivatives possess the highest potency.

8.2 Future Work

There are many avenues for furthering this project and developing a deeper knowledge of the chemistry and biological activity of halichlorine core structure derivatives. Gaining an in-depth insight into the biological capabilities of simplified analogues would be very beneficial and informative for developing a library of specific bioactive compounds. The activities determined in this thesis do provide an indication for the structure of future libraries based on this scaffold, for example, the larger alkyl chains attached at C7 displayed in figure 35. This would give the further synthetic investigations a direction, working on expansion of the most potent molecules. Comparison against a second screening would identify any effects these changes have had on the potency.

It would also be beneficial to explore the alternative methods for oxidising the free hydroxyl group of azaspirodecanes in an effort to explore how bioactivity is related to the structure of C1-side chains:

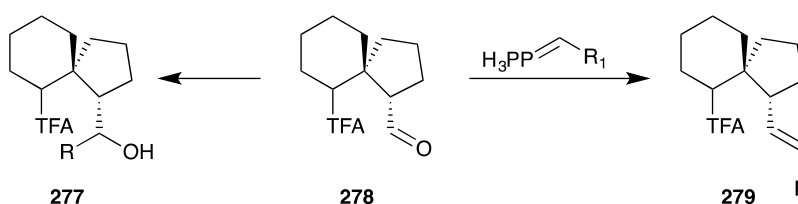


Figure 35. Alternate methods to oxidise the free hydroxyl group.

Furthermore, the RCM-based route to the core structure of both halichlorine and pinnaic acid described in schemes 52 and 53 warrants investigation once a strategy for separating diastomeric allyl adducts has been devised.

The strategy towards 6,6-spiro systems related to the HTX family of alkaloids demonstrates that a range of analogues should be accessed with some ease via cycloaddition and a thorough exploration of the scope of this process needs to be undertaken. The analogues obtained are all novel derivatives of HTX and should be tested for cholinergic activity. Given the structural similarity between halichlorine/pinnaic acid and HTX's it is also proposed to test the compounds investigated herein in a likewise manner.

As stated in the Introduction NF κ B regulates genes encoding cyclooxygenase 2 (COX2) in addition to iNOS, thus some future efforts should be directed towards determining the COX activity of the active compounds highlighted in this thesis.

Chapter 9. Experimental

All reactions were performed using oven dry glassware. All air sensitive reactions were performed with a Schlenk line under Ar. Dry solvents were collected from an Innovative Technology Pure Solv solvent drying system. All chemicals were purchased from either Sigma Aldrich or Alfa Aesar. Thin layer chromatography were performed using Sigma Aldrich silica gel 60Å F254 plates, a basic potassium permanganate solution was used as a stain. Flash column chromatography was performed using Sigma Aldrich silica gel pore size 60, 230-400 mesh as the solid support with indicated eluent. NMR spectra were recorded using a Joel ECS 400 NMR spectrometer, operating at 400 MHz for ^1H nuclei and 100 MHz for ^{13}C nuclei. Chemical shifts are reported relative to TMS (^1H 0.00 ppm) and CDCl_3 (^1H 7.26 ppm, ^{13}C 77.0 ppm) and are reported in parts per million (ppm) on the δ scale. Multiplicities are described as singlet (s), doublet (d), doublet of doublet (dd), triplet (t), doublet of triplets (dt), multiplet (m), broad (b). The symbols * is used to differentiate between two isomers present in a mixed sample, a and b protons refer to different germinal protons. Infrared spectra were recorded using a Thermo Nicolet 380 FT-IR. Mass spectra and accurate mass data were obtained on a Aligent Technologies 6540 UHD Accurate-Mass Q-TOF LC/MS. Melting points were checked on Stuart SMP10 apparatus.

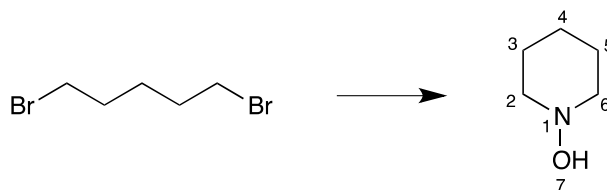
General procedure for Grignard Reagents in THF

Grignard reagents were prepared to approximately 1.5M concentration. Organohalide (4 mmol) was added to a stirred solution of Mg (15 mmol, 0.36g) in tetrahydrofuran (4 ml) with a crystal of iodine. Upon initiation, the remaining organohalide (11 mmol) was added as a solution in tetrahydrofuran (6 ml). The mixture was stirred under reflux for 30 minutes. The resulting reagent was used directly after preparation.

General procedure for Grignard reagents in diethyl ether

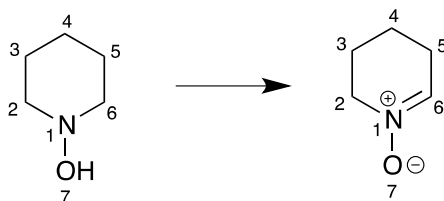
Grignard reagents were prepared to approximately 1.5M concentration. Organohalide (4 mmol) was added to a stirred solution of Mg (15 mmol, 0.36g) in diethyl ether (4 ml) with a crystal of iodine. Upon initiation, the remaining organohalide (11 mmol) was added as a solution in ether (6 ml). The mixture was stirred under reflux for 30 minutes. The resulting reagent was used directly after preparation.

Piperidin-1-ol (115)



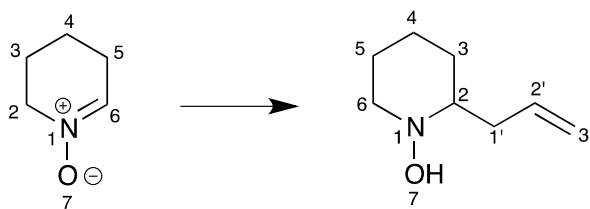
The synthesis was performed according to the literature procedure.⁶⁰ 1,5-dibromopentane **196** (0.13 mol, 30.00g) was added to a suspension of hydroxylamine hydrochloride (0.325 mol, 22.84g) in triethylamine (230 ml), before heating under reflux for 4 h. The mixture was filtered through a pad of sodium sulphate and Celite® and the residue washed with diethyl ether (3x 20 ml). The filtrate was concentrated under reduced pressure to give a pale yellow oil. Purification by flash column chromatography on silica gel using ethyl acetate: methanol (9.5:0.5) as the eluent gave *the title compound* (9.23g, 70%) as a colourless oil. R_f value 0.76; δ_H (400 MHz; CDCl₃) 1.07-1.13 (1H, m, 4a-H), 1.49-1.56 (3H, m, 3a-H, 4b-H, 5a-H), 1.69-1.71 (2H, dd *J* = 3.2 and 10.4 Hz, 3b-H, 5b-H), 2.38-2.44 (2H, dt *J* = 2 and 10.8 Hz, 2a-H, 6a-H), 3.19-3.29 (2-H, d *J* = 10 Hz, 2b-H, 6b-H); δ_C (100 MHz; CDCl₃) 22.9 (CH₂, C-4) 25.4 (CH₂, C-3) 59.0 (CH₂, C-2). IR/ cm⁻¹ 3160 (O-H br), 2973 (C-H), 2833 (C-H), 1476 (C-H). HRMS calcd for C₅H₁₁NO 101.0841: found [M+H] 102.0895.

2,3,4,5-Tetrahydropyridine 1-oxide (116)



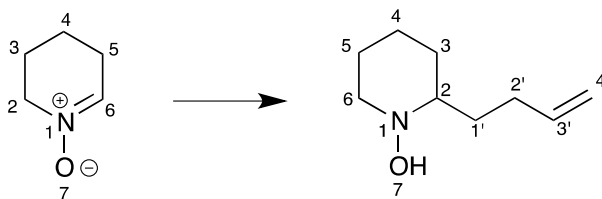
The synthesis was performed according to the literature procedure.⁶⁰ To a solution of **115** (86 mmol, 8.82g) in dichloromethane (20 ml) at 0°C, a suspension of mercuric oxide (195 mmol, 42.26g) in dichloromethane (60 ml) was added. The mixture was warmed to r.t. and stirred for 3 h. The slurry was filtered through sodium sulphate and a pad of Celite®. The filtrate was concentrated under reduced pressure to give *the title compound* as a yellow/orange oil. R_f value 0.05, the crude product was used for further synthesis without purification.

2-Allylpiperidin-1-ol (270)



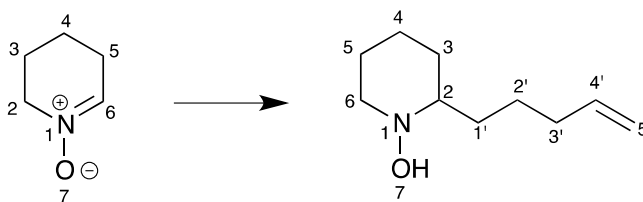
The synthesis was performed according to the literature procedure.⁶⁰ N-oxide **116** (2 g, 21 mmol) in tetrahydrofuran (20 ml) was cooled to 0°C under Ar. Commercially prepared allylmagnesium chloride (2M, 25 mmol, 0.7 ml) was added drop-wise. The resulting mixture was warmed to r.t. and gently warmed for 30 minutes to aid solubility, before leaving to stir for 10 hours. Water (3 ml) was added to quench the reaction before separation between saturated aqueous ammonium chloride (10 ml) and dichloromethane. The aqueous phase was extracted further with dichloromethane (3x 15 ml). The combined organic layers were dried with anhydrous sodium sulphate and concentrated under reduced pressure. The residue was purified by flash column chromatography using ethyl acetate: hexane as the eluent to give *the title compound* (0.7240g, 23%) as an orange oil, R_f value 0.69. δ_{H} (400 MHz; CDCl₃) 1.01-1.19 (2H, m, 4a-H, 5a-H); 1.46-1.70 (3H, m, 3a,b-H, 4b-H); 1.80 (1H, dd $J = 2.4$ and 7.2 Hz, 5b-H); 2.01 (1H, m, 1'a-H); 2.28 (1H, m, 2-H); 2.47 (1H, m, 6a-H); 2.78 (1H, m, 1'b-H); 3.24 (1H, d $J = 11.2$ Hz, 6b-H); 4.96-5.00 (2H, m, 3'a,b-H); 5.70-5.75 (1H, m, 2'-H). δ_{C} (100 MHz; CDCl₃) 23.7 (CH₂, C-4); 25.9 (CH₂, C-3); 30.8 (CH₂, C-5); 38.0 (CH₂, C-1'); 59.8 (CH₂, C-6); 67.0 (CH, C-2); 117.1 (CH₂, C-3'); 136.4 (CH, C-2'). IR/cm⁻¹ 3363 (O-H br), 2935 (C-H), 1639 (C=C), 1450 (C-H₂). HRMS calcd for C₈H₁₅NO 141.1154: found [M+H] 142.1227.

2-(But-3-en-1-yl)piperidin-1-ol (271)



A solution of nitrone **116** (2.8 g, 27.7 mmol) in tetrahydrofuran (40 ml) was cooled to 0°C under Ar. But-3-en-1-ylmagnesium bromide (42 mmol) prepared in tetrahydrofuran (30 ml) according to the general procedure, was added to the nitrone via cannula addition, which was then warmed to r.t. and left to stir overnight. Water (10 ml) was added to quench the reaction before the removal of the tetrahydrofuran and water under reduced pressure, this was followed by separation between saturated aqueous ammonium chloride (30 ml) and diethyl ether, followed by further extraction with diethyl ether (3x 20 ml). The combined organic layers were dried with anhydrous sodium sulphate and concentrated under reduced pressure. The residue was purified by flash column chromatography using ethyl acetate: hexane (1:1) as the eluent to give *the title compound* (1.55 g, 37%*) as a colourless oil, R_f value 0.69. δ_{H} (400 MHz; CDCl₃) 1.05-2.03 (9H, m, 2x 3-H, 2x 4-H, 2x 5-H, 2x 1'-H, 2'a-H); 2.36 (1H, m, 2'b-H); 3.14 (1H, m, 6a); 3.36-3.57 (2H, m, 2-H, 6b-H), 4.81-4.90 (2H, m, 2x 4'-H); 5.66-5.73 (1H, m, 3'-H). δ_{C} (100 MHz; CDCl₃) 21.8, 22.5, 26.4, 27.5, 29.8 (C1', C2', C3, C4, C5); 60.9 (C6); 76.1 (C2), 113.9 (C4'); 139.1 (C3'). IR/cm⁻¹ 3267 (O-H br), 2933 (C-H), 1639 (C=C), 1455 (C-H₂), 728 (C-H₂). HRMS calcd for C₉H₁₇NO 155.1310: found [M+H] 156.1370.

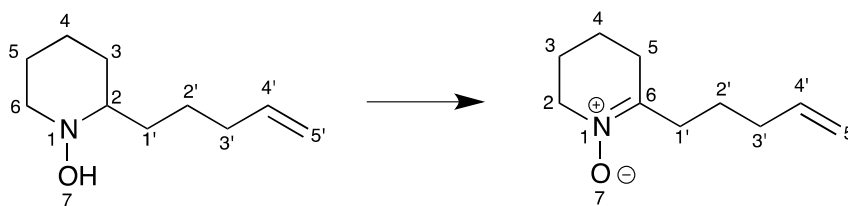
2-Pent-4-enylpiperidinol (117)



The synthesis was performed according to the literature procedure.⁶⁰ A solution of nitron **116** (86 mmol, 8.82g) in tetrahydrofuran (40 ml) was cooled to 0°C, and a solution of pent-4-enylmagnesium bromide, prepared according to the general procedure, in tetrahydrofuran, was added via cannula addition. The resulting reaction mixture was warmed to r.t. and left to stir for 15 h. The mixture was quenched with water (20 ml) followed by the removal of tetrahydrofuran and water under reduced pressure. Saturated aqueous ammonium chloride (30 ml) was added to the slurry and extracted with diethyl ether (3 x 20 ml). The combined organic extracts were dried with anhydrous sodium sulphate and concentrated under reduced pressure to a yellow/brown oil. This was purified by flash column chromatography using ethyl acetate: hexane (1:1) as the eluent to give *the title compound* (7.96g, 55%) as a pale yellow oil, R_f value 0.77. δ_{H} (400 MHz; CDCl₃) 1.05-1.67 (9H, m, 2x 1'a-H, 2x 2'-H, 3-a, 2x 4-H, 2x 5-H); 1.79-1.82 (1H, m, 3H-b); 2.00-2.12 (3H, m, 1'H-b, 2x 3'-H); 2.19-2.21 (1H, m, 2-H); 2.43-2.50 (1H, dt $J = 2.8$ and 10.4 Hz, 6H-a); 3.23-3.26 (1H, d $J = 10.4$ Hz, 6H-a); 4.84-4.97 (2H, m, 2x 5'-H); 5.71-5.82 (1H, m, 4'-H); δ_{C} (100 MHz; CDCl₃) 23.8 (C4), 25.3 (C1'), 25.9 (C5), 31.1 (C3), 32.9 (C2'), 34.2 (C3'), 59.7 (C6), 67.6 (C2), 114.4 (C5'), 138.8 (C4'). IR/cm⁻¹ 3076 (O-H br), 2932 (C-H),

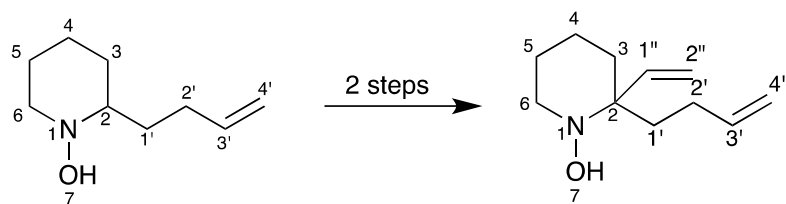
2857 (C-H), 1641 (C=C), 1442 (C-H). HRMS calcd for C₁₀H₁₉NO 169.1467: found
[M+H] 170.1505.

6-(Pent-4-en-1-yl)-2,3,4,5-tetrahydropyridine 1-oxide (118)



The synthesis was performed according to the literature procedure.⁶⁰ A solution of **116** (6.66g, 39 mmol) in dichloromethane (20 ml) was cooled to 0°C. Mercuric oxide (89 mmol, 19.2g) was added as a suspension in dichloromethane (70 ml) and the reaction mixture was warmed to r.t. and stirred for 3 h. The mixture was filtered through a pad of anhydrous sodium sulphate and Celite® and concentrated under reduced pressure to give *the title compound*, Rf value 0.05. This product was used without purification.

2-(But-3-en-1-yl)-2-vinylpiperidin-1-ol (273)

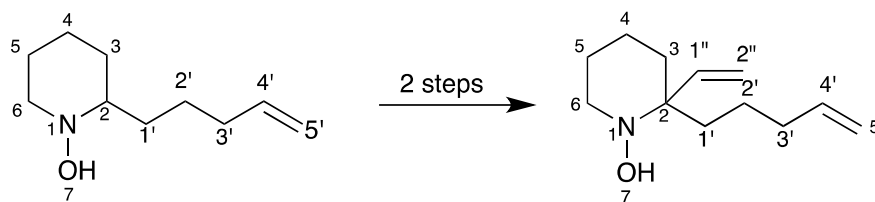


271 (3.2 mmol, 0.5g) was cooled to 0°C in dichloromethane (5 ml), before mercuric oxide (8.0 mmol, 1.74g) was added as a suspension in dichloromethane (15 ml), the reaction mixture was warmed to r.t. and stirred for 3 h. The mixture was filtered through a pad of anhydrous sodium sulphate and Celite® and concentrated under reduced pressure to give *the title compound*. This product was used without purification.

A mixture of the crude nitron was cooled to 0°C in tetrahydrofuran (15 ml) under argon. Commercially prepared vinylmagnesium bromide (1M, 4.8 mmol, 0.65 ml) was added drop-wise over 5 minutes. The reaction mixture to warm to r.t. and stirring for 4 h, then reaction mixture was quenched with saturated aqueous ammonium chloride before concentrating under reduced pressure. This mixture was extracted with diethyl ether (3 x 10 ml). The combined organic layers were dried with anhydrous sodium sulphate and concentrated under reduced pressure to give a yellow oil. This was purified by flash column chromatography on silica gel using ethyl acetate: hexane (1:1) gave *the title compound* as a pale yellow oil, R_f value 0.5. (0.19 g, 30%*) δ_H (400 MHz; CDCl₃) 1.22-2.38 (10H, m, 3-H, 4-H, 5-H, 1'-H, 2'-H); 3.60 (2H, m, 6-H); 4.92-5.03 (4H, m, 2''-H, 4'-H); 5.54-5.81 (2H, m, 1''-H, 3'-H). δ_C (100 MHz; CDCl₃) 11.0, 14.1,

23.8, 30.4, 38.8 (C3, C4, C5, C1', C2'); 68.2 (C6); 128.5, 130.9 (C2'', C4'); 132.5, 167.8 (C1', C3'). HRMS calcd for C₁₁H₁₉NO 181.1467: found [M+H] 182.1530.

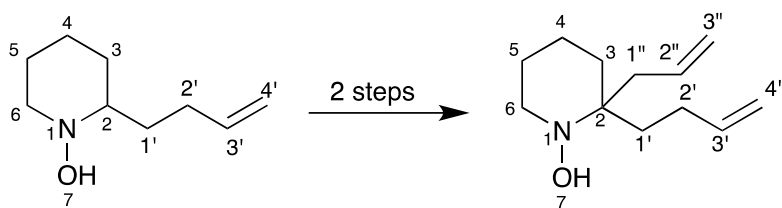
2-(Pent-4-en-1-yl)-2-vinylpiperidin-1-ol (274)



116 (0.5 g, 2.96 mmol) was cooled to 0°C in dichloromethane (5 ml), before mercuric oxide (6.66 mmol, 1.44 g) was added as a suspension in dichloromethane (15 ml), the reaction mixture was warmed to r.t. and stirred for 3 h. The mixture was filtered through a pad of anhydrous sodium sulphate and Celite[®] and concentrated under reduced pressure to give *the title compound*, Rf value 0.05. This product was used without purification.

A mixture of the crude intermediate was cooled to 0°C in tetrahydrofuran (15 ml) under argon. Commercially prepared vinylmagnesium bromide (1M, 4.4 mmol, 0.59 ml) was added drop-wise over 5 minutes, before allowing the reaction mixture to warm to r.t. and stirring for 4 h. Upon completion, the reaction mixture was quenched with saturated aqueous ammonium chloride before concentrating under reduced pressure to remove most of the tetrahydrofuran. This was then extracted with diethyl ether (3 x 10 ml). The combined organic layers were dried with anhydrous sodium sulphate and concentrated under reduced pressure to give a yellow oil. This was purified by flash column chromatography on silica gel using ethyl acetate: hexane (1:1) to give *the title compound*, Rf value 0.56, (0.24 g, 41%*). δ_{H} (400 MHz; CDCl₃) 1.06-2.09 (12H, m, 2x 1'-H, 2x 2'-H, 2x 3-H, 2x 3'-H, 2x 4-H, 2x 5-H); 2.82-3.08 (2H, m, 2x 6-H); 4.88-5.33 (4H, m, 2x 2''-H, 2x 5'-H); 5.73-5.89 (2-H, m, 1''-H, 4'-H). HRMS calcd for C₁₂H₂₁NO 195.1623: found [M+H] 196.1650.

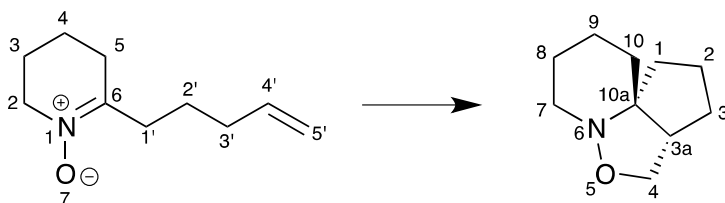
2-allyl-2-(but-3-en-1-yl)-piperidin-1-ol (272)



271 (3.3 mmol, 0.5 g) was cooled to 0°C in dichloromethane (5 ml), before mercuric oxide (7.45 mmol, 1.61 g) was added as a suspension in dichloromethane (15 ml), the reaction mixture was warmed to r.t. and stirred for 3 h. The mixture was filtered through a pad of anhydrous sodium sulphate and celite® and concentrated under reduced pressure to give *the title compound*, Rf value 0.05. This product was used without purification.

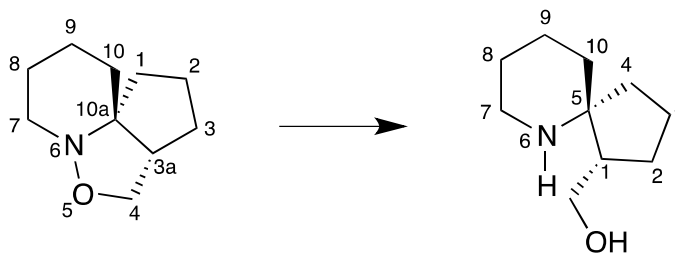
A mixture of the crude intermediate was cooled to -78°C in tetrahydrofuran (15 ml) under argon. Commercially prepared allylmagnesium chloride (2M, 6.6 mmol, 0.34 ml) was added drop-wise over 5 minutes. The mixture was stirred at -78°C for 2 h, before quenching with saturated aqueous ammonium chloride. The reaction mixture was concentrated under reduced pressure to remove most of the tetrahydrofuran, before extracting with diethyl ether (3 x 10 ml). The combined organic layers were dried with anhydrous sodium sulphate and concentrated under reduced pressure to give an orange oil. This was purified by flash column chromatography on silica gel using ethyl acetate: hexane (1:1) to give *the title compound* as an orange oil, Rf value 0.49. (0.07g, 21%*). δ_{H} (400 MHz; CDCl₃) 1.21-2.49 (12H, m, 2x 1'-H, 2x 1''-H, 2x 2'-H, 2x 3-H, 2x 4-H, 2x 5-H); 3.57-3.65 (2H, m, 2x 6-H); 4.91-5.04 (4H, m, 2x 3''-H, 2x 4'-H); 5.76-5.82 (2H, m, 2''-H, 3'-H). HRMS calcd for C₁₂H₂₁NO 195.1623: found [M+H] 196.1692.

(3*aS,10*aS**)-Octahydro-1*H*-cyclopenta[3.4]isoxazolo[2,3-*a*]pyridine (119)**



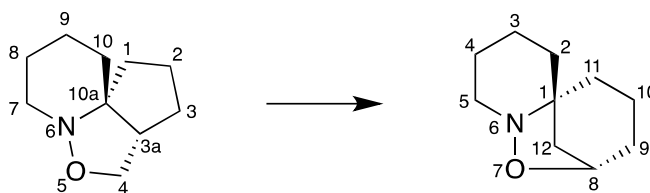
The synthesis was performed according to the literature procedure.⁶⁰ A solution of crude compound **118** in toluene (50 ml) was heated under reflux for 24 h. The mixture was cooled to r.t. and concentrated under reduced pressure to obtain a dark brown oil. This was purified by flash column chromatography on silica gel using diethyl ether: hexane (1:1) as the eluent to give *the title compound* (3.50g, 53%) as a yellow oil, R_f value 0.5. δ_{H} (400 MHz; CDCl₃) 1.29-1.53 (4H, m, 2x 2-H, 8a-H, 10a-H); 1.54-1.93 (8H, m, 2x 1-H, 2x 3-H, 8H-b, 2x 9-H, 10b-H); 2.55-2.63 (1H, m, 3a-H); 2.77-2.89 (1H, m, 7a-H); 2.99-3.10 (1H, m, 7b-H); 3.39-3.48 (1H, dd $J = 3.2$ and 8.4 Hz, 4a-H); 4.20-4.31 (1H, t $J = 8$ Hz, 4b-H). δ_{C} (400 MHz, CDCl₃) 21.6 (C1), 22.8 (C10), 24.1 (C9), 31.4 (C2), 33.2 (C3), 39.2 (C8), 49.9 (C3a), 50.4 (C7), 72.2 (C4), 75.2 (C10a). IR/cm⁻¹ 2933 (C-H), 2856 (C-H), 1444 (C-H), 850 (C-H). HRMS calcd for C₁₀H₁₇NO 167.1310: found [M+H] 168.1352.

(1*S,5*S**)-6-Azaspiro[4.5]decan-1-ylmethanol (244)**



The synthesis was performed according to the literature procedure.⁶³ A solution of **119** (3.80g, 22.5 mmol) in acetic acid: water (1:1, 60 ml) with zinc dust (179.9 mmol, 11.76g) was heated under reflux for 4 h. The reaction mixture was then cooled to r.t., before quenching with saturated aqueous sodium bicarbonate (40 ml) and extracting with chloroform (3 x 30 ml). The organic layers were combined, dried with anhydrous sodium sulphate and concentrated under reduced pressure to give a crude yellow oil. This was purified by flash column chromatography on silica gel using dichloromethane: methanol (9:1) as the eluent to give *the title compound* (3.53g, 93%) as a pale yellow oil, R_f value 0.15. δ_{H} (400 MHz; CDCl₃) 1.46-2.03 (13H, m, 2x 3-H, 2x 4-H, 2x 5-H, 6-H, 2x 7-H, 2x 8-H, 2x 9-H; 2.78-2.85 (1H, m, 2b-H), 3.18-3.21 (1H, d $J = 13.2$ Hz, 2a-H), 3.72-3.81 (2H, m, 2x 1'-H). δ_{C} (100 MHz; CDCl₃) 20.5, 22.0, 23.0, 26.9, 32.8, 34.8 (C3, C4, C5, C6, C7, C8); 41.7 (C2); 50.1 (C9); 61.7 (C10); 65.8 (C5a). IR/cm⁻¹ 3277 (O-H br), 2944 (C-H), 2869 (C-H), 1558 (N-H), 1401 (C-H). HRMS calcd for C₁₀H₁₉NO 169.1467; found [M+H] 170.1529.

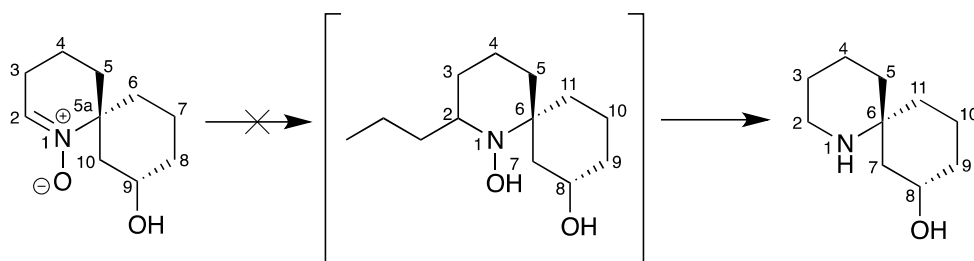
(1*R- 8*S**)-7-Oxa-6-aza-tricyclo[6.3.1.0^{1,6}]dodecane (198)**



A solution of **119** (2.0g, 11.4 mmol) in toluene (10 ml) was heated by microwave irradiation at 220°C for 2.5 h. The resulting black solution was concentrated under reduced pressure. Purification by column chromatography using diethyl ether: hexane (1:1), gave *the title compound* (1.27g, 76%) as a pale yellow oil, R_f value 0.26. The remaining starting material was recovered for further use.

δ_{H} (400 MHz; CDCl₃) 0.89-1.48 (11H, m, 4a-H, 2x 2-H, 2x 3-H, 9a-H, 2x 10-H, 2x 11-H, 12a-H); 1.64-1.67 (2H, m, 4b-H, 9b-H); 2.14-2.40 (2H, m, 12b-H, 5a-H); 3.00 (1H, m, 5b-H); 4.26 (1H, m, 8-H). δ_{C} (100 MHz; CDCl₃) 18.8, 19.7, 24.7, 31.5 (C2, C3, C10, C11), 33.2 (C4), 38.3 (C12), 40.0 (C9), 55.3 (C5), 62.4 (C1), 75.4 (C8). IR/cm⁻¹ 2928 (C-H), 1447 (c-H₂), 872 (C-H). HRMS calcd for C₁₀H₁₇NO 167.1310: found [M+H] 168.1387.

(6*R,8*S**)-8-hydroxy-1-azaspiro[5.5]undecane (280)**

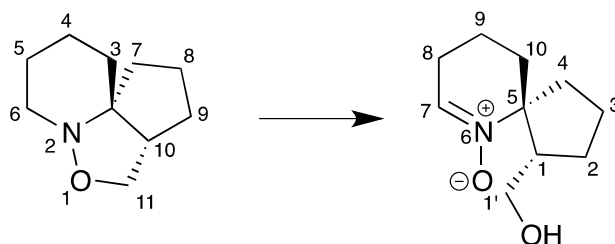


231 (0.1 g, 0.55 mmol) was cooled to 0°C in tetrahydrofuran (10 ml) under argon. Propylmagnesium bromide (0.5 ml), prepared according to the general procedure in tetrahydrofuran (10 ml) was added drop-wise over 5 minutes, before warming to r.t. and allowing to stir for 10 h. The reaction mixture was quenched with saturated aqueous ammonium chloride and extracted with diethyl ether (3 x 10 ml). The combined organic layers were dried with anhydrous sodium sulphate and concentrated under reduced pressure to give a crude oil, which was used without purification.

The crude nitronium in acetic acid: water (1:1, 10 ml) and zinc dust (4.4 mmol, 0.29g) was heated under reflux for 4 h. Upon cooling, the reaction mixture was quenched using saturated aqueous sodium bicarbonate and extracted using dichloromethane (3 x 15 ml). The combined organic extracts were dried using anhydrous sodium sulphate and concentrated under reduced pressure. The crude product was purified by flash column chromatography on silica gel using chloroform: methanol (9:1) as the eluent to give *the title compound*, R_f value 0.15 (33 mg, 35%). δ_H (400 MHz; CDCl₃) 1.14-1.73 (11 H, m, 2x 3-H, 2x 4-H, 2x 5-H, 9a-H, 2x 10-H, 2x 11-H); 1.89-2.01 (2H, m, 7a-H, 9b-H); 2.45-2.53 (2H, m, 2a-

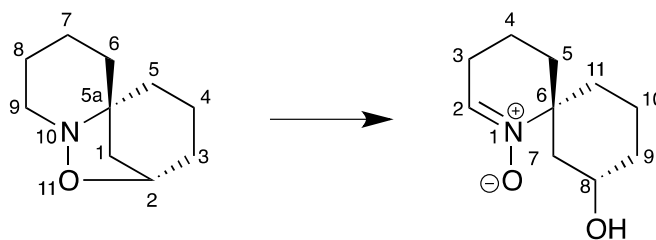
H, 7b-H); 3.24 (1H, t $J = 6.8$ Hz, 2b-H); 4.54 (1H, t $J = 5.6$ Hz, 8-H). δ_c (100 MHz; CDCl₃) 19.0, 19.9, 25.0, 31.6 (C4, C5, C10, C11), 33.4 (C3), 38.6 (C9), 40.2 (C7), 55.6 (C2), 62.7 (C8), 75.7 (C6). IR/ cm⁻¹ 3363 (O-H br), 2931 (C-H), 1481 (C-H₂), 871 (C-H). HRMS calcd for C₁₀H₁₉NO 169.1467: found [M-H] 168.1381.

(1*S,5*S**)-1-(hydroxymethyl)-6-azaspiro[4.5]-dec-6-ene 6-oxide (147)**



The synthesis was performed according to literature procedure.⁶³ A solution of isoxazolidine **119** (30.8 mmol, 5.2 g) in dichloromethane (200 ml) was cooled to 0°C under argon. mCPBA (1.5 equiv. at ~77%, 46.2 mmol, 7.96 g) in dichloromethane (150 ml) was added drop wise over 7 hours. On completion of the addition, the mixture was warmed to r.t. and left to stir for 20 hours. The reaction mixture was quenched with a solution of saturated aqueous sodium thiosulfate: saturated aqueous sodium bicarbonate (1:1) (160 ml) and extracted with dichloromethane (3 x 40 ml). The organic layers were combined, dried with anhydrous sodium sulphate and concentrated under reduced pressure to give an orange oil. Purification was performed by flash column chromatography on silica gel using dichloromethane: methanol (9.5: 0.5) as the eluent gave *the title compound*, R_f value 0.44 (2.78 g, 49%) as an orange solid. δ_{H} (400 MHz; CDCl₃) 1.41-2.05 (9H, m, 2a-H, 2x 3-H, 2x 4-H, 2x 9-H, 2x 10-H), 2.09-2.21 (1H, m, 2a-H), 2.39-2.44, (2H, m, 2x 8-H), 2.69-2.73 (1H, m, 1-H), 3.61-3.72 (2H, m, 2x 1'-H) 7.29 (1H, t *J* = 4.4 Hz, 7-H). δ_{C} (100 MHz; CDCl₃) 15.6, 24.2 (C4, C10), 26.5 (C8), 28.4 (C3), 37.2 (C9), 38.7 (C2), 52.9 (C1), 61.2 (C'1), 77.6 (C5), 141.9 (C7). IR/ cm⁻¹ 3272 (O-H br), 2936 (C-H), 1448 (C-H) 1114 (C-O), 791 (C-H). HRMS calcd for C₁₀H₁₇NO₂ 183.1259: found [M+H] 184.1331.

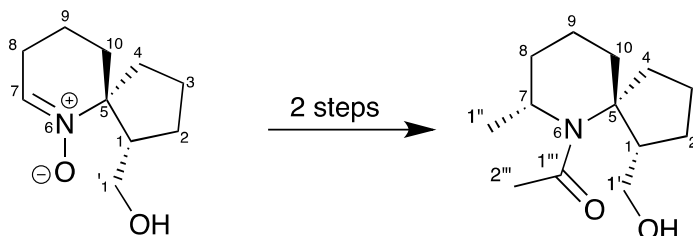
(6*R,8*S**)-8-hydroxy-1-azaspiro[5.5]undec-1-ene 1-oxide (231)**



To a cooled solution of isoxazolidine **198** (2.2 g, 13 mmol) in dichloromethane (90 ml) under argon, a solution of mCPBA (1.5 equiv. at ~77%, 20 mmol, 3.37g) in dichloromethane (70 ml) was added drop-wise over 7 hours. The mixture was then warmed to r.t. and left to stir overnight. Upon completion the reaction was quenched with a mixture of saturated aqueous sodium thiosulfate: saturated aqueous sodium bicarbonate (1:1, 50 ml), and washed with dichloromethane (3x 20 ml). The combined organic layers were dried with anhydrous sodium sulphate and concentrated under reduced pressure. Purification by flash column chromatography on silica gel using dichloromethane: methanol (9.5: 0.5) as the eluent gave *the title compound* (1.43 g, 60%) as an orange oil, R_f value 0.37 δ_H (400 MHz; $CDCl_3$) 1.39-1.83 (9H, m, 3a-H, 2x 4-H, 2x 5-H, 2x 10-H, 2x 11-H); 2.06-2.49 (5H, m, 3b-H, 2x 7-H, 2x 9-H); 3.83 (1H, m, 8-H); 7.18 (1H, t $J = 4$ Hz, 2-H). δ_C (100 MHz; $CDCl_3$) 14.4, 18.5, 26.2, 33.4 (C4, C5, C10, C11); 37.1, 35.4 (C3, C9); 42.3 (C7); 68.1 (C6); 64.6 (C8); 138.2 (C2). HRMS calcd for $C_{10}H_{17}NO_2$ 183.1259: found $[M+H]$ 184.1329.

(1S*,5S*,7R*)-1-(hydroxymethyl)-6-acetyl-7-methyl-6-azaspiro[4.5]decane

(205)



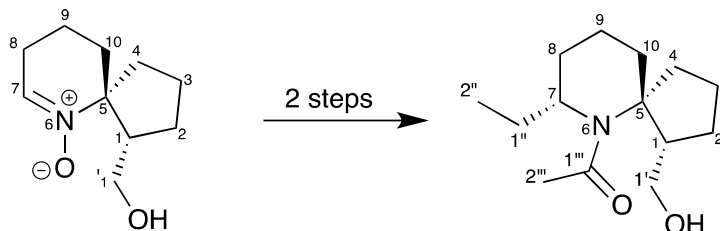
A solution of spironitrone **147** (0.13 g, 0.71 mmol) was cooled to 0°C in THF (5 ml) under Ar. Commercially prepared methylmagnesium bromide (3M, 4.3 mmol, 0.16 ml) was added drop-wise before warming to r.t. and leaving to stir for 10 hours. The reaction mixture was quenched with saturated aqueous ammonium chloride (10 ml) and extracted with diethyl ether (3x 10 ml). The combined organic layers were dried with anhydrous sodium sulphate and concentrated under reduced pressure. The crude orange residue obtained was reduced without purification.

A mixture of the crude hydroxylamine (0.085 g, 0.42 mmol) and zinc dust (3.4 mmol, 0.22g) in acetic acid: water (1:1, 10 ml) was heated under reflux for 4 h. Upon completion, the mixture was cooled to r.t. and quenched with saturated aqueous sodium bicarbonate (10 ml) and extracted with dichloromethane (4 x 15 ml). The combined organic layers were dried using anhydrous sodium sulphate and concentrated under reduced pressure. Purification by flash column chromatography using dichloromethane: methanol (9: 1) as the eluent gave *the title compound* (70 mg, 44%) as a pale yellow oil, R_f value 0.17 δ_H (400

MHz; CDCl₃) 1.21 (3H, d $J = 6.4$ Hz, 3x 1''-H); 1.39-1.81 (10H, m, 2x 2-H, 2x 3-H, 2x 4-H, 2x 9-H, 2x 10-H); 1.90 (3H, s, 2'''-H); 2.01-2.15 (1H, m, 8a-H); 2.37 (1H, m, 1-H); 3.55 (2H, m, 7-H, 1'-H); 3.70-3.78 (1H, m, 1'-H). δ_c (100 MHz; CDCl₃) 19.1, 26.1, 31.1, 33.5, 36.3 (C2, C3, C4, C9, C10); 19.8 (C1''); 20.0 (C2'''-H); 36.3 (C8); 41.5 (C1); 51.1 (C7); 63.7 (C1'); 66.4 (C5); 178.5 (C1'''). IR/ cm⁻¹ 3245 (O-H br), 2926 (C-H), 1735 (C=O), 1302 (C-H), 731 (C-H). HRMS calcd for C₁₃H₂₃NO₂ 225.1729: found [M+H] 226.1797.

(1S*,5S*,7R*)-1-(hydroxymethyl)-6-acetyl-7-ethyl-6-azaspiro[4.5]decane

(206)



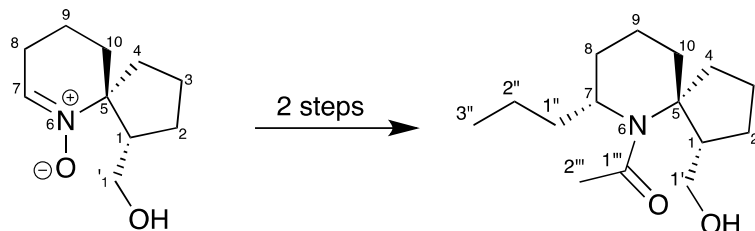
A solution of spironitrone **147** (0.10 g, 0.55 mmol) in tetrahydrofuran (5 ml) was cooled to 0°C under Ar. Ethylmagnesium bromide (1.0 ml), prepared according to the general procedure in tetrahydrofuran (10 ml), was added drop-wise before warming to r.t. and leaving to stir for 10 h. The reaction mixture was quenched with saturated aqueous ammonium chloride (10 ml) and extracted with diethyl ether (3 x 10 ml). The combined organic layers were dried with anhydrous sodium sulphate and concentrated under reduced pressure. The crude orange residue obtained was reduced without purification.

A mixture of the crude hydroxylamine (57 mg, 0.23 mmol) and zinc dust (1.9 mmol, 0.12 g) in acetic acid: water (1:1, 8 ml) was heated under reflux for 4 h. Upon completion, the mixture was cooled and quenched with saturated aqueous sodium bicarbonate (10 ml) before extracting with dichloromethane (4 x 15 ml). The combined organic layers were dried using anhydrous sodium sulphate and concentrated under reduced pressure. Purification by flash column chromatography using dichloromethane: methanol (9: 1) as the eluent gave *the title compound* (50 mg, 38%) as a pale yellow oil, R_f value 0.17 δ_H (400

MHz; CDCl₃) 0.87 (3H, t $J = 7.6$ Hz, 3x 2''-H); 1.26-1.89 (13H, m, 2x 1'-H, 2x 2-H, 2x 3-H, 2x 4-H, 8a-H, 2x 9-H, 2x 10-H); 1.93 (3H, s, 3x 1'''-H); 2.22 (1H, m, 8b-H); 2.43 (1H, m, 1-H); 3.38 (1H, m, 7-H), 3.55 (1H, m, 1'a-H); 3.81-3.87 (1H, m, 1'b-H). δ_c (100 MHz; CDCl₃) 18.8, 19.5, 25.6, 26.6, 27.7, 33.4, 35.3 (C1', C2, C3, C4, C8, C9, C10); 23.8 (C2'''); 41.5 (C1); 57.0 (C7); 63.2 (C1'); 67.0 (C5); 177.9 (C1'''). IR/ cm⁻¹ 3210 (O-H br), 2931 (C-H), 2562 (C-H), 1747 (C=O), 1264 (C-H), 1101 (O-H). HRMS calcd for C₁₄H₂₅NO₂ 239.1885: found [M+H] 240.1955.

(1S*,5S*,7R*)-1-(hydroxymethyl)-6-acetyl-7-propyl-6-azaspiro[4.5]decane

(207)



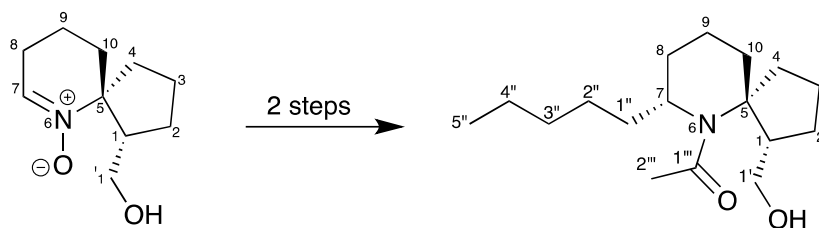
A solution of spironitrone **147** (0.10 g, 0.55 mmol) was cooled to 0°C in tetrahydrofuran (5 ml) under Ar. Propylmagnesium bromide (1.0 ml), prepared according to the general procedure in tetrahydrofuran (10 ml), was added drop-wise before warming to r.t. and leaving to stir for 10 h. The reaction mixture was quenched with saturated aqueous ammonium chloride (10 ml) and extracted with diethyl ether (3x 10 ml). The combined organic layers were dried with anhydrous sodium sulphate and concentrated under reduced pressure. The crude orange residue obtained was reduced without purification.

A mixture of the crude hydroxylamine (0.04 g, 0.15 mmol) and zinc dust (1.2 mmol, 80 mg) in acetic acid: water (1:1, 8 ml) was heated under reflux for 4 h. Upon completion, the mixture was cooled and quenched with saturated aqueous sodium bicarbonate (10 ml) before extracting with dichloromethane (4 x 15 ml). The combined organic layers were dried using anhydrous sodium sulphate and concentrated under reduced pressure. Purification by flash column chromatography using dichloromethane: methanol (9: 1) as the eluent gave *the title compound* (32 mg, 28%) as a pale yellow oil, R_f value 0.33 δ_H (400

MHz; CDCl₃) 0.87 (3H, t $J = 6.8$ Hz, 3x 3''-H); 1.19-1.82 (15H, m, 2x 1''-H, 2x 2''-H, 2x 2-H, 2x 3-H, 2x 4-H, 8a-H, 2x 9-H, 2x 10-H); 1.96 (3H, t, 3x 1'''-H); 1.96-2.05 (1H, m, 8b-H); 2.29 (1H, m, 1-H); 3.12-3.15 (1H, m, 7-H); 3.60 (1H, m, 1'a-H); 3.73 (1H, m, 1'b-H). δ_c (100 MHz; CDCl₃) 14.2 (C3''); 18.9, 19.6, 20.2, 26.6, 30.3, 35.2, 37.7, 38.0 (C1'', C2'', C2, C3, C4, C8a, C9, C10); 24.4 (C2'''); 41.5 (C1); 54.6 (C7); 64.5 (C1'); 65.8 (C5); 178.1 (C1'''). IR/ cm⁻¹ 3220 (O-H br), 2943 (C-H), 1736 (C=O), 1124 (C-H). HRMS calcd for C₁₅H₂₇NO₂ 253.2042 (211.194 -COCH₃): found [M+H] 212.201 -COCH₃ observed.

(1S*,5S*,7R*)-1-(hydroxymethyl)-6-acetyl-7-pentyl-6-azaspiro[4.5]decane

(208)



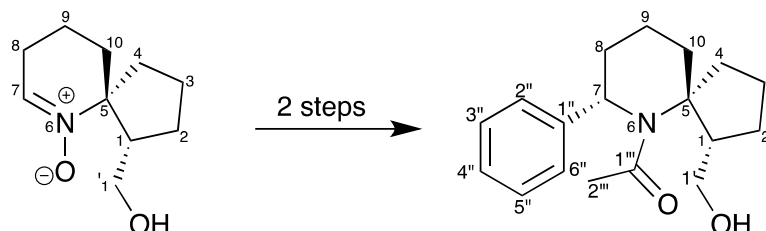
A solution of spironitrone **147** (0.10 g, 0.55 mmol) was cooled to 0°C in tetrahydrofuran (5 ml) under Ar. Pentylmagnesium bromide (1.0 ml), prepared according to the general procedure, was added drop-wise before warming to r.t. and leaving to stir for 10 h. The reaction mixture was quenched with saturated aqueous ammonium chloride (10 ml) and extracted with diethyl ether (3x 10 ml). The combined organic layers were dried with anhydrous sodium sulphate and concentrated under reduced pressure. The crude orange residue obtained was reduced without purification.

A mixture of the crude hydroxylamine (60 mg, 0.33 mmol) and zinc dust (1.9 mmol, 0.12 g) in acetic acid: water (1:1, 8 ml) was heated under reflux for 4 h. Upon completion, the mixture was cooled and quenched with saturated aqueous sodium bicarbonate (6 ml) before extracting with dichloromethane (4 x 15 ml). The combined organic layers were dried using anhydrous sodium sulphate and concentrated under reduced pressure. Purification by flash column chromatography using dichloromethane: methanol (9: 1) as the eluent gave the title compound (43 mg, 33%) as a pale yellow oil. R_f value 0.45 δ_H (400

MHz; CDCl₃) 0.81 (3H, t $J = 6.8$ Hz, 3x 5''-H); 1.20-1.94 (19H, m, 2x 1''-H, 2x 2''-H, 2x 3''-H, 2x 4''-H, 2x 2-H, 2x 3-H, 2x 4-H, 8a-H, 2x 9-H, 2x 10-H); 1.94 (3H, s, 3x 1'''-H); 2.22 (1H, m, 8b-H); 2.45 (1H, m, 1-H); 2.86-2.91 (1H, m, 7-H); 3.50-3.54 (1H, m, 1'-H); 3.80-3.88 (1H, m, 8b-H). δ_c (100 MHz; CDCl₃) 14.2 (C5''); 20.5, 21.0, 25.6, 27.8, 32.1, 33.0, 37.7, 37.9, 41.1 (C1'', C2'', C2, C3'', C3, C4'', C4, C8, C8, C9, C10); 41.7 (C1); 53.5 (C7); 64.2 (C1'); 65.8 (C5), 178.1 (C1'''). IR/ cm⁻¹ 3201 (O-H br), 2931 (C-H), 1754 (C=O), 921 (C-H), 727 (C-H). HRMS calcd for C₁₇H₃₁NO₂ 281.2355 (239.225 -COCH₃): found [M+H] 240.2318.

(1*S,5*S**,7*R**)-1-(hydroxymethyl)-6-acetyl-7-phenyl-6-azaspiro[4.5]decane**

(209)



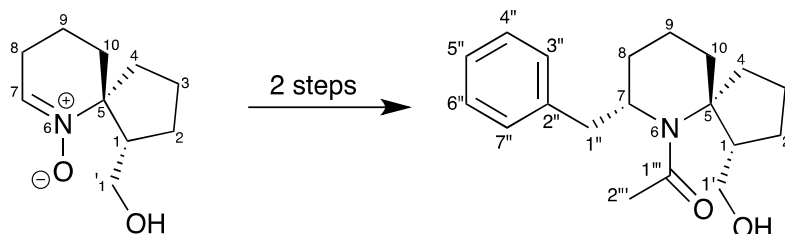
A solution of nitronium **147** (0.2 g, 0.1 mmol) in tetrahydrofuran (10 ml) was cooled to 0°C under Ar. Phenylmagnesium bromide in tetrahydrofuran (1.8 ml), prepared according to the general procedure, was added drop-wise, before warming to r.t and leaving to stir for 2 hours. Upon completion, the reaction mixture was quenched with water (3 ml) and saturated aqueous ammonium chloride and extracted with diethyl ether (3 x 10 ml). The combined organic extracts were dried with anhydrous sodium sulphate and concentrated under reduced pressure. The crude orange residue obtained was reduced without purification.

The crude starting material (0.15 mmol, 40 mg) in glacial acetic acid: water (1:1, 10 ml) with zinc dust (1.2 mmol, 79 mg) was heated under reflux for 4 h. Once cooled the reaction mixture was quenched with saturated aqueous sodium bicarbonate (10 ml) before extracting with dichloromethane (3 x 15 ml). The combined organic layers were dried with anhydrous sodium sulphate and concentrated under reduced pressure. Purification by flash column chromatography on silica gel using dichloromethane: methanol (9.5: 0.5) as the

eluent gave *the title compound* (0.008g, 6%) as a colourless oil, R_f value 0.69 δ_{H} (400 MHz; CDCl₃) 1.42-2.0 (12H, m, 2x 2-H, 2x 3-H, 2x 4-H, 2x 8-H, 2x 9-H, 2x 10-H); 2.45 (1H, m, 1-H); 2.98 (1H, t $J = 26.8$ Hz, 1'a-H); 3.30 (1H, dd $J = 6.8$ and 12 Hz, 1'b-H); 4.33-4.37 (1H, m, 7-H); 7.2-7.3 (3H, m, 3''-H, 4''-H, 5''-H); 7.4 (2H, m, 2''-H, 6''-H). δ_{C} (100MHz; CDCl₃) 18.8, 20.5, 25.4, 31.1, 33.6, 36.0 (C-2, C-3, C-4, C-8, C-9, C-10); 23.6 (C-2''); 40.6 (C-1); 59.1 (C-7); 63.3 (C-1'); 67.2 (C-5); 127.9 (C-2'', C6''); 128.4 (C4''); 128.8 (C3'', C5''). IR/cm⁻¹ 3220 (O-H br), 2950 (C-H), 1717 (C=O), 1491 (C-H₂), 852 (=C-H). HRMS calcd for C₁₈H₂₅NO₂ 287.1885 (-COCH₃ 245.178): found [M+H] 246.1853 – COCH₃ observed.

(1*S,5*S**,7*R**)-1-(hydroxymethyl)-6-acetyl-7-benzyl-6-azaspiro[4.5]decane**

(209)

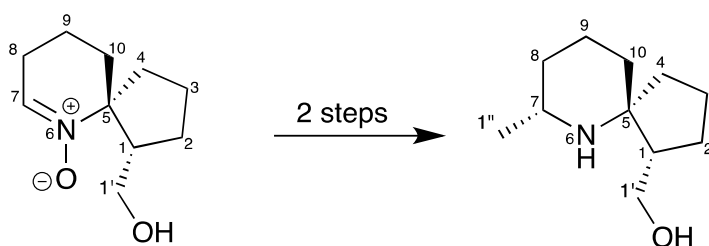


A solution of spironitrone **147** (0.10 g, 0.55 mmol) was cooled to 0°C in tetrahydrofuran (5 ml) under Ar. Benzylmagnesium bromide (0.4 ml), prepared according to the general procedure in tetrahydrofuran, was added drop-wise before warming to r.t. and leaving to stir for 10 h. The reaction mixture was quenched with saturated aqueous ammonium chloride (10 ml) and extracted with diethyl ether (3 x 10 ml). The combined organic layers were dried with anhydrous sodium sulphate and concentrated under reduced pressure. The crude orange residue obtained was reduced without purification.

A mixture of the crude intermediate (60 mg, 0.33 mmol) and zinc dust (1.9 mmol, 0.12 g) in acetic acid: water (1:1, 8 ml) was heated under reflux for 4 h. Upon completion, the mixture was cooled and quenched with saturated aqueous sodium bicarbonate (10 ml) before extracting with dichloromethane (4 x 15 ml). The combined organic layers were dried using anhydrous sodium sulphate and concentrated under reduced pressure. Purification by flash column chromatography using dichloromethane: methanol (9: 1) as the eluent gave *the title compound* (69 mg, 42%) as a white solid, R_f value 0.69 δ_H (400

MHz; CDCl₃) 1.19-1.67 (12H, m, 2x 2-H, 2x 3-H, 2x 4-H, 2x 8-H, 2x 9-H, 2x 10-H); 1.78-1.88 (2H, m, 2x 1''-H); 1.98-2.12 (4H, m, 2x 1'-H, 2x 2'''-H); 3.69-3.72 (1H, d $J = 11.6$ Hz, C7); 4.09 (1H, dd $J = 3.2$ and 11.2 Hz, 1'a-H); 4.35-4.39 (1H, dd $J = 4.8$ and 11.2 Hz, 1'b-H), 7.20-7.31 (4H, m, 2''-H, 4''-H, 5''-H, 6''-H); 7.37-7.38 (2H, m, 3''-H, 7''-H). δ_c (100MHz; CDCl₃) 21.3 (C2'''); 21.8, 23.1, 28.2, 34.6, 35.5, 35.8 (C2, C3, C4, C8, C9, C10); 49.3 (C1); 56.7 (C7); 63.5 (C5); 65.7 (C1'); 127.0 (C3'', C7''); 128.4 (C4'', C6''); 146.5 (C5''); 171.5 (C1'''). IR/cm⁻¹ 3210 (O-H br), 2926 (C-H), 1731 (C=O), 1590 (C=C), 1397 (C-H), 984 (C-H), 802 (C-H₂), m.p. 63-64°C.

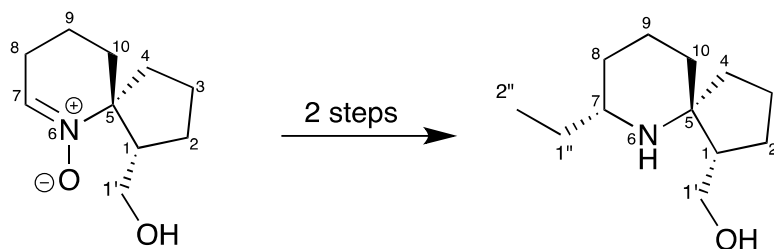
(1S*,5S*,7R*)-1-(hydroxymethyl)-7-methyl-6-azaspiro[4.5]decane (211)



A solution of spironitrone **147** (0.18 g, 0.98 mmol) was cooled to 0°C in tetrahydrofuran (10 ml) under Ar. Commercially prepared methylmagnesium bromide (3M, 2.9 mmol, 0.11 ml) was added drop-wise before warming to r.t. and leaving to stir for 10 hours. The reaction mixture was quenched with ethanol: saturated aqueous ammonium chloride (2:1, 10 ml) and indium powder (0.55 mmol, 0.06 g) was added before heated under reflux for 4 h. Upon cooling, diethyl ether and saturated aqueous ammonium chloride were added and the aqueous layer further extracted with diethyl ether (3 x 10 ml). The combined organic extracts were dried using anhydrous sodium sulphate and concentrated under reduced pressure. This was purified by flash column chromatography on silica gel using dichloromethane: methanol (9:1) as the eluent gave *the title compound* (76 mg, 42%) as a pale white solid, R_f value 0.48. δ_{H} (400 MHz; CDCl₃) 1.44-1.46 (3H, d $J = 6.4$ Hz, 1''-H); 1.56-1.83 (11H, m, 2x 2-H, 2x 3-H, 2x 4-H, 8a-H, 2x 9-H, 2x 10-H); 2.29-2.38 (1H, m, 8b-H); 2.49 (1H, m, 1-H); 3.54-3.58 (1H, m, 1'a-H); 3.70 (1H, m, 7-H); 4.00-4.06 (1H, m, 1'b-H). δ_{C} (100MHz; CDCl₃) 19.4 (C1''); 18.6, 19.6, 25.2, 27.6, 30.3, 32.4 (C2, C3, C4, C8, C9, C10); 41.0 (C1); 52.7 (C7); 63.1 (C1'); 67.7 (C5). IR/cm⁻¹ 3310 (O-H br), 2940, (C-

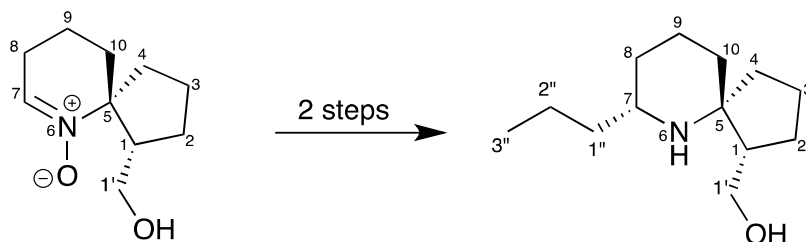
H), 1448 (C-H₂), 7.26 (C-H₂), m.p. 161-163°C. HRMS calcd for C₁₁H₂₁NO
183.1623: found [M+H] 184.1696.

(1*S,5*S**,7*R**)-1-(hydroxymethyl)-7-ethyl-6-azaspiro[4.5]decane (212)**



A solution of spirinitrone **147** (0.17 g, 0.93 mmol) was cooled to 0°C in tetrahydrofuran (10 ml) under Ar. Ethylmagnesium bromide (1.5 ml), prepared according to the general procedure in tetrahydrofuran, was added drop-wise before warming to r.t. and leaving to stir for 10 hours. The reaction mixture was quenched with ethanol: saturated aqueous ammonium chloride (2:1, 10 ml) and indium powder (0.55 mmol, 0.06 g) was added before heated under reflux for 4 h. Upon cooling, diethyl ether and saturated aqueous ammonium chloride were added and the aqueous layer further extracted with diethyl ether (3 x 10 ml). The combined organic extracts were dried using anhydrous sodium sulphate and concentrated under reduced pressure. This was purified by flash column chromatography on silica gel using dichloromethane: methanol (9:1) as the eluent gave *the title compound* (49 mg, 27%) as a pale yellow oil, R_f value 0.47 δ_H (400 MHz; CDCl₃) 0.83-0.87 (3H, t *J* = 7.6 Hz, 3x 2''-H); 1.41-1.90 (14H, m, 2x 2''-H, 2x 2-H, 2x 3-H, 2x 4-H, 2x 8-H, 2x 9-H, 2x 10-H); 2.43 (1H, m, 1-H); 3.38 (1H, m, 7-H); 3.60 (1H, m, 1'a-H); 3.78 (1H, m, 1'b-H). δ_C (100MHz; CDCl₃) 10.4 (C2''); 18.7, 19.4, 23.2, 25.0, 26.7, 28.6, 35.1 (C1'', C2, C3, C4, C8, C9, C10); 42.3 (C1); 50.3 (C7); 62.4 (C1). IR/cm⁻¹ 3268 (O-H br), 2937 (C-H), 1458 (C-H₂), 725 (C-H₂). HRMS calcd for C₁₂H₂₃NO 197.1780: found [M+H] 198.1849.

(1*S,5*S**,7*R**)-1-(hydroxymethyl)-7-propyl-6-azaspiro[4.5]decane (213)**

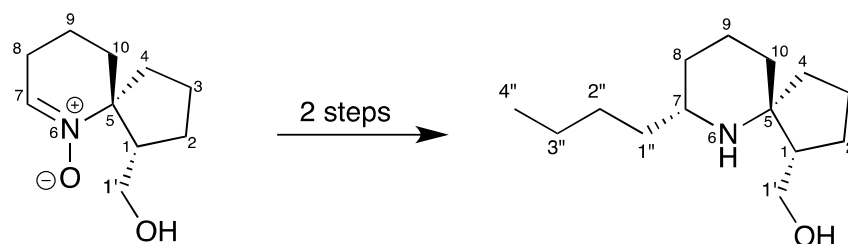


A solution of spironitrone **147** (0.18 g, 0.98 mmol) was cooled to 0°C in tetrahydrofuran (10 ml) under Ar. Propylmagnesium bromide (1.6 ml), prepared according to the general procedure in tetrahydrofuran, was added drop-wise before warming to r.t. and leaving to stir for 10 hours. The reaction mixture was quenched with ethanol: saturated aqueous ammonium chloride (2:1, 10 ml) and indium powder (0.55 mmol, 0.06g) was added before heated under reflux for 4 h. Upon cooling, diethyl ether and saturated aqueous ammonium chloride were added and the aqueous layer further extracted with diethyl ether (3 x 10 ml). The combined organic extracts were dried using anhydrous sodium sulphate and concentrated under reduced pressure. This was purified by flash column chromatography on silica gel using chloroform: methanol (9:1) as the eluent to give *the title compound* (60 mg, 29%) as a white solid. δ_{H} (400 MHz; CDCl_3) 0.83-0.87 (3H, t $J = 7.6$ Hz, 3x 3''-H); 1.24-2.07 (15H, m, 2x 2''-H, 2x 2-H, 2x 3''-H, 2x 3-H, 2x 4-H, 8a-H, 2x 9-H, 2x 10-H); 2.34-2.46 (2H, m, 1-H, 8b-H); 3.50-3.54 (2H, dd $J = 3.2$ and 11.6 Hz, 1'-H, 7-H); 3.99-4.05 (1H, t $J = 11.6$ Hz, 1'-H). δ_{C} (100MHz; CDCl_3) 13.8 (C3''); 18.5, 18.7, 19.4, 25.1, 27.6, 32.7, 34.8, 35.4 (C1'', C2'', C2, C3, C4, C8, C9, C10); 41.0 (C1); 56.6 (C7); 62.3 (C1'); 68.0 (C5). IR/ cm^{-1} 3161 (O-H br), 2934 (C-H), 1616 (N-H), 1466 (O-H), 1064 (C-

C), 739 (C-H₂), m.p. 167-169°C, HRMS calcd for C₁₃H₂₅NO 211.1936: found [M+H]

212.2008.

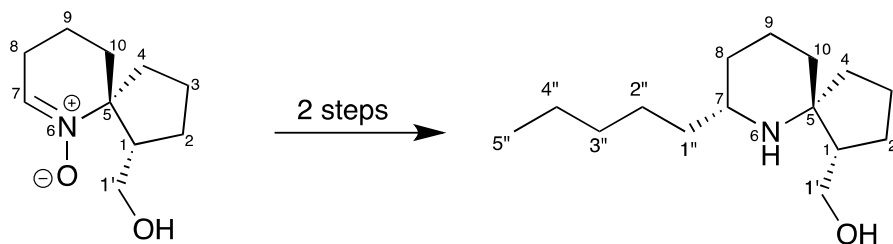
(1S*,5S*,7R*)-1-(hydroxymethyl)-7-butyl-6-azaspiro[4.5]decane (214)



A solution of spironitrone **147** (0.15 g, 0.82 mmol) was cooled to 0°C in tetrahydrofuran (10 ml) under Ar. Butylmagnesium bromide (1.5 ml), prepared according to the general procedure in tetrahydrofuran, was added drop-wise before warming to r.t. and leaving to stir for 10 hours. The reaction mixture was quenched with ethanol: saturated aqueous ammonium chloride (2:1, 10 ml) and indium powder (0.55 mmol, 0.06 g) was added before heated under reflux for 4 h. Upon cooling, diethyl ether and saturated aqueous ammonium chloride were added and the aqueous layer further extracted with diethyl ether (3 x 10 ml). The combined organic extracts were dried using anhydrous sodium sulphate and concentrated under reduced pressure. This was purified by flash column chromatography on silica gel using dichloromethane: methanol (9:1) as the eluent gave *the title compound* (79 mg, 43%) as a yellow oil, R_f value 0.51 δ_{H} (400 MHz; CDCl₃) 0.84-0.90 (3H, t J = 7.6 Hz, 3x 4''-H); 1.21-2.03 (17H, m, 2x 1''-H, 2x 2''-H, 2x 2-H, 2x 3''-H, 2x 3-H, 2x 4-H, 8a-H, 2x 9-H, 2x 10-H); 2.34-2.48 (2H, m, 1-H, 8b-H); 3.53-3.56 (2H, m, 1'-H, 7-H); 4.01-4.07 (1H, t J = 11.6 Hz, 1'-H). δ_{C} (100MHz; CDCl₃) 14.0 (C4''); 18.5, 19.5, 22.4, 22.6, 25.1, 27.6, 32.8, 33.3, 34.9 (C1'', C2'', C2, C3'', C3, C4, C8, C9, C10); 41.0 (C1); 56.7 (C7); 63.1 (C1'); 67.8

(C5). IR/cm⁻¹ 3354 (O-H br), 2926 (C-H), 1440 (C-H₂).HRMS calcd for C₁₄H₂₇NO
225.2093: found [M+H] 226.2165.

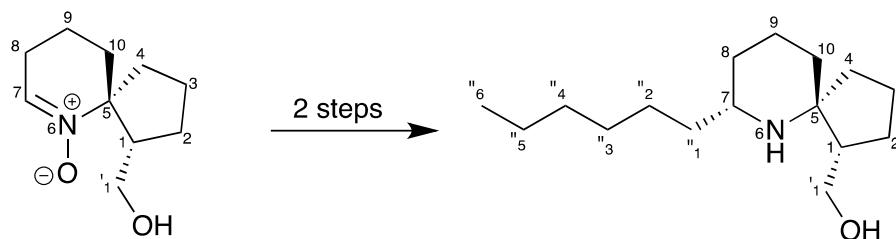
(1S*,5S*,7R*)-1-(hydroxymethyl)-7-pentyl-6-azaspiro[4.5]decane (215)



A solution of spironitrone **147** (0.15 g, 0.82 mmol) was cooled to 0°C in tetrahydrofuran (10 ml) under Ar. Pentylmagnesium bromide (1.5 ml), prepared according to the general procedure in tetrahydrofuran (10 ml), was added drop-wise before warming to r.t. and leaving to stir for 10 hours. The reaction mixture was quenched with ethanol: saturated aqueous ammonium chloride (2:1, 10 ml) and indium powder (0.55 mmol, 0.06 g) was added before heated under reflux for 4 h. Upon cooling, diethyl ether and saturated aqueous ammonium chloride were added and the aqueous layer further extracted with diethyl ether (3 x 10 ml). The combined organic extracts were dried using anhydrous sodium sulphate and concentrated under reduced pressure. This was purified by flash column chromatography on silica gel using dichloromethane: methanol (9:1) as the eluent gave *the title compound* (79 mg, 43%) as a yellow oil, R_f value 0.47 δ_H (400 MHz; $CDCl_3$) 0.69-0.91 (5H, m, 3x 5''-H, 2x 4''-H); 1.21-2.19 (18H, m, 2x 1''-H, 2x 2''-H, 2x 2-H, 2x 3''-H, 2x 3-H, 2x 4-H, 2x 8-H, 2x 9-H, 2x 10-H); 2.43-2.52 (1H, m, 1-H); 3.51-3.56 (1H, m, 7-H); 3.82-4.03 (2H, m, 2x 1'-H). δ_C (100MHz; $CDCl_3$) 14.1 (C5''); 18.5, 19.4, 22.7, 25.1, 27.5, 31.5, 32.6, 32.7, 33.2, 34.7 (C1'', C2'', C2, C3'', C3, C4'', C4, C8, C9, C10); 40.9

(C1); 56.8 (C7); 63.1 (C1'); 68.0 (C5). IR/cm⁻¹ 3362 (O-H br), 2954 (C-H), 1458 (C-H₂). HRMS calcd for C₁₅H₂₉NO 239.2249: found [M+H] 240.2322.

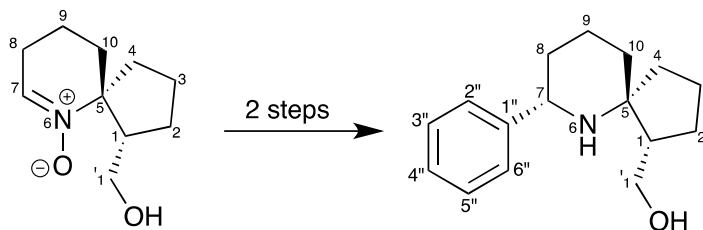
(1*S,5*S**,7*R**)-1-(hydroxymethyl)-7-hexyl-6-azaspiro[4.5]decane (216)**



A solution of spironitrone **147** (0.2 g, 1.0 mmol) was cooled to 0°C in diethyl ether (12 ml) under Ar. Hexylmagnesium bromide (0.4 ml), prepared according to the general procedure in diethyl ether (10 ml), was added drop-wise before warming to r.t. and leaving to stir for 10 hours. The reaction mixture was quenched with ethanol: saturated aqueous ammonium chloride (2:1, 12 ml) and indium powder (0.55 mmol, 0.06g) was added before heated under reflux for 4 h. Upon cooling, diethyl ether and saturated aqueous ammonium chloride were added and the aqueous layer further extracted with diethyl ether (3 x 10 ml). The combined organic extracts were dried using anhydrous sodium sulphate and concentrated under reduced pressure. This was purified by flash column chromatography on silica gel using dichloromethane: methanol (9:1) as the eluent to give *the title compound* (87 mg, 34%) as a pale yellow oil, R_f value 0.32 δ_H (400 MHz; $CDCl_3$) 0.82-0.84 (3H, t $J = 6.8$ Hz, 3x 6''-H); 1.23-1.39 (8H, m, 2x 3''-H, 2x 4''-H, 2x 5''-H); 1.58-2.04 (15H, 2x 1''-H, 2x 2''-H, 2x 2-H, 2x 3-H, 2x 4-H, 8a-H, 2x 9-H, 2x 10-H); 2.36-2.51 (2H, m, 1-H, 8b-H); 3.47-3.57 (2H, dd $J = 3.2$ and 11.6 Hz, 1'-H, 7-H); 4.03-4.09 (1H, t $J = 11.6$ Hz, 1'-H). δ_C (100MHz; $CDCl_3$) 14.3 (C6''); 18.5, 19.6, 22.6, 25.0, 25.6, 27.6, 29.1, 31.8, 33.4, 34.7, 35.0 (C1'',

C2", C2, C3", C3, C4", C4, C5", C8, C9, C10); 41.0 (C1); 57.0 (C7); 63.1 (C1'); 67.9
(C5). HRMS calcd for C₁₆H₃₁NO 253.2406: found [M+H] 254.2478.

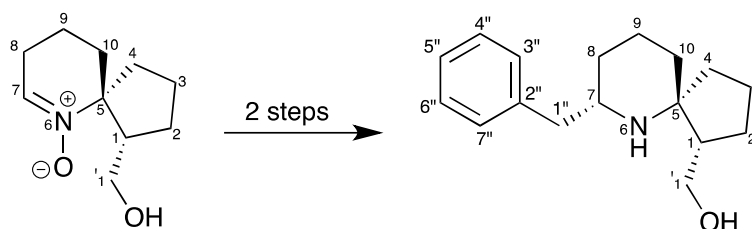
(1*S,5*S**,7*R**)-1-(hydroxymethyl)-7-phenyl-6-azaspiro[4.5]decane (217)**



A solution of spironitrone **147** (0.2 g, 1.0 mmol) was cooled to 0°C in tetrahydrofuran (10 ml) under Ar. Commercially prepared phenylmagnesium bromide (3M, 3 mmol, 0.2 ml) was added drop-wise before warming to r.t. and leaving to stir for 10 hours. The reaction mixture was quenched with ethanol: saturated aqueous ammonium chloride (2:1, 12 ml) and indium powder (1.0 mmol, 0.11 g) was added before heated under reflux for 4 h. Upon cooling, diethyl ether and saturated aqueous ammonium chloride were added and the aqueous layer further extracted with diethyl ether (3 x 15 ml). The combined organic extracts were dried using anhydrous sodium sulphate and concentrated under reduced pressure. This was purified by flash column chromatography on silica gel using dichloromethane: methanol (9:1) as the eluent to give *the title compound* (165 mg, 67%) as a white solid, R_f value 0.48 δ_H (400 MHz; CDCl₃) 1.23-1.90 (12H, m, 2x 2-H, 2x 3-H, 2x 4-H, 2x 8-H, 2x 9-H, 2x 10-H); 2.36 (1H, m, 1-H); 3.64 (2H, m, 2x 1'-H); 4.07 (1H, m, 7-H); 7.22-7.41 (5H, m, 2''-H, 3''-H, 4''-H, 5''-H, 6''-H). δ_C (100MHz; CDCl₃) 20.2, 21.5, 27.6, 32.8, 36.7, 40.9 (C2, C3, C4, C8, C9, C10); 41.7 (C1); 57.8 (C7); 64.9 (C5); 65.5 (C1'); 126.7 (C3'', C5''); 127.4 (C4''); 128.4 (C2'', C6''). IR/cm⁻¹ 3284 (O-H br), 2931 (C-H), 1440 (C=C), 1068 (C-

C), 698 (C=C); m.p. 161-163°C. HRMS calcd for C₁₆H₂₃NO 245.1780: found [M+H]
246.1851.

(1*S,5*S**,7*R**)-1-(hydroxymethyl)-7-benzyl-6-azaspiro[4.5]decane (218)**

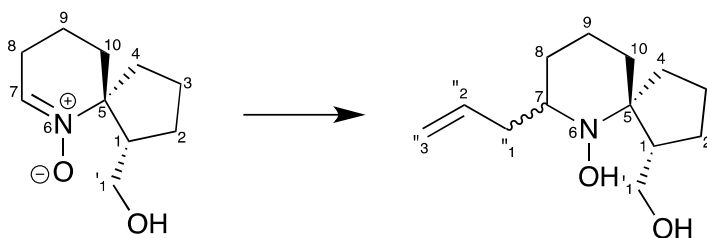


A solution of spironitrone **147** (0.2 g, 1 mmol) was cooled to 0°C in diethyl ether (10 ml) under Ar. Benzylmagnesium bromide (1.8 ml), prepared according to the general procedure in diethyl ether (10 ml), was added drop-wise before warming to r.t. and leaving to stir for 10 hours. The reaction mixture was quenched with ethanol: saturated aqueous ammonium chloride (2:1, 12 ml) and indium powder (1.0 mmol, 0.11 g) was added before heated under reflux for 4 h. Upon cooling, diethyl ether and saturated aqueous ammonium chloride were added and the aqueous layer further extracted with diethyl ether (3 x 15 ml). The combined organic extracts were dried using anhydrous sodium sulphate and concentrated under reduced pressure. This was purified by flash column chromatography on silica gel using dichloromethane: methanol (9:1) as the eluent gave *the title compound* (89 mg, 34%) as a pale yellow solid, R_f value 0.62

δ_{H} (400 MHz; CDCl₃) 1.23-2.09 (14H, m, 2x 1''-H, 2x 2-H, 2x 3-H, 2x 4-H, 2x 8-H, 2x 9-H, 2x 10-H); 2.49 (1H, m, 1-H); 3.54 (1H, dd $J = 3.2$ and 11.6 Hz, 7-H); 3.73 (1H, t $J = 11.6$ Hz, 1'a-H); 4.34 (1H, d $J = 12$ Hz, 1'b-H); 7.24-7.33 (4H, m, 3''-H, 4''-H, 6''-H, 7''-H); 7.55 (1H, m, 5''-H). δ_{C} (100MHz; CDCl₃) 128.3, 128.4, 128.7 (C3'', C4'', C5'', C6'', C7''). IR/cm⁻¹ 3290 (O-H br), 2930 (C-H), 1449 (C=C), 1070

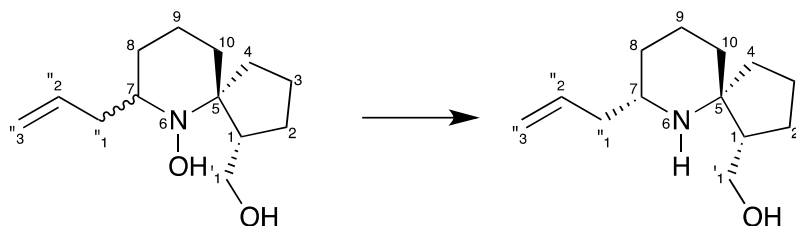
(C-C), 698 (C=C); m.p. 165-168°C. HRMS calcd for C₁₇H₂₅NO 259.1936: found
[M+H] 260.1654.

(1*S,5*S**,7*R**)-7-allyl-(hydroxymethyl)-6-azaspiro[4.5]decan-6-ol (281)**



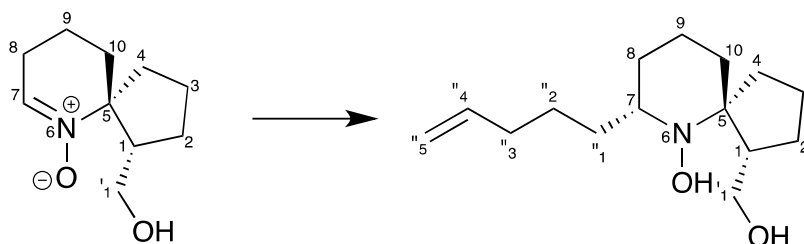
A solution of spironitrone **147** (0.10 g, 0.55 mmol) was cooled to 0°C in THF (10 ml) under Ar. Commercially prepared allylmagnesium chloride (2M, 1.65 mmol, 0.2 ml) was added drop-wise over 5 minutes. The resulting mixture was warmed to r.t., before leaving to stir for 10 hours. Water (2 ml) was added to quench the reaction before separation between saturated aqueous ammonium chloride (10 ml) and dichloromethane (10 ml), followed by further extraction with dichloromethane (3x 15 ml). The combined organic layers were dried with anhydrous sodium sulphate and concentrated under reduced pressure. The residue was purified by flash column chromatography gave *the title compound* (0.7240g, 28%*, 25.5 mg, 3%) as an orange oil, R_f value 0.63 δ_{H} (400 MHz; CDCl₃) 1.23-2.33 (14H, m, 1''-H, 2-H, 3-H, 4-H, 8-H, 9-H, 10-H); 3.08 (1H, m, 7-H); 3.42-3.60 (2H, m, 1'-H); 5.00-5.02 (2H, m, 3''-H); 5.81 (1H, m, 2''-H). δ_{C} (100MHz; CDCl₃) 20.0, 20.4, 24.1, 27.7, 28.6, 37.6 (C2, C3, C4, C8, C9, C10); 38.3 (C1''); 43.4 (C1); 61.6 (C7); 65.4 (C1'); 73.0 (C5); 116.7 (2''-H); 136.3 (3''-H). IR/cm⁻¹ 3272 (O-H br), 2938 (C-H), 1495 (C=C), 1038 (C-C). HRMS calcd for C₁₃H₂₃NO₂ 225.1729: found [M+H] 226.1813.

(1*S,5*S**,7*R**)-1-(hydroxymethyl)-7-allyl-6-azaspiro[4.5]decane (219)**



A solution of **281** (0.1g, 0.55 mmol) in acetic acid: water (1:1, 10 ml) with zinc dust (4.4 mmol, 0.29 g) was heated under reflux for 4 h. The reaction mixture was then cooled to r.t., before quenching with saturated aqueous sodium carbonate (10 ml), before extracting with chloroform (3 x 30 ml). The organic layers were combined, dried with anhydrous sodium sulphate and concentrated under reduced pressure to give a crude yellow oil. This was purified by flash column chromatography on silica gel using dichloromethane: methanol (9:1) as the eluent gave *the title compound* (64 mg, 55%) as a yellow oil, R_f value 0.30 δ_H (400 MHz; $CDCl_3$) 1.42-2.16 (13H, m, 1''a-H, 2x 2-H, 2x 3-H, 2x 4-H, 2x 8-H, 2x 9-H, 2x 10-H); 2.51-2.54 (1''b-H); 2.87 (1H, m, 1-H); 3.06 (1H, m, 7-H); 3.93-4.02 (2H, m, 2x 1'-H); 5.16-5.24 (2H, m, 2x 3''-H); 5.64-5.72 (1H, m, 2''-H). δ_C (100MHz; $CDCl_3$) 20.4, 23.0, 27.4, 28.0, 33.4, 34.7 (C2, C3, C4, C8, C9, C10); 37.9 (C1''); 50.2 (C1); 54.0 (C7); 61.5 (C1'); 68.2 (C5); 120.4 (C2''); 132.0 (C3''). IR/ cm^{-1} 3268 (O-H br), 2938 (C-H), 1458 (C=C), 1054 (C-C). HRMS calcd for $C_{13}H_{23}NO$ 209.1780: found [M+H] 210.1850.

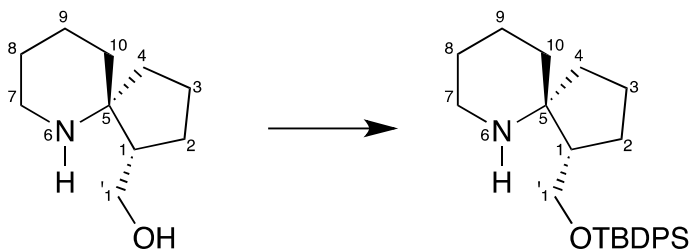
(1*S,5*S**,7*R**)-1-(hydroxymethyl)-7-pentyl-6-azaspiro[4.5]decan-6-ol (282)**



A solution of spironitrone **147** (0.10 g, 0.55 mmol) was cooled to 0°C in tetrahydrofuran (10 mL) under Ar. Freshly prepared pentenylmagnesium bromide (1.0 ml) was added drop-wise before warming to r.t. and leaving to stir for 10 h. The mixture was quenched with water (5 ml) followed by the removal of tetrahydrofuran and water under reduced pressure. Saturated aqueous ammonium chloride (10 ml) was added to the slurry and extracted with diethyl ether (3 x 10 ml). The combined extracts were dried with anhydrous sodium sulphate and concentrated under reduced pressure to a yellow oil. This was purified by flash column chromatography using ethyl acetate: hexane (1:1) as the eluent to give *the title compound* (23 mg, 17%) as a clear oil, R_f value 0.54 δ_{H} (400 MHz; CDCl₃) 1.16-2.23 (19H, m, 1-H, 2x 1''-H, 2x 2''-H, 2x 2-H, 2x 3''-H, 2x 3-H, 2x 4-H, 2x 8-H, 2x 9-H, 2x 10-H); 2.91 (1H, m, 7-H); 3.58 (2H, m, 2x 1'-H); 4.75-4.98 (2H, m, 2x 4''-H); 5.76 (1H, m, 5''-H). δ_{C} (100MHz; CDCl₃) 20.6, 21.1, 25.3, 27.9, 33.1, 34.0, 37.4, 41.3, 41.7 (C1', C2', C2, C3', C3, C4, C8, C9, C10); 50.3 (C1); 53.3 (C7); 63.6 (C1'); 65.9 (C5); 114.7 (C4'); 138.8 (C5'). IR/cm⁻¹ 3279 (O-H br), 2926 (C-H), 1456 (C=C), 907 (C-C). HRMS calcd for C₁₅H₂₇NO₂ 253.2042: found [M+H] 254.2125.

1-((1*S, 5*S**)-1-(((*tert*-butyldiphenylsilyl)oxy)methyl)-6-azaspiro[4.5]decane**

(242)



Method 1

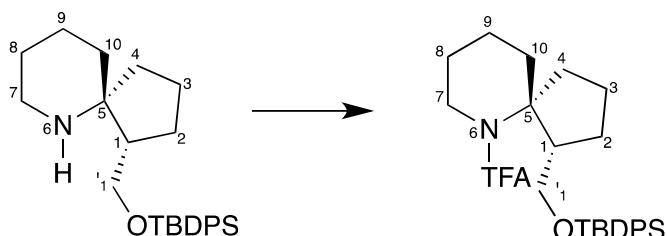
244 (2.7 g, 15.9 mmol) was dissolved in minimal amounts of dimethylformamide (8 ml) with 4-dimethylaminopyridine (3.2 mmol, 0.39 g) and imidazole (47.7 mmol, 3.25 g) before the drop-wise addition of *tert*-butyldiphenylsilyl chloride (31.8 mmol, 8.2 ml) over 10 minutes, before stirring at r.t. for 48 h. The thick white solution was separated between dichloromethane and brine, before extraction with dichloromethane (3 x 20 ml). The combined organic layers were dried using anhydrous sodium sulphate and concentrated under reduced pressure. This was purified by flash column chromatography using a dichloromethane: methanol gradient elution 100% dichloromethane to 9:1 dichloromethane: methanol to give *the title compound* (0.45 g, 54%) as a yellow oil.

Method 2

Spiroamine **244** (2.0 g, 12.1 mmol) in dichloromethane (20 ml) was cooled to 0°C with 4-dimethylaminopyridine (0.6 mmol, 0.73 g), and triethylamine (74.9

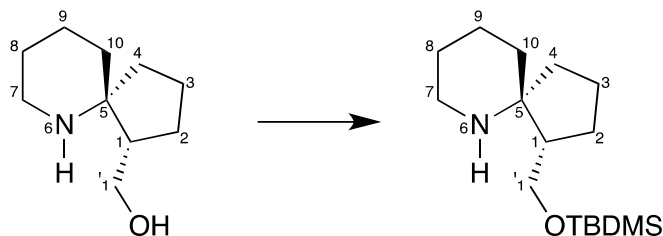
mmol, 10.5 ml) before the drop-wise addition of *tert*-butyldiphenylsilyl chloride (24.2 mmol, 6.2 ml). The mixture was warmed to r.t. and stirred overnight. Upon completion, the reaction mixture was separated between dichloromethane and brine, before extraction with dichloromethane (3 x 20 ml). The combined organic layers were dried using anhydrous sodium sulphate and concentrated under reduced pressure. This was purified by flash column chromatography using a dichloromethane: methanol gradient elution 100% dichloromethane to 9:1 dichloromethane: methanol to give *the title compound* (2.84 g, 59%) as a yellow oil, R_f value 0.68 δ_{H} (400 MHz; CDCl₃) 1.03 (9H, s, *t*Bu); 1.46-2.01 (12H, m, 2x 2-H, 2x 3-H, 2x 4-H, 2x 8-H, 2x 9-H, 2x 10-H); 2.21 (1H, m, 7a-H); 2.30 (1H, m, 7b-H); 2.88-2.99 (1H, m, 1'a-H); 3.39-3.47 (1H, m, 1'b-H); 7.38-7.59 (10H, m, Ph-H). δ_{C} (100MHz; CDCl₃) 18.7, 19.2, 21.3, 24.3, 25.7, 34.8 (C2, C3, C4, C8, C9, C10); 27.0 (3C-*t*Bu); 43.6 (C7); 48.9 (C1); 62.9 (C1'); 70.9 (C5); 127.9, 130.5, 132.9, 135.1, 135.9 (C-Ph); IR/cm⁻¹ 2856 (C-H), 2732 (C-H), 1428 (C-H₃), 1109 (C-H); 706 (C-C); m.p.92-93°C. HRMS calcd for C₂₆H₃₇NOSi 407.2643: found [M+H] 408.2717.

1-((1*S*, 5*S*)-1-(((*tert*-butyldiphenylsilyl)oxy)methyl)-6-azaspiro[4.5]decan-6-yl)-2,2,2-trifluoroethanone (258)



Silyl ether **242** (0.9 g, 2.2 mmol) with triethylamine (4.9 mmol, 0.7 ml) in dichloromethane (15 ml) was cooled to 0°C, before the cautious drop-wise of trifluoroacetic anhydride (4.4 mmol, 0.6 ml). The reaction mixture was stirred for 30 minutes at 0°C, before warming to r.t. and stirring for 6 h. When complete, the solution was quenched with a PH7 aqueous buffer and extracted with dichloromethane (3 x 20 ml). The combined organic layers were dried using anhydrous sodium sulphate and concentrated under reduced pressure. This was purified by flash column chromatography using a ethyl acetate: hexane as the eluent to give *the title compound* (0.74 g, 68%) as a pale orange oil, R_f value 0.91 δ_H (400 MHz; CDCl₃) 1.03 (9H, s, ^tBu); 1.53-2.06 (12H, m, 2x 2-H, 2x 3-H, 2x 4-H, 2x 8-H, 2x 9-H, 2x 10-H); 2.21 (1H, m, 7a-H); 2.33 (1H, m, 7b-H); 2.92-2.98 (1H, m, 1'a-H); 3.47-3.49 (1H, m, 1'b-H); 7.35-7.6 (10H, m, Ph-H). δ_C (100MHz; CDCl₃) 18.4, 19.3, 21.6, 24.7, 25.9, 34.9 (C2, C3, C4, C8, C9, C10); 27.0 (3C-^tBu); 43.6 (C7); 48.7 (C1); 63.7 (C1'); 70.3 (C5); 127.8, 129.8, 133.5, 135.6, 135.7 (C-Ph); 133.8 (C-F₃); 157.0 (C=O). IR/cm⁻¹ 2931 (C-H), 2744 (C-H), 1741 (C=O), 1446 (C-H₃), 1127 (C-H); 703 (C-C). HRMS calcd for C₂₈H₃₆F₃NO₂Si 503.2466: found [M+H].

**1-((1S, 5S)-1-(((*tert*-butyldimethylsilyl)oxy)methyl)-6-azaspiro[4.5]decane
(243)**



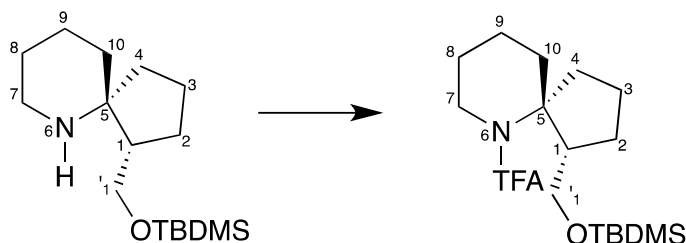
Method 1

244 (1.6 g, 9.5 mmol) was dissolved in minimal amounts of dimethylformamide (6 ml) with 4-dimethylaminopyridine (4.7 mmol, 0.58 g) and imidazole (28.3 mmol, 1.93) before the portion-wise addition of *tert*-butyldimethylsilyl chloride (18.9 mmol, 2.6 g) over 10 minutes. The mixture was heated at 120°C for 5 h. When complete, the mixture was separated between dichloromethane and brine, before extraction with dichloromethane (3 x 20 ml). The combined organic layers were dried using anhydrous sodium sulphate and concentrated under reduced pressure. This was purified by flash column chromatography using a dichloromethane: methanol gradient elution 100% dichloromethane to 9:1 dichloromethane: methanol to give *the title compound* (1.38 g, 52%) as a pale yellow oil.

Method 2

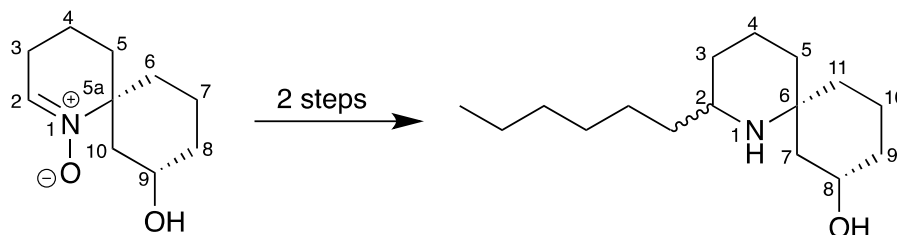
Spiroamine **244** (2.0 g, 11.8 mmol) in dichloromethane (20 ml) with 4-dimethylaminopyridine (0.6 mmol, 0.73 g), and imidazole (29.5 mmol, 2.0 g) before the portion-wise addition of *tert*-butyldimethylsilyl chloride (24.2 mmol, 63.5 g). The mixture was warmed to r.t. and stirred for 48 h. Upon completion, the reaction mixture was separated between dichloromethane and brine, before extraction with dichloromethane (3 x 20 ml). The combined organic layers were dried using anhydrous sodium sulphate and concentrated under reduced pressure. This was purified by flash column chromatography using a dichloromethane: methanol gradient elution 100% dichloromethane to 9:1 dichloromethane: methanol to give *the title compound* (2.11 g, 63%) as a pale yellow oil, R_f value 0.33 δ_{H} (400 MHz; CDCl₃) 0.10-0.15 (6H, d J = 3.6 Hz, (CH₃)₂); 0.89 (9H, s, ^tBu); 1.41-2.10 (12H, m, 2x 2-H, 2x 3-H, 2x 4-H, 2x 8-H, 2x 9-H, 10-H); 2.17-2.25 (1H, m, 7a-H); 2.97 (1H, m, 1-H); 3.35-3.38 (1H, m, 7b-H); 3.96 (1H, m, 1'a-H); 4.14 (1H, m, 1'b-H). δ_{C} (100MHz; CDCl₃) -5.3 (CH₃)₂; 20.4, 22.8, 24.1, 28.1, 33.8, 36.0 (C2, C3, C4, C8, C9, C10); 41.5 (C7); 51.0 (C1); 63.6 (C1'); 66.8 (C5). IR/cm⁻¹ 2928 (C-H), 1461 (C-H₃), 1079 (C-H); 835 (C-C). HRMS calcd for C₁₆H₃₃NOSi 283.2331: found [M+H] 284.2373.

1-((1*S, 5*S**)-1-(((*tert*-butyldimethylsilyl)oxy)methyl)-6-azaspiro[4.5]decan-6-yl)-2,2,2-trifluoroethanone (242)**



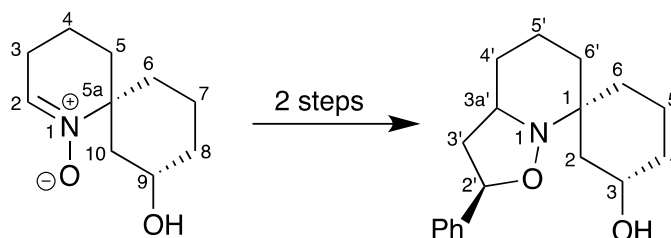
Silyl ether **243** (0.9 g, 3.1 mmol) with triethylamine (6.7 mmol, 1.0 ml) in CH₂Cl₂ (10 ml) was cooled to 0°C, before the cautious drop-wise of trifluoroacetic anhydride (6.2 mmol, 0.9 ml). The reaction mixture was stirred for 30 minutes at 0°C, before warming to r.t. and stirring overnight. When complete, the solution was quenched with a PH7 aqueous buffer and extracted with dichloromethane (3 x 20 ml). The combined organic layers were dried using anhydrous sodium sulphate and concentrated under reduced pressure. This was purified by flash column chromatography using a ethyl acetate: hexane as the eluent to give *the title compound* (0.87 g, 86%) as a pale yellow solid. Rf value 0.65 δ_H (400 MHz; CDCl₃) 0.05 (6H, d *J* = 3.6 Hz, (CH₃)₂); 0.85 (9H, s, ^{*t*}Bu); 1.44-1.97 (12H, m, 2x 2-H, 2x 3-H, 2x 4-H, 2x 8-H, 2x 9-H, 2x 10-H); 2.21-2.26 (1H, m, 7a-H); 2.47 (1H, m, 1-H); 3.21-3.22 (1H, m, 7b-H); 3.43-3.48 (2H, m, 2x 1'-H). δ_C (100MHz; CDCl₃) -3.3 (CH₃)₂; 19.3, 20.8, 22.9, 28.1, 33.8, 36.0 (C2, C3, C4, C8, C9, C10); 40.9 (C7); 51.3 (C1); 64.2 (C1'); 66.9 (C5); 134.2 (C-F₃); 154.3 (C=O). IR/cm⁻¹ 2942 (C-H), 1734 (C=O), 1453 (C-H₃), 1058 (C-H), 830 (C-C); m.p. 46-49°C. HRMS calcd for C₁₈H₃₂F₃NO₂Si 379.2154: found [M+H].

(6*R, 8*S**)-2-hexyl-1-azaspiro[5.5]undecan-8-ol (240)**



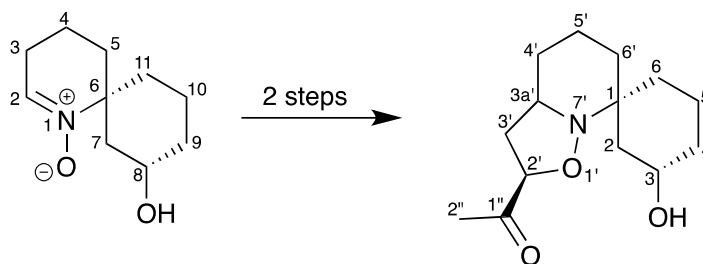
A solution of spironitrone **231** (0.06 g, 0.33 mmol) was cooled to 0°C in diethyl ether (10 ml) under Ar. Freshly prepared hexylmagnesium bromide (0.2 ml) was added drop-wise before warming to r.t. and leaving to stir for 10 hours. The reaction mixture was quenched with ethanol: saturated aqueous ammonium chloride (2:1, 10 ml) and indium powder (0.33 mmol, 0.04 g) was added before heated under reflux for 4 h. Upon cooling, the reaction mixture was separated using diethyl ether and saturated aqueous ammonium chloride and washed with diethyl ether (3 x 10 ml). The combined organic extracts were dried using anhydrous sodium sulphate and concentrated under reduced pressure. This was purified by flash column chromatography on silica gel using chloroform: methanol (9:1) as the eluent to give *the title compound* (19 mg, 23%) as a clear oil. R_f value 0.65; δ_H (400 MHz; CDCl₃) 0.85 (3H, t *J* = 7.6 Hz, 6'-H); 1.23-1.94 (22H, m, 2x 1'-H, 2x 2'-H, 2x 3'-H, 2x 3-H, 2x 4'-H, 2x 4-H, 2x 5'-H, 2x 5-H, 2x 9-H, 2x 10-H, 2x 11-H); 2.19-2.2 (1H, m, 7a-H); 2.5 (1H, m, 7b-H); 2.88 (1H, m, 2-H); 3.6-3.8 (1H, m, 8-H). δ_C (100MHz; CDCl₃) 14.2, 20.2, 20.7, 22.7, 25.9, 26.7, 27.4, 29.4, 31.8, 36.6, 37.1, 41.6 (C1', C2', C3', C3, C4', C4, C5', C5, C9, C10, C11); 46.9 (C7); 54.0 (C2); 64.8 (C8); 65.4 (C6). IR/cm⁻¹ 3362 (O-H br), 2936 (C-H), 1457 (C-C), 1069 (C-H₂). HRMS calcd for C₁₆H₃₁NO 253.2406: found [M+H] 254.2480.

(1*R, 2'*R**, 3*S*')-2'-phenylhexyhydrospiro[cyclohexane-1,7'-isoxazolo[2,3-a]pyridine]-3-ol (232)**



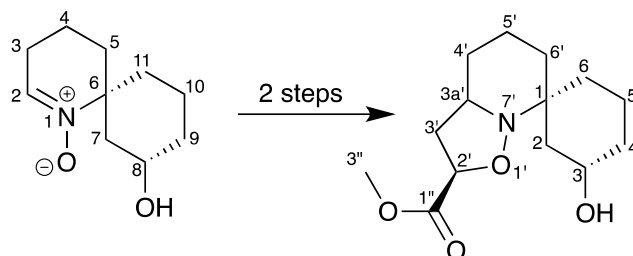
Spironitrone **231** (0.02 g, 0.1 mmol) and styrene (0.7 mmol, 0.08 ml) in toluene (6 ml) was heated under reflux for 4 h. When complete the toluene was removed under reduced pressure. This was purified by flash column chromatography using ethyl acetate: hexane (1: 1) as the eluent to give *the title compound* (0.87 g, 86%) as a clear oil, *R_f* value 0.63; δ_{H} (400 MHz; CDCl_3) 1.42-1.9 (12H, m, 2x 4-H, 2x 4'-H, 2x 5-H, 2x 5'-H, 2x 6-H, 2x 6'-H); 2.17-2.47 (4H, m, 2x 2-H, 2x 3'-H); 3.67 (2H, m, 2'-H, 3a'-H); 5.06 (1H, m, 3-H); 7.19-7.37 (5H, m, Ph-H). δ_{C} (100MHz; CDCl_3) 19.3, 21.5, 26.1, 27.6, 38.0, 44.6, 45.7, 65.6 (C2, C3', C4, C4', C5, C5', C6, C6'); 58.6 (C3a'); 69.9 (C1); 76.5 (C3); 86.7 (C2'); 125.5, 127.2, 128.6 (C-Ph); IR/ cm^{-1} 3347 (O-H br), 2913 (C-H), 1446 (C-C), 975 (C-H). HRMS calcd for $\text{C}_{18}\text{H}_{25}\text{NO}_2$ 287.1885: found [M+H] 469.3051.

1-((1*R,3*S**)-3-hydroxyhexahydrospiro[cyclohexane-1,7'-isoxazolo[2,3-a]pyridine]-3'-yl)ethanone (233)**



Spironitrone **231** (0.06 g, 0.3 mmol) and methyl vinyl ketone (2.0 mmol, 0.16 ml) in ethanol (5 ml) was stirred at r.t.. When complete the ethanol was removed under reduced pressure. This was purified by flash column chromatography using ethyl acetate: hexane (1: 1) as the eluent to give *the title compound* (0.87 g, 86%) as a clear oil. R_f value 0.26; δ_H (400 MHz; CDCl₃) 1.01-2.34 (19H, 2x 2-H, 2'-H, 2x 2''-H, 2x 4-H, 2x 4'-H, 2x 5-H, 2x 5'-H, 2x 6-H, 2x 6'-H); 3.62-3.65 (1H, m, 3a'-H); 3.97 (1H, m, 3-H); 4.28-4.33 (1H, m, 3'-H). δ_C (100MHz; CDCl₃) 15.6, 18.4, 25.7, 31.0, 33.4, 36.6, 38.4, 39.1 (C2, C2' C4, C4', C5, C5', C6, C6'); 25.5 (C2''); 55.0 (C3a); 59.2 (C1); 67.0 (C3); 79.3 (C2'); 211.4 (C1''). IR/cm⁻¹ 3346 (O-H br), 2968 (C-H), 1725 (C=O), 1455 (C-C) 1048 (C-H₂). HRMS calcd for C₁₄H₂₃NO₃ 253.1678: found [M+H] 254.1746.

(1*R, 2'*R**, 3*S**)-2'-methyl 3-hexyhydrospiro[cyclohexane-1,7'-isoxazolo[2,3-a]pyridine]-2'-carboxylate (234)**



Spironitrone **231** (0.10 g, 0.5 mmol) and methyl acrylate (3.3 mmol, 0.3 ml) in toluene (10 ml) was heated under reflux for 4 h. When complete the toluene was removed under reduced pressure. This was purified by flash column chromatography using ethyl acetate: hexane (1: 1) as the eluent to give *the title compound* (0.68 g, 39%*) as a clear oil. R_f value 0.34; δ_H (400 MHz; CDCl₃) 1.03-2.53 (16H, 2.71-3.07 (2x 2-H, 2x 2*-H, 2x 3'-H, 2x 3'*-H, 2x 4-H, 2x 4*-H, 2x 4'-H, 2x 4'*-H, 2x 5-H, 2x 5*-H, 2x 5'-H, 2x 5'*-H, 2x 6-H, 2x 6*-H, 2x 6'-H, 2x 6'*-H); (1H, m, 3a-H, 3a*-H); 3.43-4.11 (3H, m, 3''-H, 3''*-H); 4.12-4.56 (1H, m, 3-H, 3*-H); 5.11-5.39 (1H, m, 2'-H, 2'*-H). δ_C (100MHz; CDCl₃) 15.0, 15.3, 18.3, 25.9, 26.2, 31.3, 31.4, 32.1, 33.6, 36.8, 37.1, 38.8, 39.0, 39.6, 52.2, 52.4, 53.5, 54.3, 58.3, 58.7, 66.7, 67.0, 67.4, 67.8 (C2, C2*, C3, C3*, C3', C3'*, C3'', C3''*, C3a', C3a'*), C4, C4*, C4', C4'*, C5, C5*, C5', C5'', C6, C6*, C6', C6''); 65.9 (C1); 72.5 (C2'); 173.2, 173.5 (C1'', C1''*). IR/cm⁻¹ 3353 (O-H br), 2936 (C-H), 1734 (C=O), 1436 (C-C) 1058 (C-H₂). HRMS calcd for C₁₄H₂₃NO₄ 269.1628: found [M+H]⁺ 270.1699.

Chapter 9 References

1. M. Kuramoto, C. Tong, K. Yamada, T. Chiba, Y. Hayashi and D. Uemura, *Tet. Lett.*, 1996, **37**, 3867-3870.
2. J. W. Daly and C. W. Myers, *Science*, 1967, **156**, 970-973.
3. D. A. Dias, S. Urban and U. Roessner, *Metabolites*, 2012, **2**, 303-336.
4. F. Von Nussbaum, M. Brands, B. Hinzen, S. Weigand and D. Häbich, *Angew. Chem. Int. Ed.*, 2006, **45**, 5072-5129.
5. A. Harvey, *DDT*, 2000, **5**, 294-300.
6. M. J. Balunas and A. D. Kinghorn, *Life Sciences*, 2005, **78**, 431-441.
7. G. M. Cragg and D. J. Newman, *Biochimica et Biophysica Acta*, 2013, 3670-3695.
8. Y. W. Chin, M. J. Balunas, H. B. Chai and A. D. Kinghorn, *The AAPS Journal*, 2006, **8**, 239-253.
9. G. P. Hu, J. Yuan, L. Sun, Z. G. She, J. H. Wu, X. J. Lan, X. Zhou, Y. C. Lin and S. P. Chen, *Mar. Drugs*, 2011, **9**, 514-525.
10. W. Bergmann and R. J. Feeney, 1951, **16**.
11. T. F. Molinski, D. S. Dalisay, S. L. Livens and J. P. Saludes, *Nature Reviews*, 2009, **8**, 69-85.
12. G. M. Konig, S. Kehraus, S. F. Sober, A. Abdel-Lateff and D. Muller, *ChemBioChem*, 2006, **7**, 229-238.
13. B. Hefner, *DDT*, 2003, **8**, 536-544.
14. T. Chou, M. Kuramoto, Y. Otani, M. Shikano, K. Yazawa and D. Uemura, *Tet. Lett.*, 1996, **37**, 3871-3874.
15. S. Pericaris, T. Vlachogianni and A. Valavanidis, *Nat. Prod. Chem. Res.*, 2013, **1**, 1-8.
16. R. M. Kramer and J. D. Sharp, *FEBS Letters*, 1997, 49-53.
17. Y. Tsubosaka, T. Murata, K. Yamada, D. Uemura, M. Hori and H. Ozaki, *J. Pharma. Sci.*, 2010, **113**, 208-213.
18. M. Kuramoto, H. Arimoto and D. Uemura, *Mar. Drugs*, 2004, 39-54.
19. A. U. Ahmed, *Front. Biol.*, 2011, **6**, 274-281.
20. D. Sarkar and P. B. Fisher, *Cancer Letters*, 2006, **236**, 13-23.
21. N. A. Campbell and J. B. Reece, *Biology*, Eighth edn., 2008.
22. A. Mantovani, P. Allavena, A. Sica and F. Balkwill, *Nature*, 2008, **454**, 436-444.
23. R. Sen and D. Baltimore, *Cell*, 1986, **47**, 921-928.
24. S. Ghosh, *Annu. Rev. Immunol.*, 1998, **16**, 225-260.
25. F. S. Laroux, K. P. Pavlick, I. N. Hines, S. Kawachi, H. Harada, S. Bharwani, J. M. Hoffman and M. B. Grisham, *Acta. Physiol. Scand.*, 2001, **173**, 113-118.
26. A. A. Beg and A. S. Baldwin Jr, *Genes and Development*, 1993, 2064-2070.
27. R. Korhonen, A. Lahti, H. Kankaanranta and E. Moilanen, *Current Drug Targets*, 2005, **4**, 471-479.
28. P. J. Barnes and M. Karin, *New England Journal of Medicine*, 1997, **336**, 1066-1071.
29. E. Ricciotti and G. A. Fitzgerald, *Arteriocler. Thromb. Vasc. Biol.*, 2011, **31**, 986-1000.
30. R. M. Clancy, A. R. Amin and S. B. Abramson, *Arthritis & Rheumatism*, 1998, **47**, 1141-1151.
31. H. Kim, *Heterocycles*, 2006, **70**, 143-146.
32. D. L. J. Clive, *Strategies and tactics in organic synthesis*, 2012, **8**, 25-54.

33. D.-Y. Zhu, *Adv. Synth. Catal.*, 2015, **357**, 747-752.
34. C. Gignoux, *Org. Biomol. Chem.*, 2012, **10**, 67-69.
35. C. Kibayashi and S. Aoyagi, *J. Syn. Org. Chem.*, 2011, **69**, 1005-1019.
36. B. Stevenson, W. Lewis and J. Dowden, *Synlett*, 2010, 672-674.
37. G. E. Keck and S. A. Neumann, *Org. Lett.*, 2008, **10**, 4783-4786.
38. D. L. J. Clive, M. Yu, J. Wang, V. S. C. Yeh and S. Kang, *Chem. Rev.*, 2005, **105**, 4483-4514.
39. D. Trauner, J. B. Schwarz and S. J. Danishefsky, *Angew. Chem. Int. Ed.*, 1999, **38**, 3542-3545.
40. D. Trauner and S. J. Danishefsky, *Tet. Lett.*, 1999, **40**, 6513-6516.
41. E. P. Boden and G. E. Keck, *J. Org. Chem.*, 1985, **50**, 2394-2395.
42. H. Arimoto, I. Hayakawa, M. Kumamoto and D. Uemura, *Tet. Lett.*, 1998, **39**, 861-862.
43. I. Hayakawa, H. Arimoto and D. Uemura, *Heterocycles*, 2003, **59**, 441-444.
44. I. Hayakawa, H. Arimoto and D. Uemura, *Chem. Comm.*, 2004, **10**, 1222-1223.
45. S. Xu, D. Unabara, D. Uemura and H. Arimoto, *Chemistry - An Asian Journal*, 2014, **9**, 367-375.
46. S. Xu, H. Arimoto and D. Uemura, *Angew. Chem. Int. Ed.*, 2007, **46**, 5746-5749.
47. H. Arimoto, S. Asano and D. Uemura, *Tet. Lett.*, 1999, **40**, 3583-3586.
48. D. L. J. Clive and V. S. C. Yeh, *Tet. Lett.*, 1999, **40**, 8503-8507.
49. M. Yu, D. L. J. Clive, V. S. C. Yeh, S. Kang and J. Wang, *Tet. Lett.*, 2004, **45**, 2879-2881.
50. D. L. J. Clive, J. Wang and M. Yu, *Tet. Lett.*, 2005, **46**, 2853-2855.
51. D. L. J. Clive, M. Yu and Z. Li, *Chem. Comm.*, 2005, 906-908.
52. D. Liu, H. P. Acharya, M. Yu, J. Wang, V. S. C. Yeh, S. Kang, C. Chiruta, S. M. Jachak and D. L. J. Clive, *J. Org. Chem.*, 2009, **74**, 7417-7428.
53. J. D. White, P. R. Blakemore, E. A. Korf and A. F. T. Yokochi, *Org. Lett.*, 2001, **3**, 413-415.
54. S. Lee and Z. Zhao, *Org. Lett.*, 1999, **1**, 681-683.
55. S. Lee and Z. Zhao, *Tet. Lett.*, 1999, **40**, 7921-7924.
56. J. W. Daly, I. Karle, C. W. Myers, T. Tokuyama, J. A. Waters and B. Witkop, *Proc. Natl. Acad. Sci. U. S. A.*, 1971, **68**, 1870.
57. A. Sinclair and R. Stockman, *Nat. Prod. Rep.*, 2007, **24**, 298-326.
58. J. W. Daly, H. M. Garraffo, P. Jain, T. F. Spande, R. R. Snelling, C. Jaramillo and A. S. Rand, *J. Chem. Ecol.*, 2000, **26**, 73-85.
59. D. Evans, E. W. Thomas and R. E. Cherpeck, *J. Am. Chem. Soc.*, 1982, **104**, 3695-3700.
60. E. Gossinger, R. Imhof and H. Wehrli, *Helv. Chim. Acta*, 1975, **58**, 96-103.
61. G. M. Williams, S. D. Roughley, J. E. Davies and A. B. Holmes, *J. Am. Chem. Soc.*, 1999, 4900-4901.
62. W. Gessner, K. Takahashi, B. Witkop and A. Brossi, *Helv. Chim. Acta.*, 1985, **68**, 49-55.
63. S. H. Yang, G. R. Clark and V. Caprio, *Org. Biomol. Chem.*, 2009, **7**, 2981-2990.
64. R. A. Floyd, *Aging Cell*, 2006, **5**, 51-57.
65. E. Janzen, J and J. L. Ferlock, *Nature*, 1969, **222**, 867-868.
66. R. A. Floyd, K. Hensley, M. J. Forster, J. A. Kelleher-Andersson and P. L. Wood, *Mechanisms of Ageing and Development*, 2002, **123**, 1021-1031.
67. R. A. Floyd, R. D. Kopke, C.-H. Choi and F. S. B., *Free Radical Biology and Medicine*, 2008, **45**, 1361-1374.

68. R. A. Floyd, K. Hensley, M. J. Forster, J. A. Kelleher-Anderson and P. L. Wood, *Journal*, 2002, **959**, 321-329.
69. E. Sakiniene and L. V. Collins, *Arthritis Res*, 2002, **4**, 196-200.
70. J. Clayden, *Organic chemistry*, Oxford University Press, Oxford, 2001.
71. S. Cicchi, M. Marradi, A. Goti and A. Brandi, *Tet. Lett.*, 2001, **42**, 6503-6505.
72. G. D'Adamio, C. Parmeggiani, A. Goti and F. Cardona, *Eur. J. Org. Chem.*, 2015, **29**, 6541-6546.
73. D. V. Nguyen, P. Prakash, E. Gravel and E. Doris, *RSC Adv.*, 2016, **92**, 89283-89241.
74. S. Cicchi, M. Corsi and A. Goti, *J. Org. Chem.*, 1999, **19**, 7243-7245.
75. P. A. S. Smith and S. E. Gloyer, *J. Org. Chem.*, 1975, **17**, 2504-2508.
76. C. Matassini, C. Parmeggiani, F. Cardona and A. Goti, *Org. Lett.*, 2015, **16**, 4082-4085.
77. T. Shono, Y. Matsumura and K. Inoue, *J. Org. Chem.*, 1986, **4**, 549-551.
78. M. Forcato, M. Mba, W. A. Nugent and G. Licini, *Eur. J. Org. Chem.*, 2010, **4**, 740-748.
79. S. Murahashi, H. Mitsui, T. Shiota, T. Tsuda and S. Watanabe, *J. Org. Chem.*, 1990, **55**, 1736-1744.
80. C. Gella, E. Ferrer, R. Alibes, F. Busque, P. March, M. Figueredo and J. Font, *J. Org. Chem.*, 2009, **74**, 6365-6367.
81. A. Goti and L. Nannelli, *Tet. Lett.*, 1996, **33**, 6025-6028.
82. E. Marcantoni, M. Petrini and O. Polimanti, *Tet. Lett.*, 1995, **20**, 3561-3562.
83. K. Suzuki, T. Watanabe and S. I. Murahashi, *J. Org. Chem.*, 2013, **6**, 2301-2310.
84. F. Nikbakht and A. Heydari, *Tet. Lett.*, 2014, **15**, 2513-2516.
85. M. Gulla, L. Bierer, L. Redcliffe, S. Schmidt and V. Jager, *Artivoc*, 2006, 76-88.
86. E. Breuer, H. G. Aurich and A. Nielsen, *Nitrones, Nitronates and Nitroxides*, 1989.
87. G. R. Delpierre and M. Lamchen, *Quart. Rev.*, 1965, **19**, 329-349.
88. M. Lombardo and C. Trombini, *Synthesis*, 2000, 759-774.
89. M. F. Schlectt, *J. Chem. Soc. Chem. Commun.*, 1985, 1239-1241.
90. H. Ohtake, Y. Imada and S. Murahashi, I, *J. Org. Chem*, 1999, **64**, 3790-3791.
91. S. Cicchi, M. Bonanni, F. Cardona, J. Revuelta and A. Goti, *Org. Lett.*, 2003, **5**, 1773-1776.
92. Y. Matsumura, S. Aoyagi and C. Kibayashi, *Organic Letters*, 2004, **6**, 965-968.
93. Y. Matsumura, S. Aoyagi and C. Kibayashi, *Org. Lett.*, 2003, **5**, 3249-3252.
94. F. D. Ferrari, A. J. Ledgard and R. Marquez, *Tetrahedron*, 2011, **67**, 4988-4994.
95. H. Wang, M. Yu, M. Ochani, A. C. Amella, M. Tanovic, S. Susaria, J. H. Li, H. Wang, M. Yang, L. Ulloa, Y. Al-Abed, C. J. Czura and K. J. Tracey, 2003, **421**, 384-388.
96. H. Mitsui, S. I. Zenki, T. Shiota and S. I. Murahashi, *J. Chem. Soc. Chem. Commun.*, 1984, 874-875.
97. M. Forcato, W. A. Nugent and G. Licini, *Tet. Lett.*, 2003, **44**, 49-52.
98. D. A. Morozov, I. A. Kirilyuk, D. A. Komarov, A. Goti, I. Y. Bagryanskaya, N. V. Kuratiera and I. A. Grigor'ev, *J. Org. Chem.*, 2012, **77**, 10688-10698.
99. D. Bach, R. D. Andrzejewski and L. R. Dusold, *J. Org. Chem.*, 1973, **38**, 1742-1743.

Chapter 10 Appendix

10.1 Statistical data

Statistical data obtained from the ANOVA test calculated using SPSS stats package, showing the untreated cells against the treated cells.

Growth and viability data for undifferentiated U937 cells.

Untreated cells			95% Confidence Interval		
VS	Mean		Sig.	Lower	Upper
ALL treatments	Difference	Std. Error	(P)	Bound	Bound
Propyl 10 ⁻⁴ M	.20383	.09972	.990	-.1889	.5966
Propyl 10 ⁻⁵ M	.17250	.09972	1.000	-.2202	.5652
Phenyl 10 ⁻⁴ M	.10667	.09972	1.000	-.2861	.4994
Phenyl 10 ⁻⁵ M	.21900	.09972	.972	-.1737	.6117
Ethyl Ac 10 ⁻⁴ M	-.27983	.09972	.669	-.6726	.1129
Ethyl Ac 10 ⁻⁵ M	-.12217	.09972	1.000	-.5149	.2706
Phenyl Ac 10 ⁻⁴ M	-.32483	.09972	.318	-.7176	.0679
Phenyl Ac 10 ⁻⁵ M	-.24467	.09972	.895	-.6374	.1481
Ethyl 10 ⁻⁴ M	-.47833*	.09972	.002	-.8711	-.0856
Ethyl 10 ⁻⁵ M	-.28917	.09972	.594	-.6819	.1036
Allyl 10 ⁻⁴ M	-.39167	.09972	.052	-.7844	.0011
Allyl 10 ⁻⁵ M	-.13300	.09972	1.000	-.5257	.2597
Pentenyl OH 10 ⁻⁴ M	-.28667	.09972	.614	-.6794	.1061
Pentenyl OH 10 ⁻⁵ M	-.10900	.09972	1.000	-.5017	.2837

Allyl OR 10 ⁻⁴ M	.75950*	.09972	.000	.3668	1.1522
Allyl OR 10 ⁻⁵ M	.06967	.09972	1.000	-.3231	.4624
Methyl Ac 10 ⁻⁴ M	.11383	.09972	1.000	-.2789	.5066
Methyl Ac 10 ⁻⁵ M	.22600	.09972	.958	-.1667	.6187
Methyl 10 ⁻⁴ M	-.40167*	.09972	.037	-.7944	-.0089
Methyl 10 ⁻⁵ M	-.32083	.09972	.345	-.7136	.0719
Butyl 10 ⁻⁴ M	.05750	.09972	1.000	-.3352	.4502
Butyl 10 ⁻⁵ M	.13050	.09972	1.000	-.2622	.5232
Hexyl 10 ⁻⁴ M	-.32083	.09972	.345	-.7136	.0719
Hexyl 10 ⁻⁵ M	-.05183	.09972	1.000	-.4446	.3409
Benzyl Ac 10 ⁻⁴ M	.19717	.09972	.994	-.1956	.5899
Benzyl Ac 10 ⁻⁵ M	.33300	.09972	.265	-.0597	.7257
Benzyl 10 ⁻⁴ M	-.52583*	.09972	.000	-.9186	-.1331
Benzyl 10 ⁻⁵ M	-.43667*	.09972	.011	-.8294	-.0439
Pentyl 10 ⁻⁴ M	-.19050	.09972	.997	-.5832	.2022
Pentyl 10 ⁻⁵ M	-.35167	.09972	.168	-.7444	.0411
TBDMS 10 ⁻⁴ M	.26267	.09972	.795	-.1301	.6554
TBDMS 10 ⁻⁵ M	.17667	.09972	.999	-.2161	.5694
TBDPS 10 ⁻⁴ M	.16783	.09972	1.000	-.2249	.5606
TBDPS 10 ⁻⁵ M	-.12367	.09972	1.000	-.5164	.2691
N-Ac OH 10 ⁻⁴ M	-.40500*	.09972	.033	-.7977	-.0123
N-Ac OH 10 ⁻⁵ M	-.19367	.09972	.996	-.5864	.1991
TFA-PS 10 ⁻⁴ M	.18117	.09972	.999	-.2116	.5739
TFA-PS 10 ⁻⁵ M	.21617	.09972	.977	-.1766	.6089

Growth and viability data for LPS activated U937 cells.

Untreated cells				95%	Confidence
VS	Mean		Sig.	Interval	
ALL Treatments	Difference	Std. Error	(P)	Lower Bound	Upper Bound
Propyl 10 ⁻⁴ M	-.02100	.08395	1.000	-.3516	.3096
Propyl 10 ⁻⁵ M	-.09733	.08395	1.000	-.4280	.2333
Phenyl 10 ⁻⁴ M	-.07467	.08395	1.000	-.4053	.2560
Phenyl 10 ⁻⁵ M	.08933	.08395	1.000	-.2413	.4200
Ethyl Ac 10 ⁻⁴ M	-.39083*	.08395	.004	-.7215	-.0602
Ethyl Ac 10 ⁻⁵ M	-.34917*	.08395	.024	-.6798	-.0185
Phenyl Ac 10 ⁻⁴ M	-.49117*	.08395	.000	-.8218	-.1605
Phenyl Ac 10 ⁻⁵ M	-.46617*	.08395	.000	-.7968	-.1355
Ethyl 10 ⁻⁴ M	-.23683	.08395	.658	-.5675	.0938
Ethyl 10 ⁻⁵ M	-.17000	.08395	.992	-.5006	.1606
Allyl 10 ⁻⁴ M	-.35017*	.08395	.023	-.6808	-.0195
Allyl 10 ⁻⁵ M	-.45850*	.08395	.000	-.7891	-.1279
Pentenyl OH 10 ⁻⁴ M	-.49200*	.08395	.000	-.8226	-.1614
Pentenyl OH 10 ⁻⁵ M	-.36683*	.08395	.011	-.6975	-.0362
Allyl OR 10 ⁻⁴ M	.46633*	.08395	.000	.1357	.7970
Allyl OR 10 ⁻⁵ M	-.03033	.08395	1.000	-.3610	.3003
Methyl Ac 10 ⁻⁴ M	-.04700	.08395	1.000	-.3776	.2836
Methyl Ac 10 ⁻⁵ M	.01483	.08395	1.000	-.3158	.3455
Methyl 10 ⁻⁴ M	-.19217	.08395	.953	-.5228	.1385
Methyl 10 ⁻⁵ M	.06100	.08395	1.000	-.2696	.3916
Butyl 10 ⁻⁴ M	-.12917	.08395	1.000	-.4598	.2015

Butyl 10 ⁻⁵ M	-.11317	.08395	1.000	-.4438	.2175
Hexyl 10 ⁻⁴ M	.13883	.08395	1.000	-.1918	.4695
Hexyl 10 ⁻⁵ M	.17750	.08395	.984	-.1531	.5081
Benzyl Ac 10 ⁻⁴ M	.31417	.08395	.092	-.0165	.6448
Benzyl Ac 10 ⁻⁵ M	.14850	.08395	.999	-.1821	.4791
Benzyl 10 ⁻⁴ M	-.34433*	.08395	.029	-.6750	-.0137
Benzyl 10 ⁻⁵ M	-.36100*	.08395	.014	-.6916	-.0304
Pentyl 10 ⁻⁴ M	-.48450*	.08395	.000	-.8151	-.1539
Pentyl 10 ⁻⁵ M	-.28583	.08395	.228	-.6165	.0448
TBDMS 10 ⁻⁴ M	-.18133	.08395	.978	-.5120	.1493
TBDMS 10 ⁻⁵ M	-.24500	.08395	.579	-.5756	.0856
TBDPS 10 ⁻⁴ M	-.19433	.08395	.946	-.5250	.1363
TBDPS 10 ⁻⁵ M	-.29150	.08395	.193	-.6221	.0391
N-Ac OH 10 ⁻⁴ M	.11117	.08395	1.000	-.2195	.4418
N-Ac OH 10 ⁻⁵ M	-.09717	.08395	1.000	-.4278	.2335
TFA-PS 10 ⁻⁴ M	-.08267	.08395	1.000	-.4133	.2480
TFA-PS 10 ⁻⁵ M	-.16500	.08395	.995	-.4956	.1656

NO data for undifferentiated U937 cells.

Untreated cells				95% Interval	Confidence
Vs	Mean		Sig.	Lower	Upper
ALL Treatments	Difference	Std. Error	(P)	Bound	Bound
Propyl 10 ⁻⁴ M	128.91667*	30.76323	.018	8.8038	249.0295
Propyl 10 ⁻⁵ M	72.22250	30.76323	.939	-47.8903	192.3353
Phenyl 10 ⁻⁴ M	110.00000	30.76323	.139	-10.1128	230.1128
Phenyl 10 ⁻⁵ M	64.16750	30.76323	.988	-55.9453	184.2803
Ethyl Ac 10 ⁻⁴ M	85.55667	30.76323	.691	-34.5562	205.6695
Ethyl Ac 10 ⁻⁵ M	31.11333	30.76323	1.000	-88.9995	151.2262
Phenyl Ac 10 ⁻⁴ M	64.44583	30.76323	.988	-55.6670	184.5587
Phenyl Ac 10 ⁻⁵ M	-28.33250	30.76323	1.000	-148.4453	91.7803
Ethyl 10 ⁻⁴ M	56.94583	30.76323	.999	-63.1670	177.0587
Ethyl 10 ⁻⁵ M	7.50167	30.76323	1.000	-112.6112	127.6145
Allyl 10 ⁻⁴ M	55.02750	30.76323	.999	-65.0853	175.1403
Allyl 10 ⁻⁵ M	-36.08167	30.76323	1.000	-156.1945	84.0312
Pentenyl OH 10 ⁻⁴ M	92.22333	30.76323	.511	-27.8895	212.3362
Pentenyl OH 10 ⁻⁵ M	72.77750	30.76323	.934	-47.3353	192.8903
Allyl OR 10 ⁻⁴ M	91.38917	30.76323	.534	-28.7237	211.5020
Allyl OR 10 ⁻⁵ M	56.39000	30.76323	.999	-63.7228	176.5028
Methyl Ac 10 ⁻⁴ M	115.00083	30.76323	.086	-5.1120	235.1137
Methyl Ac 10 ⁻⁵ M	72.77833	30.76323	.934	-47.3345	192.8912
Methyl 10 ⁻⁴ M	108.61250	30.76323	.158	-11.5003	228.7253
Methyl 10 ⁻⁵ M	76.39000	30.76323	.886	-43.7228	196.5028
Butyl 10 ⁻⁴ M	102.27326	31.45462	.314	-20.5391	225.0856

Butyl 10 ⁻⁵ M	73.33417	30.76323	.927	-46.7787	193.4470
Hexyl 10 ⁻⁴ M	105.00167	30.76323	.215	-15.1112	225.1145
Hexyl 10 ⁻⁵ M	66.39000	30.76323	.981	-53.7228	186.5028
Benzyl Ac 10 ⁻⁴ M	104.39508	31.45462	.270	-18.4173	227.2074
Benzyl Ac 10 ⁻⁵ M	70.00083	30.76323	.959	-50.1120	190.1137
Benzyl 10 ⁻⁴ M	120.00083	30.76323	.051	-.1120	240.1137
Benzyl 10 ⁻⁵ M	78.05583	30.76323	.858	-42.0570	198.1687
Pentyl 10 ⁻⁴ M	107.33317	32.26475	.265	-18.6422	233.3086
Pentyl 10 ⁻⁵ M	76.11250	30.76323	.890	-44.0003	196.2253
TBDMS 10 ⁻⁴ M	50.00083	30.76323	1.000	-70.1120	170.1137
TBDMS 10 ⁻⁵ M	.27917	30.76323	1.000	-119.8337	120.3920
TBDPS 10 ⁻⁴ M	33.61167	30.76323	1.000	-86.5012	153.7245
TBDPS 10 ⁻⁵ M	-8.05500	30.76323	1.000	-128.1678	112.0578
N-Ac OH 10 ⁻⁴ M	29.72250	30.76323	1.000	-90.3903	149.8353
N-Ac OH 10 ⁻⁵ M	10.00000	30.76323	1.000	-110.1128	130.1128
TFA-PS 10 ⁻⁴ M	48.88833	30.76323	1.000	-71.2245	169.0012
TFA-PS 10 ⁻⁵ M	-15.27667	30.76323	1.000	-135.3895	104.8362

NO data for LPS activated U937 cells.

Untreated cells				95% Interval	Confidence
VS	Mean		Sig.	Lower	Upper
ALL Treatments	Difference	Std. Error	(P)	Bound	Bound
Propyl 10 ⁻⁴ M	152.22333*	20.55686	.000	71.9297	232.5170
Propyl 10 ⁻⁵ M	87.77667*	20.55686	.013	7.4830	168.0703
Phenyl 10 ⁻⁴ M	129.24182*	20.97729	.000	47.3060	211.1776
Phenyl 10 ⁻⁵ M	72.88000	20.97729	.184	-9.0558	154.8158
Ethyl Ac 10 ⁻⁴ M	114.72333*	20.55686	.000	34.4297	195.0170
Ethyl Ac 10 ⁻⁵ M	34.72250	20.55686	1.000	-45.5711	115.0161
Phenyl Ac 10 ⁻⁴ M	124.99917*	20.55686	.000	44.7055	205.2928
Phenyl Ac 10 ⁻⁵ M	71.38833	20.55686	.184	-8.9053	151.6820
Ethyl 10 ⁻⁴ M	163.00000*	21.47094	.000	79.1360	246.8640
Ethyl 10 ⁻⁵ M	77.33300	21.47094	.129	-6.5310	161.1970
Allyl 10 ⁻⁴ M	203.33300*	21.47094	.000	119.4690	287.1970
Allyl 10 ⁻⁵ M	122.27273*	20.97729	.000	40.3369	204.2085
Pentenyl OH 10 ⁻⁴ M	206.33300*	21.47094	.000	122.4690	290.1970
Pentenyl OH 10 ⁻⁵ M	68.61083	20.55686	.259	-11.6828	148.9045
Allyl OR 10 ⁻⁴ M	205.63500*	21.47094	.000	121.7710	289.4990
Allyl OR 10 ⁻⁵ M	74.16667	20.55686	.127	-6.1270	154.4603
Methyl Ac 10 ⁻⁴ M	147.49917*	20.55686	.000	67.2055	227.7928
Methyl Ac 10 ⁻⁵ M	56.66667	20.55686	.710	-23.6270	136.9603
Methyl 10 ⁻⁴ M	118.05667*	20.55686	.000	37.7630	198.3503
Methyl 10 ⁻⁵ M	50.27667	20.55686	.903	-30.0170	130.5703
Butyl 10 ⁻⁴ M	111.66583*	20.55686	.000	31.3722	191.9595

Butyl 10 ⁻⁵ M	81.66667*	20.55686	.040	1.3730	161.9603
Hexyl 10 ⁻⁴ M	131.11083*	20.55686	.000	50.8172	211.4045
Hexyl 10 ⁻⁵ M	95.27833*	20.55686	.003	14.9847	175.5720
Benzyl Ac 10 ⁻⁴ M	133.05500*	20.55686	.000	52.7614	213.3486
Benzyl Ac 10 ⁻⁵ M	53.66900	21.47094	.877	-30.1950	137.5330
Benzyl 10 ⁻⁴ M	223.52000*	22.05930	.000	137.3580	309.6820
Benzyl 10 ⁻⁵ M	177.33400*	21.47094	.000	93.4700	261.1980
Pentyl 10 ⁻⁴ M	188.88917*	20.55686	.000	108.5955	269.1828
Pentyl 10 ⁻⁵ M	180.27833*	20.55686	.000	99.9847	260.5720
TBDMS 10 ⁻⁴ M	121.94500*	20.55686	.000	41.6514	202.2386
TBDMS 10 ⁻⁵ M	163.88833*	20.55686	.000	83.5947	244.1820
TBDPS 10 ⁻⁴ M	113.61167*	20.55686	.000	33.3180	193.9053
TBDPS 10 ⁻⁵ M	144.00100*	21.47094	.000	60.1370	227.8650
N-Ac OH 10 ⁻⁴ M	131.66583*	20.55686	.000	51.3722	211.9595
N-Ac OH 10 ⁻⁵ M	131.66583*	20.55686	.000	51.3722	211.9595
TFA-PS 10 ⁻⁴ M	175.60636*	20.97729	.000	93.6706	257.5422
TFA-PS 10 ⁻⁵ M	106.38917*	20.55686	.000	26.0955	186.6828
